TÉCNICO LISBOA

Radiotherapy bunker design as a function of technique used: 3D-CRT, IMRT, TBI and SRS. Economic impact evaluation.

Victoria Corregidor Berdasco

Thesis to obtain the Master of Science Degree in

Radiation Protection and Safety

Supervisor(s): Dr. Esmeralda Poli
Dr. Mário João Capucho dos Reis

Examination Committee

Chairperson: Prof. Pedro Vaz
Supervisor: Dr. Esmeralda Poli
Member of the Committee: Dr. Yuriy Romanets

October 2018

To Rafael and Carlos,
who gave me the strength and support to
write it and probably will never read it,

with love.

Acknowledgments

This document would not have been possible without the support of my supervisor Dr. Esmeralda Poli, from Hospital Santa Maria, over the past few months. I am grateful for the Time dedication and Guidance she provided and also for the radiotherapy classes.

I am grateful to Dr. Mário Reis, for his availability and support.

I would also like to thank Prof. Pedro Vaz, coordinator of the Master on Radiation Protection and Safety, for his efforts and coaching sessions. Also, thanks to the teachers who dedicated their energies to us, sometimes too much energy...

Thank you, thank you, thank you to my colleagues: Ana, Bianca, Catarina, Daniel, João, Luís, Mariana, Marisa, Maria José, and Pêro. We learned together and from each other, and we suffered together...

Thanks to my friends and family (both Spanish and Portuguese) for their support and encouragement.

Doing a master requires Time. Since Time is limited, Time was mainly taken from Rafael, Carlos, family, and friends. I apologize and I thank all of you, for allowing me to do so without any reproval.

Resumo

Quando se pretende desenhar uma sala de radioterapia externa, o planeamento das barreiras de proteção deve ter em conta diversos fatores: tipo de acelerador, técnicas de radioterapia empregues, tipo e energia dos feixes utilizados, número de tratamentos, área disponível para a construção, etc.

A determinação das espessuras das barreiras de proteção, incluindo a porta, deve considerar também os materiais de construção: betão normal ou betão de alta densidade para as paredes e chumbo e/o polietileno com boro para as portas. A escolha destes materiais será refletida no orçamento final e no espaço utilizado, que na maioria dos casos são limitados.

Este trabalho explora como diferentes fatores afetam o dimensionamento das barreiras de proteção, assim como ao volume construído e ao orçamento. Os fatores considerados são: energia do feixe de fotões (6 e/ou 15 MV) e as técnicas de radioterapia empregues: 3D-CRT, IMRT, SRS e TBI. O método de cálculo utilizado está baseado no documento NCRP-151.

As situações estudadas e os resultados obtidos podem ser aplicados a salas reais instaladas há uma década em Portugal. Na maioria dos casos, a sala foi projetada para executar 3D-CRT, a mais utilizada em radioterapia na época. Contudo, hoje em dia, o mesmo acelerador (e sala) também é usado para realizar técnicas como IMRT ou SRS. Considerando os resultados obtidos, nestes casos deveria haver uma reavaliação das barreiras de proteção e um levantamento radiométrico, uma vez que estas alterações introduzem variações nas espessuras das barreiras, principalmente devido à radiação de fuga e geração de neutrões.

Palavras-chave: NCRP-151, desenho de barreiras, proteção radiológica, instalações de radioterapia, radiação de fuga, barreiras para neutrões

Abstract

When considering a radiotherapy bunker design, there are many parameters that should be taken into account as type of linear accelerator, intended techniques for treatment, type of beams and energy to use to deliver those techniques, number of patients, area available for construction, etc.

Barrier thickness and door composition will depend also on the materials to be used, usually concrete or high density concrete and lead and/or borated polyethylene respectively. The choice of these materials will be reflected on the budget an also on the space to be used, which in most of the cases are limited.

This master thesis explores how different parameters affect the barriers of a bunker in different scenarios, and how they are reflected in both: volume and budget. The parameters considered are: the photon beam energy (6 and/or 15 MV) and the techniques to be delivered: 3D-CRT, IMRT, SRS and TBI. The methodology followed is that described in the NCRP-151 report.

The different scenarios studied and results obtained can be applied to real bunkers already installed a decade ago, for instance, in Portugal. Most of them were designed to perform 3D-CRT, the most used technique in radiotherapy in that time but, nowadays the same accelerator (and bunker) is also used to deliver IMRT or SRS techniques. According to the results obtained, a re-evaluation of structural shielding design and a radiation survey should take place on those bunkers, since these changes introduce variations on barrier thicknesses, mostly due to the leakage radiation and neutron generation.

Keywords:: NCRP-151, shielding design, radiation protection, radiotherapy room, leakage radiation, neutron shielding

Contents

List of Tables

List of Figures

Nomenclature

β	Transmission factor for neutrons that penetrate the head shielding
φ_A	Total neutron fluence per unit absorbed dose of x-rays at the isocenter (1/(m^2 Gy))
$\dot{\mathrm{D}}_0$	Maximum absorbed-dose output rate at isocenter (Gy/h)
$\bar{\mathrm{N}}_h$	Average number of treatments per hour
α_0	Reflection coefficient scattering from surface A_0
α_1	Reflection coefficient scattering from surface A_1
α_z	Reflection coefficient scattering from surface A_z
n	Number of TVLs of material needed for a barrier
w_R	Radiation weighting factor
A_0	Beam area at the first scattering surface (m^2)
A_1	Area of wall that can be seen from maze door (m^2)
A_z	Cross-sectional area of maze inner entry (A_0 projected into the maze inner entry) (m^2)
a(θ)	Fraction of the primary beam that scatters from the patient
B	Transmission factor
C_{IMRT}	IMRT factor, ratio of MU_{IMRT} to MU_{conv}
C_{SRT}	SRT factor, ratio of MU_{SRT} to MU_{conv}
C_{TBI}	TBI factor, ratio of MU_{TBI} to MU_{conv}
D	Absorbed dose to the patient at isocenter per treatment (Gy/treatment)
d_0	Distance of 1.41 m, used in an application of Kersey's method (m)
d_{hd}	Accelerator head-to-maze door distance (m)
d_h	Perpendicular distance from the target to the first reflection surface (m)
d_{LS}	Distance from x-ray target to the maze centerline in area A_1 (m)

d_l Distance from isocenter or closest approach of the accelerator head target to the center of the maze door through the inner maze (m)

d_{pp} Perpendicular distance from isocenter to the wall (m)

d_{pri} Distance from the x-ray target to the point protected (m)

d_r Distance from beam center at the first reflection to midline of maze, passing the edge of maze wall (m)

d_{sca} Distance from the x-ray target to the patient or scattering surface (m)

d_{sec} Distance from the scattering object to the point protected (m)

d_{TBI} Total-body irradiation treatment distance (m)

d_{zz} Centerline distance along the maze length from a scattering surface to the door (m)

d_z Centerline distance along the maze (ending d_r) to the door (m)

E Effective dose (Sv)

eV Electron-volt

F Field area at mid-depth of the patient at isocenter (cm^2)

Gy Gray

H Dose equivalent per week (Sv/week)

h hour

h_φ Dose equivalent from neutron capture gamma rays outside the door per unit of absorbed dose of x-rays at the isocenter (Sv/week)

H_{cg} Dose equivalent per week at the maze door due to the contribution of neutron capture gamma rays (Sv/week)

H_{LS} Dose equivalent per week due to head-leakage photons scattered by the room surfaces (Sv/week)

H_{LT} Dose equivalent per week due to leakage radiation that is transmitted through the inner maze wall (Sv/week)

H_n Neutron dose equivalent per week (Sv/week)

H_{ps} Dose equivalent per week at the maze door due to primary beam scattered from the patient (Sv/week)

H_{sum} Sum of dose equivalent contributions beyond a barrier from photon leakage and patient scattered radiation (Sv/week)

H_s Dose equivalent per week due to scatter of the primary beam from the room surfaces (Sv/week)

H_{tot} Total dose equivalent beyond the door from photon leakage and patient scattered radiation (Sv/week)

m meter

n	neutrons
P	Shielding design goal, expressed as dose equivalent (mSv/week)
Q_n	Neutron source strength (n/Gy)
R_h	Time averaged dose equivalent rate in-any-one-hour (Sv)
R_w	Weekly time averaged dose-equivalent rate (Sv/h)
S_0	Inner maze entrance cross-sectional area (m^2)
S_1	Maze cross-sectional area (m^2)
S_r	Total surface area of the bunker (m^2)
Sv	Sievert
T	Occupancy factor
t	Thickness of barrier (cm)
U	Use factor, fraction of time that the beam is likely to be incident on the barrier
V	Volt
W	Weekly workload (Gy/week)
w	Width of barrier (cm)

Acronyms

AAPM American Association of Physicists in Medicine

ALARA As low as reasonably achievable

BPE Borated polyethylene

BPE Decree Law

CT Computed tomography

DIRAC Directory of Radiotherapy Centres, DIRAC

FFF Flattening filter free beams

GTV Gross tumour volume

HDC High density

HERO Health Economics in Radiation Oncology

HVL Half-value layer

IAEA International Atomic Energy Agency

ICRP International Commission on Radiological Protection

ICRU International Commission on Radiation Units and Measurements

IDR Instantaneous dose-equivalent rate

IMRT Intensity modulated radiation therapy

LET Linear energy transfer

LINAC Linear accelerator

MLC Multileaf collimators

MR Magnetic resonance

MU Monitor units

NCRP National Council on Radiation Protection and Measurements

NRC U.S. Nuclear Regulatory Commission

Pb Lead

QC Quality control

RT Radiotherapy

SRT Stereotactic radiation therapy

SSD Surface to surface distance

TADR Time averaged dose-equivalent rate

TBI Total body irradiation

TRS Technical Reports Series, IAEA

TVD Tenth-value distance

TVL Tenth-value layer

UNSCEAR United Nations Scientific Committee on the Effects of Atomic Radiation

3D-CRT 3D conformal radiotherapy

Chapter 1

Introduction

1.1 Motivation

Fortunately, due to the technological advances made in radiation oncology jointly with the developments in other related specialties and the early detection strategies, the number of cured cancer patients is rising. According to IAEA [1] about 50% of all cancer patients would require radiotherapy, and of all patients healed, about 40 % were treated by external radiotherapy (RT) techniques alone or in combination with other modalities.

According to Van Dyk *et at.* [2], RT is an affordable and feasible therapeutic treatment, despite the core investments required (capital and specialised human resources). Among the capital investment, the construction cost, and especially the bunker is one of the cost components with higher impact when installing a radiotherapy department. At the same time, the successful of RT is based on the use of the latest technical improvements which requires access to modern equipment and the latest RT treatments as intensity modulated radiotherapy (IMRT) or stereotactic radiotherapy (SRT). These improvements entails changes in parameters used to calculate the shielding needed in a bunker, which usually imply a reinforcement of the barriers. For example, IMRT is among the RT techniques high higher growth rate in most of the countries in the latest years, which imply an increment of the leakage workload by a factor between 2 and 5 when compared with 3D conformal radiotherapy (3D-CRT) technique, thus secondary barriers projected for 3D-CRT should be revaluated, and eventually increased. Other changes as energy of the primary beam, patient position or even the usage pattern distribution will have an impact in the shielding parameters and, as a consequence, in the radiation protection of both, workers and public.

In Portugal, there were 41 linear accelerators (LINACs) dedicated to radiotherapy in 2014 [3] (52 LINACs and 1 LINAC robotic according to DIRAC database consulted in 2018 [4, 5]) and about 68 % of them can perform IMRT. 50 % of the LINACs were installed between 1996 and 2008 (see figure 1.1), and according to projected requirements for 2020 computed from the IAEA-DIRAC database [5] Portugal has a deficit of about 20 teletherapy units.

The needs of new units and the equipment renewal requires investment [6], and it must include an important slice to bunker design, construction and modifications, being the main goal the proper radiation protection to the public and workers.

On the other hand, the distribution and objectives of the LINACs should be carefully planned considering

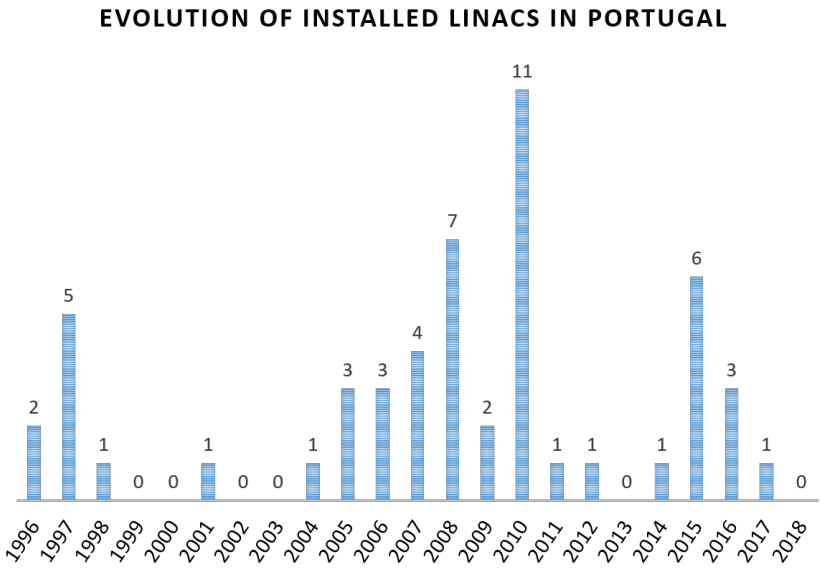

Figure 1.1: *Evolution of LINACs installed in Portugal since 1996 (data from IAEA-DIRAC database [5].*

the national outlook and when possible, following the international guidelines. Rodriguez *et at.* [7] point out that Departments with high number of accelerators as in Netherlands (5.7 accelerators per center), enables the subspecialisation by pathology (and technique) by means of dedicated rooms resulting in better performance [3, 8].

The present thesis emerges as an effort to show how the RT techniques applied in a bunker and its usage pattern can affect the bunker design, for both dedicated bunkers to a specific technique or for a mix of techniques, a more realistic situation in Portugal.

1.2 Topic Overview

Construction costs, available space and aesthetics will be major contributions affecting the bunker design for radiotherapy purpose. Long-term maintenance, quick access to the patient in case of emergency, and the typical number of trips in and out of the room prior to and during treatment should also be considered. The choice of barrier materials (e.g. concrete, lead, and/or steel) is also an influence in the final costs and available space.

On the other hand, barrier thicknesses will depend, among other factors, on the radiation protection shielding design goals for each protected area and its occupancy factor. Also, given the investment needed to construct this type of rooms, it is desirable to achieve the thinnest possible structure consistent with the radiation protection goals, and that approach is generally taken by a multidisciplinary team, speaking in the same language.

Throughout this master thesis the nomenclature followed by the NCRP-151 report [9] and generally accepted by the radiotherapy community, will be followed. ”MV” will be used when referring to accelerating voltages and the endpoint energy of a bremsstrahlung spectrum of the x-rays, while ”MeV” will be used when referring only to monoenergetic photons or electrons.

1.3 Objectives

The main objective of this document is to evaluate the differences in the barrier thicknesses of an external radiotherapy bunker and how they are reflected in the budget for material construction depending on:

- Nominal beam energy of the photons: 6 MV or 15 MV;
- Radiotherapy treatment performed: 3D-CRT, IMRT, TBI and SRS.

Both, dedicated bunkers for each RT treatment and bunkers where a mix of treatments is delivered (more realistic situation) have been studied.

The materials considered for the construction of the barriers are: ordinary and high density (HD) concrete for walls and a combination of lead (Pb) and borated polyethylene (BPE) for door.

This work assumes that initial considerations and requirements to install the facility have been established, as for example:

- There is a multidisciplinary team of professionals able to design, construct and commission a radiotherapy programme of the institution that will host the radiotherapy unit;
- The workflow is known;
- Data to calculate the workload for each technique (or combination of techniques) are known.

The methodology used to calculate the thickness of the barriers is that described in the NCRP-151 [9]. Although the current Portuguese regulation by the Decree Law 180/2002 of 8 August 2002 (DL 180/2002) [10] follows the DIN-6847 standard [11] (from 1977), in this work this methodology is not going to be followed since it does not consider the leakage radiation due to IMRT or SRS technologies.

1.4 Thesis Outline

The document is divided in 6 main chapters.

This first chapter is focused on introducing the reader to the topic and objectives of this master thesis.

The second one is dedicated to introduce the radiation protection area in the medicine field, starting from a historic contextualization, followed by a brief description of the biological effects of radiation and then a brief description of the therapeutical radiotherapy techniques used in the frame of this document. Also a short description of how a linear accelerator works and the mechanism of interaction between radiation and matter is given.

Chapter 3 is dedicated to introduce the NCRP-151 methodology that will be used to calculate the barriers of the radiotherapy bunker and how it was implemented in this document. In this section is also presented the actual dose limits for exposed workers and public considering the actual Portuguese legislation (DL 222/2008 of 17 November 2008 [12]) and the last Council Directive of 5 December 2013 published, (2013/59/EURATOM) [13].

Chapter 4 shows the results obtained for a hypothetical room that will change according to the technique (dedicated bunker) or to multiple techniques performed inside. It is also shown how the distribution of treatments can affect the barrier thickness, which is one of the most usual situation, and can affect not only the walls but also the door entrance composition.

Chapter 5 is dedicated to the cost analysis, how parameters as beam energy, shielding design goal, occupancy factor or maze barrier can affect the project budget, considering only the cots of construction materials: ordinary and high density concrete for walls and lead and borated polyethylene for door.

Chapter 6 is for main conclusions and future work to be developed.

Finally, there are two appendixes. Appendix A summarizes the data used along this document and Appendix B presents examples of how barriers were calculated for different scenarios.

Chapter 2

Background

This chapter is dedicated to introduce the reader into the origins of the radiation protection and into the effects of radiation in biological tissues. This will help to understand the link between these two concepts: the beneficial effects obtained when radiation is ”controlled” and ”desired” and, on the other hand, the harmful effects when it is neither ”controlled” nor ”desired” and the need of protection from this radiation by means of shielding barriers.

2.1 The beginning...

The end of the XIX century is characterized by two main discoveries: x-rays and radioactivity.

The x-rays were discovered by Roentgen on November, 1895 [14]. Using a Crooke´s tube to produce x-rays and crystals of barium platino-cyanide as detector radiation, Roentgen was able to see the shadow outline of the bones of his hand. In this way, he “reported” the first hand radiography. The medical application of the x-rays was realized and widely applied without any concern.

In fact, until the patients (subjected to long time exposures) and the operators (who handled the x-ray generators) developed inflammatory changes and epilation on the exposed areas nobody thought about the biological effects of this new technology. Once they were appreciated, new designs of generators were developed to be used for therapy and diagnosis under safer conditions [15]. Thus, they were classified according to the penetration of the emitted radiation (hard, medium and soft).

In 1896, Becquerel discovered the radioactivity phenomenon when he was using naturally fluorescent minerals to study the properties of x-rays [16]. Only two years later, in 1898, Marie and Pierre Curie discovered the radium [17].

The biological effects of radioactivity were evidenced by Becquerel itself in 1901: he was carrying a tube of pure radium in his waistcoat pocket and the tissues beneath developed a severe inflammation a fortnight after, attributing this effect to the radium. P. Curie, realizing that this property of radium might have medical applications, decided to perform similar experiments on his own arm [15]. Also in 1901 Becquerel and Curie reported their experiences and soon after they gave 0.394 g radium sulphate in a rubber covered capsule to Dr. H. Danlos of St. Louis Hospital, in Paris [15, 17], who used it to treat a patient with cutaneous lupus.

Figure 2.1 shows some examples about the evolution along the last century on radiation protection applying the three main parameters that should be optimised to minimize the exposure to radiation: time, distance, and shielding.

- **Time**: as the time of exposition to radiation increases, the dose received increases in direct proportion,
- **Distance**: the most effective of the principles. As distance from the radiation source increases, the dose received decreases in proportion to the inverse of the distance from the source squared,
- **Shielding**: when the use of time and distance principles are not possible, shielding should be always used to minimize the dose.

In figure 2.1a (published in 1896) no precautions against radiation exposure is visible, since hazards were still unknown [18]. Years later, the concept of protection appears as can be seen in figures 2.1b [19] and c [20], by using physical barrier and/or the use of lead aprons and lead impregnated gloves (although implementation can be optimised). In figure 2.1d (from 1932, [21]) improved safety measures can be observed: leaded walls, indication lights, a radiation clock fixed to the wall on the right of the door and a sort of mechanical egg timer which rings when the defined radiation time is reached. In figure 2.1e (1953) barriers are becoming thicker and distance has been increased. Finally, figure 2.1f, from 1972, shows the stacking of concrete blocks surrounding a treatment room of a megavoltage irradiation facility [21].

Since 1928, the International Commission on Radiological Protection (ICRP) has contributed to the development and elaboration of the International System of Radiological Protection used world-wide as the common basis for radiological protection standards, legislation, guidelines, programmes and practices.

Documentation produced by reference non-governmental organizations as ICRP and ICRU (International Commission on Radiation Units and Measurements) provide the scientific basis to the governmental organizations to produce documentation as: Safety Standards and Technical Documents from the IAEA, documents from the National Council on Radiation Protection and Measurements (NCRP) or documents from the United Nations Scientific Committee on the Effects of Atomic Radiation (UNSCEAR).

From the early years of the XX century up to now, and thanks to the work of many multidisciplinary research groups, the knowledge has dramatically increased in many scientific and technological fields, which lead to an improvement in radiological protection. Can be highlighted:

- Physics: development of models for the different mechanisms involved between radiation and matter, among other issues,
- Biology: how changes in atoms produced by radiation are transferred to the cell, tissue or organs environment,
- Engineering: development of new devices, detectors, computation algorithms, etc.,
- Dosimetry: quantities definition, development of primary and secondary standards, measurements guidelines improvement, etc.

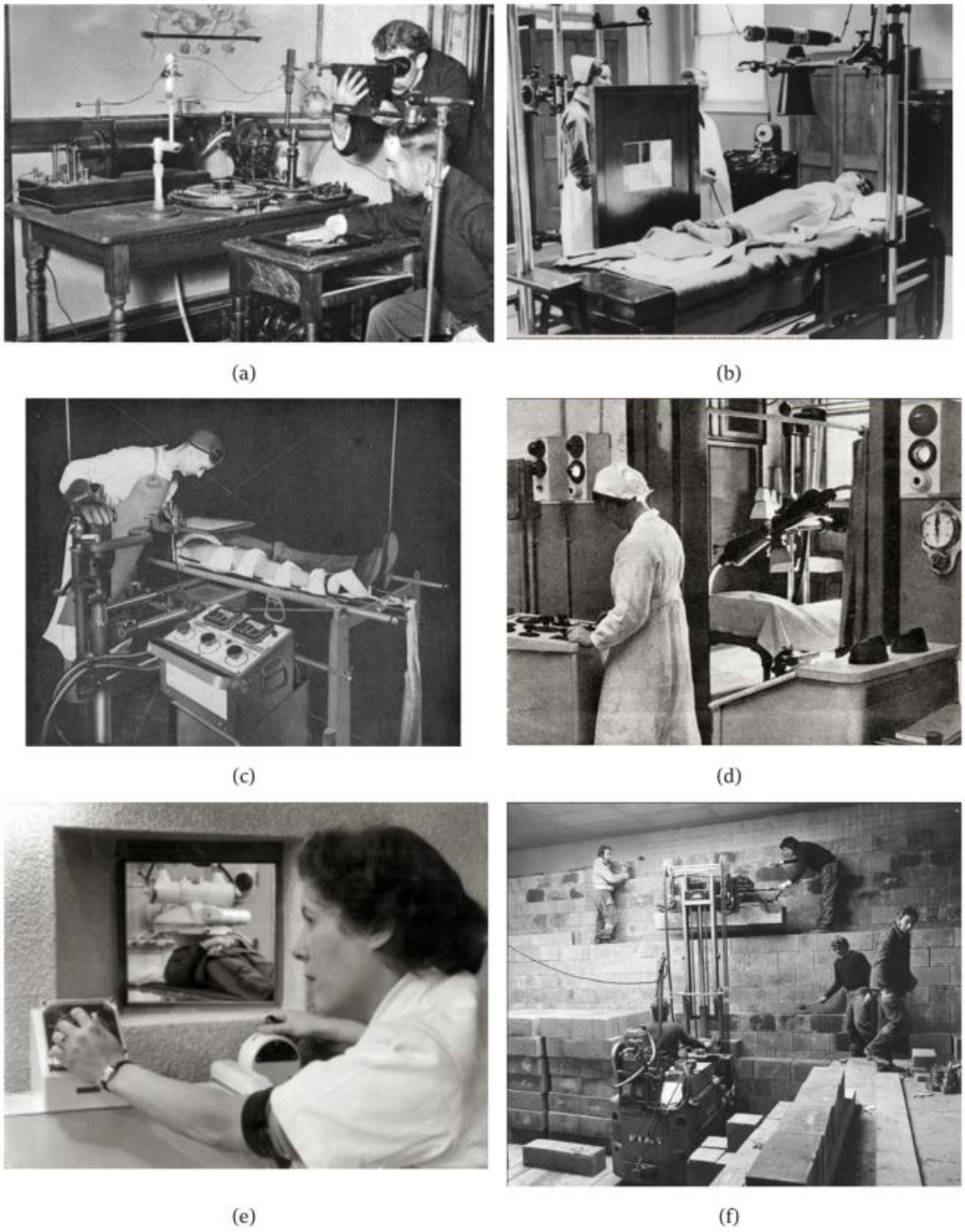

Figure 2.1: *Evolution of the radiation protection along the years. a) 1896. Taking an x-ray image with early Crookes tube apparatus (center), the standing man is viewing a hand with a fluoroscope screen. The seated man is taking a radiograph of his hand by placing it on a photographic plate. No precautions against radiation exposure are taken [18]; b) 1903. Great Ormond Street Hospital in UK acquired its first x-ray machine [19], there is a physical barrier (partially used); c) 1930. An x-ray technician from USA performs foreign body localization using the x-ray field unit [20], wearing lead aprons and lead-impregnated gloves; d) 1932. The x-ray department from the Cancer Institute Science in the Netherlands, a 15 cm thick leaded wall protects the staff when operating the controls [21]; e) 1953. Radiation therapist at the control panel of the Siemens convergence machine. Barriers are thicker and distance is increased [21]; f) 1972. Stacking of the concrete blocks surrounding a treatment room in the new megavoltage irradiation facility [21].*

2.2 Radiation and biological effects

The evolution in radiation protection is closely related with the increasing in knowledge about the biological effects of radiation, which at the same time are related with the increasing in knowledge about the interaction mechanisms between the radiation and atoms (figure 2.2).

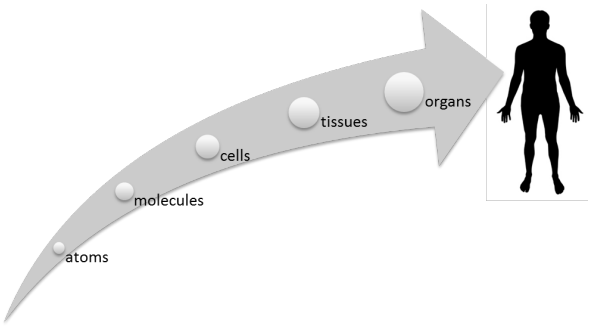

Figure 2.2: *Radiation interacts with atoms, provoking effects to the cells, tissues, organs and eventually the whole body.*

There are two mechanisms by which radiation may affect cells: direct and indirect (figure 2.3, [22]).

- **Direct**. When radiation interacts with the atoms of the DNA molecule or some other cellular component critical to the survival of the cell. As a consequence, the ability of the cell to reproduce (or survive) is compromised. Because the DNA molecule is a small part of the cell, the probability of the radiation interacting with them is very small. This mechanism is dominant when interaction is due to high LET (linear energy transfer) particles, as neutrons and alpha particles.
- **Indirect**. When radiation interacts with water may break the bonds producing hydrogen (H) and hydroxyls radicals ($^{\cdot}$OH). Then, they can recombine either with other fragments or ions to form compounds such as water (the best of the cases), or they could combine to form toxic substances, ionized water (H_2O^+) or hydrogen peroxide (H_2O_2), which can contribute to the destruction of the cell. As cells are mostly composed of water, there is a much higher probability of radiation interacts with the water than with the DNA molecule. About two thirds of the biological damage caused by low LET radiation, as x-rays or electrons, occur through indirect mechanism.

Against the destructive character of radiation, the cells have a tremendous ability to repair the damage produced. In many cases the cells are able to repair any damage completely but, if the damage is severe enough, the affected cells (or the daughter cells) will die. There is another possibility, the cell is affected in such a way that it does not die but is simply mutated. The mutated cell reproduces and thus perpetuates the mutation which, in the worst case scenario, could be the beginning of a malignant tumour.

It is also known that the cellular sensitivity to radiation depends on the cell cycle, being more sensitive during mitosis (cell division) than through the preceding substages [23, 24]. Also, according to the Law of Bergonie and Tribondeau [25], the cell radiosensitivity is directly proportional to the rate of cell division and inversely proportional to the degree of cell differentiation. The consequences of radiation in cells is also dependent on the presence of molecular oxygen in the cell. In this way, those cells with high oxygenation level will be more radiosensitive than those with low oxygenation level, being this effect even more important for low LET radiations.

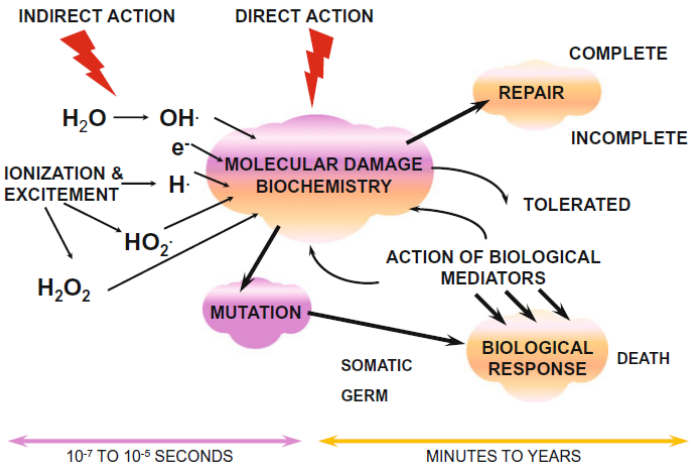

Figure 2.3: *Physical, biochemical and biological response mechanisms to radiation [22].*

2.3 External radiation in therapeutic medicine

External radiation therapy uses ionizing radiation to reduce or kill cancer cells by means of the biological effects that this radiation induces in them. These cells are characterized, among others, by: an abnormal high mitotic rates and less differentiation degree when compared with normal cells. Furthermore, in malignant tumours the outer layer of cells reproduces rapidly and has also a good supply of blood and oxygen while the cells located in the interior tend to be inactive, with low concentration of oxygen. In this sense, malignant cells and boundaries tumours will be much more radiosensitive to radiation than healthy cells.

The aim of external radiotherapy is to deliver enough radiation to the tumour, also known as gross target volume (GTV), to destroy it while avoiding damage to the surrounding healthy tissues with a dose that will lead to serious complications (morbidity) [26].

Usually the treatment given for a specific situation is fractionated, which means that the radiation is given during short periods (minutes) over specific intervals. Under this situation, the total dose delivered is higher when compared with the dose needed in a single treatment, but the therapeutic benefit is also higher. This affirmation is based on empirical results and the knowledge of the biological effects of radiation, also called the five Rs of radiotherapy [26]:

- **R**adiosensitivity. Mammalian cells have different radiosensitivities.
- **R**epair. Mammalian cells can repair sublethal damage provoked by radiation, by a variety of repair enzymes and pathways. Fractionating the dose, healthy cells can repair themselves between intervals.
- **R**epopulation. Cells can repopulate while receiving fractionated doses of radiation, reducing side effects.
- **R**edistribution. In a fractionated treatment redistribution of cell populations throughout the cell cycle phases increases the possibility to kill the cell, when compared to a single session treatment.
- **R**eoxygenation. Reoxygenation of hypoxic cells occurs during a fractionated course of treatment, making them more radiosensitive to subsequent doses of radiation.

During the last decades new external RT techniques have been developed in order to treat specific therapeutic situations. These techniques are based on the use of a linear accelerator that produces high energy x-ray beams,

high dose rates and can reach the target with more precision. The main goals of these radiotherapy techniques are:

- Increase the conformal degree of the GTV and increase the radiation dose to be delivered on it,
- Decrease toxicity of radiation to normal tissue improving the regional control and overall survival of healthy cells.

In the following sub-sections those techniques that are considered in this document are briefly described but before also a brief description of how a linear accelerator works is given.

2.3.1 How a linear accelerator works

Linear accelerators (also called LINAC) offer excellent versatility for use in external radiotherapy through isocentric mounting, providing either electron or x-ray therapy of megavoltage beam energies, or both.

X-ray beams, typically with energies between 10 kV and 50 MV[1], are produced when electrons with kinetic energies between 10 keV and 50 MeV hit a metallic target. Most of the kinetic energy is transformed in the target into heat and a small fraction is emitted as x-ray photons, which are divided into: characteristic and bremsstrahlung x-rays.

While the characteristic x-rays have discrete energies (which depend on the target atoms), the bremsstrahlung x-rays are due to radiative losses and have a continuous spectrum of energies (from zero to the kinetic energy of the incident electron). In the megavoltage range (as the case of accelerators used for radiotherapy) the contribution of characteristic x-rays to the total spectrum is negligible.

The medical accelerators accelerate electrons using non-conservative microwave radio frequency (RF) fields in the frequency range from 10^3 to 10^4 MHz, although most of them work at 2856 MHz. The electrons follow straight trajectories in accelerating waveguides which length will depend on the final electron kinetic energy: approximately 30 cm for 4 MeV or $\sim$ 150 cm for 25 MeV.

The operational system of a LINAC is distributed over five major and distinct sections which can change according to the final electron beam kinetic energy or the manufacturer [26]: gantry, gantry stand or support, modulator cabinet, patient support assembly and control console.

Schematic diagrams with a general layout of a modern LINAC are shown in figures 2.4 and 2.5. The main components can be described as [26]:

- Injection system or electron gun. It consist of a filament (cathode) and a grounded anode (some models can have also a grid). When heated, the filament emits electrons and then they are accelerated towards anode through which they enter the accelerating waveguide.
- RF power generation system (a magnetron or a klystron) which produces high power RF fields for electron acceleration. A magnetron is a source of high power RF while a klystron is an RF power amplifier that amplifies the low power RF generated by an RF oscillator commonly called the RF driver.

[1] As mentioned in Chapter 1, the nomenclature used is that from the NCRP-151 report. "MV" refers to endpoint energy of the bremsstrahlung spectrum of the x-rays and "MeV" is sued for monoenergetic photons or electrons. In fact, according to Maruyama *et al* [27] the average energy of the primary spectrum in the treatment room is 3.22 MeV for 10 MV photons and 4.53 MeV for 20 MV photons.

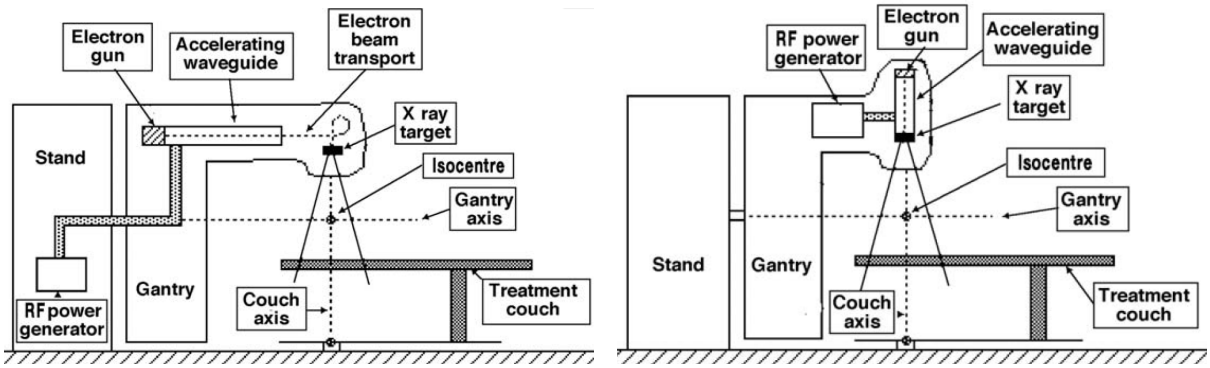

Figure 2.4: *Design configurations for isocentric medical LINACs which produces megavoltage x-rays and electrons [26]. a) The accelerating waveguide is in the gantry parallel to the isocenter axis and the RF power generator is located in the gantry stand. b) The electron gun and target are permanently embedded into the accelerating waveguide.*

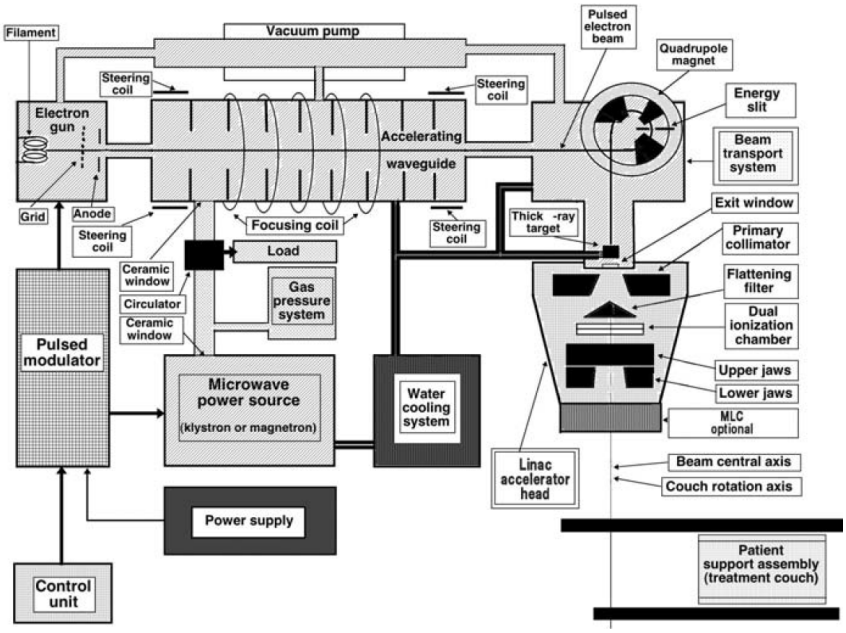

Figure 2.5: *General layout of a LINAC's components [26].*

- Accelerating waveguide: evacuated or gas filled metallic structures used in the transmission of microwaves. The simplest waveguide is obtained from a cylindrical tube and adding a series of discs with circular holes at the center, placed at equal distances along the tube (cavities) to provide a suitable electric field pattern for the acceleration of electrons. Two types of accelerating waveguide have been developed: travelling and standing wave structure.
- Auxiliary systems, which comprises: a vacuum pumping system, a water cooling system for the accelerating guide, target and RF generator; an optional air pressure system for pneumatic movement of the target or other beam shaping components; shielding against leakage radiation, designed to attenuate the average primary x-ray beam intensity to less than 0.1% [28].
- Electron beam transport for transporting the electron beam from the waveguide to the x-ray target (or to the LINAC exit window for electron beam therapy). The system consists of evacuated drift tubes and bending

magnets (90º, 270º (achromatic) or 112.5º (slalom)), steering and focusing coils.

- LINAC treatment head, which contains the components that influence the production, shaping, localizing and monitoring the photon or electron beams. It incorporates: several retractable x-ray targets, flattening filters and electron scattering foils, primary and adjustable secondary collimators, transmission ionization chambers, field defining light and a range finder, optional retractable wedges and optional multileaf collimators (MLC), see figure 2.5. The primary collimator defines a maximum circular field, which is further truncated by adjustable rectangular collimators with a maximum dimension of 40x40 cm^2 at the isocenter. The clinical photon beams are produced with a specific target–flattening filter combination, while the clinical electron beams are produced by retracting the target and flattening filter from the electron pencil beam. Modern LINACs can produce high dose rates beams by removing the flattening filter, known as flattening filter free (FFF) beams. The transmission ionization chambers are used for monitoring the beam output as well as the radial and transverse beam flatness.

For patient safety, the LINAC dosimetry system usually consists of two independent sealed ionization chambers to monitor the beam output continuously during treatment. The primary ionization chamber measures monitor units (MU). According to the IAEA TRS-398 document [29], the accelerator should be calibrated in a way to obtain a ratio of machine monitor units to absorbed dose delivered to the target volume equals to 1 MU/cGy at the depth of dose maximum on the central beam axis when irradiated with a 10x10 cm^2 field at a source to surface distance (SSD) of 100 cm. Additionally, the dose monitoring system also monitors other parameters such as the flatness and symmetry of the beam.

2.3.2 3D conformal radiation therapy (3D-CRT)

In three-dimensional conformal radiation therapy, the radiation beams are shaped to match the shape of the target by means of multileaf collimators (MLC), in which the position is set before the initiation of the treatment. This 3D technique represents a significant advance in comparison with the 2D technique (see figure 2.6) where radiation beams only matched the height and width of the tumour exposing both, healthy and unhealthy tissues, to radiation [26].

3D-CRT requires 3D images of the patient acquired by computer tomography (CT) scans or by magnetic resonance (MR) and the delineation of the gross tumour volume (GTV), the close surrounding volume or clinical target volume, and the surrounding organs at risk. Based on these CT (and/or MR) images, complex plans are developed (forward treatment planning) to deliver a radiation dose distribution to the GTV considering different angles on the beam, shape of collimators, weight or beam energy (see figure 2.7). When needed, beam intensity modulation can be obtained by using blocks or wedges to provide more uniform target coverage.

Nowadays, 3D-CRT is used to treat tumours that in the past might have been considered too close to vital organs and structures for radiation therapy. For example, it allows radiation to be delivered to head and neck tumours in a way that minimizes exposure of the spinal cord or optic nerve.

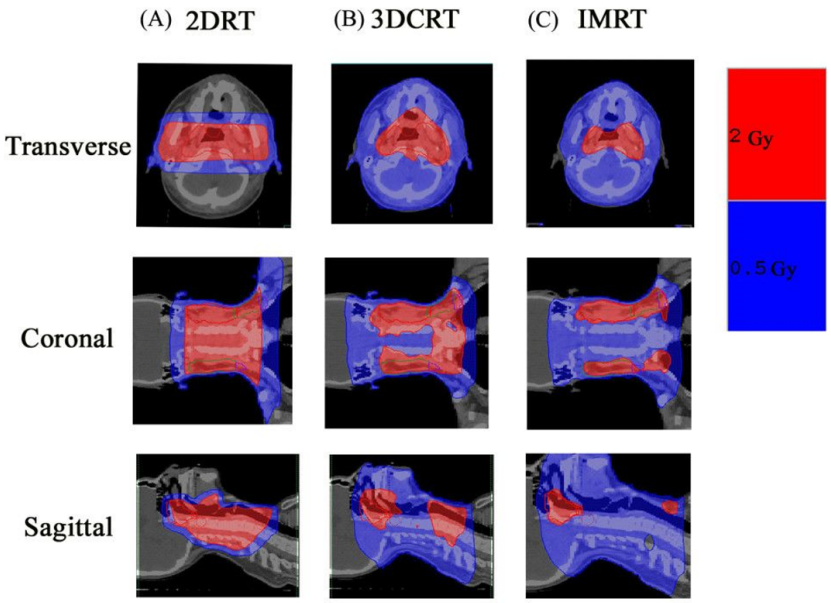

Figure 2.6: *Example of isodose distribution using different irradiation techniques delivering 2Gy to the target: transverse, coronal and sagittal view. a) Conventional radiation therapy, 2DRT; b) 3D conformal radiotherapy, 3D-CRT; c) Intensity modulated radiotherapy, IMRT [30].*

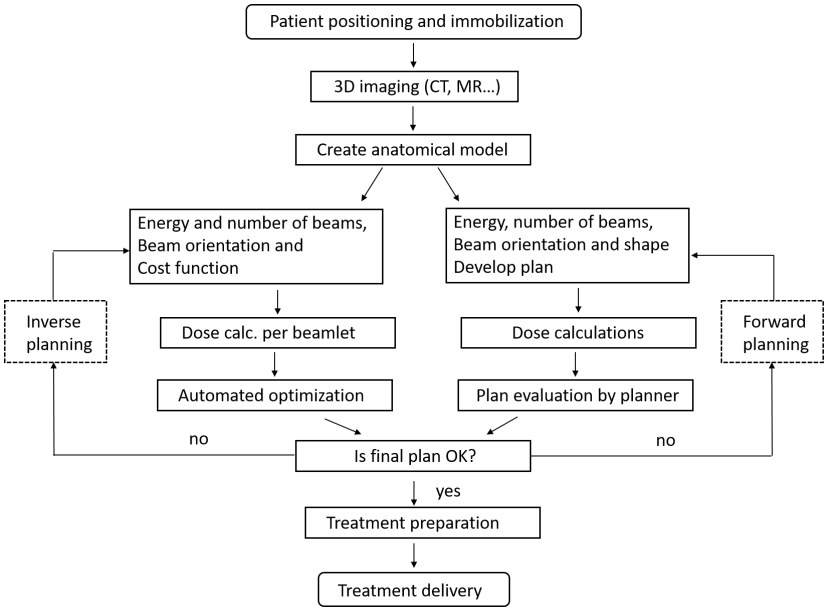

Figure 2.7: *Schematic chart of the basic components for forward and inverse planning processes, adapted from [31].*

2.3.3 Intensity-modulated radiation therapy (IMRT)

IMRT, intensity-modulated radiotherapy therapy, is also a 3D high-precision technique that uses computer-controlled LINAC to deliver high precise radiation doses to a specific volume target as shown in figure 2.6 with less damage to healthy tissues compared with 3D-CRT. IMRT is generally delivered with MLCs (figure 2.8) of tungsten which are used to shape irregular fields [26]. Each leaf can be controlled individually along the treatment with an accuracy better than 1 mm supplying intensity modulated fields in conformal radiotherapy, either in the step and shoot mode or in a continuous dynamic mode.

IMRT also needs 3D images of the patient to get information about the volume target, but in this case the dose distribution is inversely determined [32] using the inverse treatment planning (as schematized in figure 2.7) meaning that the dose distribution goal is introduced into a dedicated software and then a group of fluence maps are calculated to generate, as nearly as possible, the desired dose distribution inside the patient.

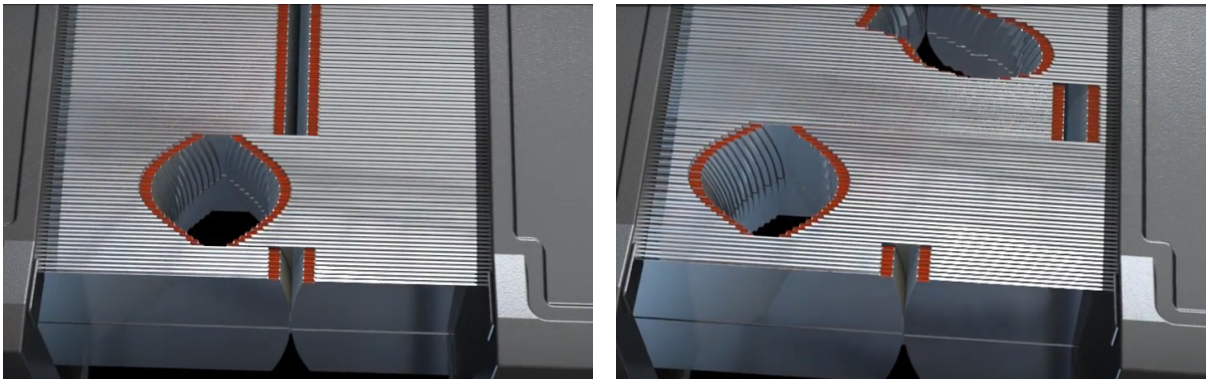

(a) (b)

Figure 2.8: *Multileaf collimators moving during treatment to shape irregular fields of the target volume (Elekta), [33].*

2.3.4 Total body irradiation (TBI)

Total body irradiation is another therapeutic radiotherapy technique that delivers to a patient an uniform dose to whole body, half body or total lymphoid. The uniformity, about 10% of the prescribed dose, is achieved with the use of bolus, partial attenuators and/or compensators [26]. Few specific organs, as lung, are partially or fully shielded from the prescribed dose, as shown in figure 2.9.

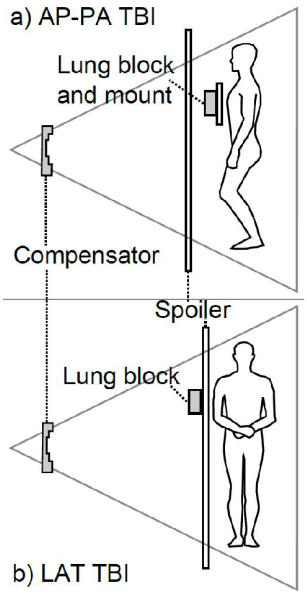

Figure 2.9: *TBI patient treatment geometry (whole body) showing the lung block and attenuator in front of the patient for (a) opposing anterior and posterior (AP-PA) technique and (b) right–left lateral (LAT) technique [34].*

TBI can be applied with either a stationary beam with large field sizes in the order of 70x200 cm^2 encompassing the whole patient, or moving the beams with smaller field sizes in translational or rotational motion to

cover the whole patient [35]. TBI treatment techniques are carried out with treatment machines specially designed for total body irradiation or, in most cases, by using a conventional LINAC at large SSD.

TBI is used primarily as part of a preparatory cytoreductive conditioning regimen prior to bone marrow transplantation. Depending on the specific clinical situation, TBI technique can be divided into four categories [35]:

- High dose TBI, with dose delivered in a single session or up to six fractions of 2 Gy each in three days, with a total dose of 12 Gy,
- Low dose TBI, with dose delivery in 10–15 fractions of 10–15 cGy each,
- Half-body irradiation, with a dose of 8 Gy delivered to the upper or lower half body in a single session,
- Total lymphoid irradiation, with a typical lymphoid dose of 36 Gy delivered in 16 fractions.

2.3.5 Stereotactic radiation therapy (SRT)

Stereotactic radiation therapy comprises high-precision irradiation techniques that use multiple and non-coplanar photon radiation beams, delivering a high dose of radiation (in the order of 10-50 Gy, $\pm$ 5 %) to stereotactically localized small lesions (1-35 cm^2), applying frame-based and frameless techniques [36]. These techniques were originally used to treat lesions mainly located in the brain, and nowadays also include a number of extra-cranial malignancies.

Requirements for SRT comprise secure patient immobilization, accurate target relocalization during treatment, and also needs to follow the respiratory motion.

SRT can be given using a wide variety of treatment devices and may incorporate specialized dose delivery methods as IMRT. Because of the small target volume, the most important requirement of an accelerator used for SRT is the mechanical stability and accuracy of its isocenter while dose homogeneity requirement is often relaxed.

There are also dedicated SRT equipments, such as:

- GammaKnife, which incorporates 201 Cobalt-60 sources;
- CyberKnife, that incorporates a miniature accelerator mounted on a robotic arm and an image guidance system which is constantly monitoring the target volume motion and automatically correcting its position by the robotic arm throughout treatment delivery;
- LINACs with FFF beams to provide high dose rates at the isoceter, combined with image guided system, patient immobilization and respiratory motion technology.

With regard to dose fractionation, SRT can be divided into stereotactic radiosurgery (SRS), in which the total dose is delivered in a single treatment session, and stereotactic radiotherapy (SRT), in which the total dose is delivered in multiple fractions.

2.4 The need of barriers. Dimension and composition

In external radiotherapy treatments, high dose of radiation is delivered into a specific volume target to provoke the appearance of deterministic effects (or ”tissue reactions” as adopted in 2012 by the ICRP-118 [37]).

On the other hand, low dose radiation exposure over long periods of time (an analogue situation to which workers of a radiotherapy department can be subjected) or even during short periods of time (as public) may have stochastics effects. The relationship between low dose radiation exposure and the appearance of stochastics effects is not totally well understood [37, 38]. Figure 2.10 shows the different hypotheses accepted nowadays for the excess relative risk (ERR) as a function of the exposure radiation dose. Briefly, these hypotheses are (see [38] and references therein):

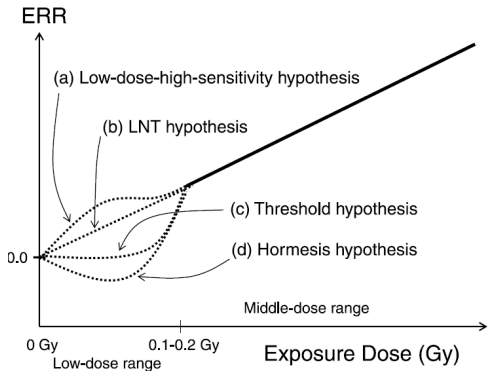

Figure 2.10: *Excess relative risk (ERR) vs dose-response model hypotheses in the low dose range (below 0.1-0.2 Gy) [38]. a) low dose vs high sensitivity hypothesis; b) the linear no-threshold (LNT) hypothesis; c) the threshold hypothesis; d) the hormesis hypothesis*

a) The low-dose-high-sensitivity hypothesis assumes that there is a set of the population who is highly sensitive to radiation and react at a lower level of radiation exposure than others, or assumes differences in the relation between the amount of damage and corresponding repair elicited by low dose radiation;

b) The linear no-threshold hypothesis, where it is supposed that the disease risk is proportional to the amount of radiation exposure at any low dose value;

c) The threshold hypothesis indicates that the disease risk becomes higher when level of exposure is larger than a fixed dose called “threshold dose”;

d) The hormesis hypothesis assumes a beneficial effect on health at small dose of radiation exposure.

The ICRP-60 established in 1991 [39] ten principles as fundamental for the system of radiation protection, also published in 2006 by the IAEA as a safety standard series document [40]. They are summarized as:

1. Responsibility for safety. The prime responsibility for safety must rest with the person or organization responsible for facilities and activities that give rise to radiation risks.

2. Role of government. An effective legal and governmental framework for safety, including an independent regulatory body, must be established and sustained.

3. Leadership and management for safety. Effective leadership and management for safety must be established and sustained in organizations concerned with, and facilities and activities that give rise to, radiation risks.

4. Justification of facilities and activities. Facilities and activities that give rise to radiation risks must yield an overall benefit.

5. Optimisation of protection. Protection must be optimised to provide the highest level of safety that can reasonably be achieved.

6. Limitation of risks to individuals. Measures for controlling radiation risks must ensure that no individual bears an unacceptable risk of harm.

7. Protection of present and future generations. People and the environment, present and future, must be protected against radiation risks.

8. Prevention of accidents. All practical efforts must be made to prevent and mitigate nuclear or radiation accidents.

9. Emergency preparedness and response. Arrangements must be made for emergency preparedness and response for nuclear or radiation incidents.

10. Protective actions to reduce existing or unregulated radiation risks. Protective actions to reduce existing or unregulated radiation risks must be justified and optimised.

Years later, in 2007, the Commission formulated a single set of principles (3) in the ICRP-103 [41] that can be applied to different situations: planned, emergency and existing exposure situations. They are:

Principle of Justification. Any decision that alters the radiation exposure situation should do more good than harm.

Principle of Optimisation of Protection. Doses should all be kept as low as reasonably achievable, taking into account economic and societal factors, also known as ALARA principle.

Principle of Application of Dose Limitation. The total dose to any individual should not exceed the appropriate limits.

As a consequence, radiation risks to workers, public and to the environment that may arise from the use of radiation have to be assessed and, if necessary, controlled. Thus, dose constraints are used for optimisation of protection against radiation and they are regulated by national laws.

Among the three main parameters that should be optimised to minimize the exposure to radiation (time, distance and shield) an efficient shielding for an external beam radiation facility is the most efficient way to reduce the radiation exposure delivered to workers and public.

In this way, since need of barriers is mandatory, it is highly recommended to know the composition of the radiation field inside the treatment room, because materials have different shielding properties which are quite dependent on the type of radiation to block. While alpha particles can be restrained by a sheet of paper, neutrons can pass through lead sheets [22], as shown in figure 2.11. A variety of materials may be required in a barrier design, depending on the type of radiation, space constraints, pre-existing structure, or budget.

Considering the interaction mechanisms of radiation with matter, the Compton effect is the predominant mode of photon interaction with shielding material with low-medium atomic number (Z) in the megavoltage energy range [42], see figure 2.12. For this reason, to reduce the barrier thickness high density materials are recommended as thickness is approximately inversely proportional to the density of the shielding material. For higher energies, the pair-production interaction can be also important when materials have Z higher than $\sim$25, nevertheless, materials incorporating these elements are even more effective as absorbers than lighter materials.

Concrete is the most commonly used material to construct barriers, providing good x-ray shielding and structural strength as well as neutron shielding due to the high hydrogen content at relatively low prices. According

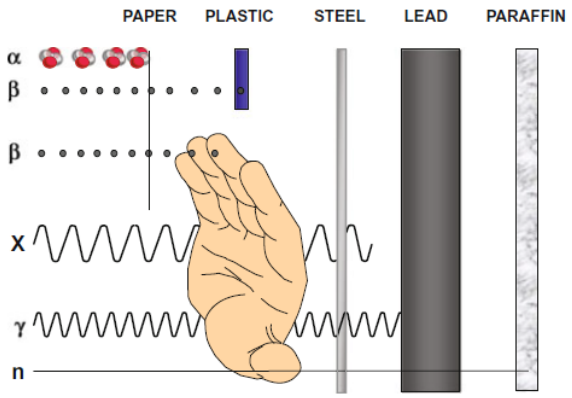

Figure 2.11: *Penetrating properties of ionizing radiations [22].*

to Barish [43], for a LINAC working at 15 - 25 MV, the TVL for neutrons in ordinary concrete is 25 cm. The density used for calculations is 2.35 g/cm^3, which should be tested and verified during construction.

Heavy concrete is also often used in construction of radiotherapy rooms. It has a density higher than 2.35 g/cm^3, and it is achieved by adding higher density material aggregates to concrete, as iron, steel or lead. The main disadvantage is the cost, and usually its use is limited to primary barriers to obtain thinner walls, saving space. The hydrogen content continues high, so the properties for shielding neutrons continue [43].

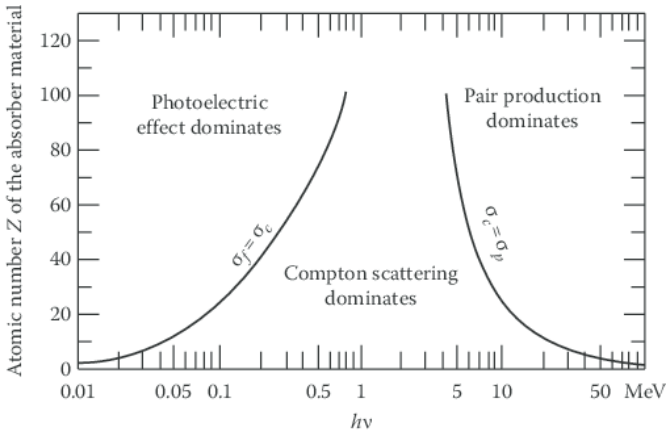

Figure 2.12: *Dominant interaction process according to photon energy and atomic number (Z) of the absorber [42].*

Besides the high energy radiation produced by the linear accelerator directed towards the volume to be treated (primary beam), other radiations are produced (figure 2.13), where can be highlighted:

- Leakage radiation (emitted in all directions isotropically) from the head of accelerator, inlcuding the MLCs;
- Patient-scattered radiation, also emitted in all directions isotropically and it is treated as if coming from isocenter, usually at 1 m from the target producing the primary beam;
- Surfaces of the treatment room scattered radiation;
- Photoneutrons produced by the primary beam (generated when accelerating voltage is above 10 MV [9]).

Among them, when the accelerating voltage is higher than 10 MV the neutron production in the head of the accelerator becomes relevant. They are produced primarily in the primary collimator and to a lesser extent by

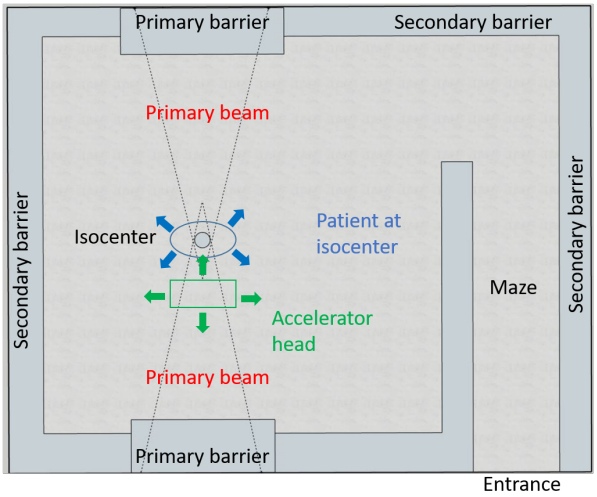

Figure 2.13: *Radiation distribution in a typical external radiotherapy bunker with a maze. Red: primary beam directed towards the primary barriers; Green: leakage radiation coming from the accelerator head in all directions; Blue: patient scatter radiation, also in all directions, and usually located at the isocenter (blue circle).*

the target and flattening filters. The MLCs can also be a major source of neutrons when they are intersected by the primary photon beam while neutrons are negligible in the patient due to the low (γ,n) cross section of the low atomic number of tissue. Neutron production in the accelerator head (thresholds are around 13 MeV for Al and Fe, 10 MeV for Cu and 6.5 MeV for W and Pb) results in isotropic neutron emissions, exposing the patient, workers and barriers to them.

Secondary neutron spectra measured in air in the patient plane are shown in figure 2.14 [44]. It includes a fast neutron peak centered between 0.1 and 1 MeV, a maximum energy of approximately 10 MeV, and a low energy tail that arises from neutrons being elastically scattered throughout the treatment room. As can be seen in the figure 2.14, the shape of the spectra is independent of the accelerating voltage, but the number of neutrons produced increases with the photon beam energy, and it is slightly dependent on the accelerator manufacturer [45] because some introduce additional borated hydrogenous shielding outside the photon shielding in LINAC head [46].

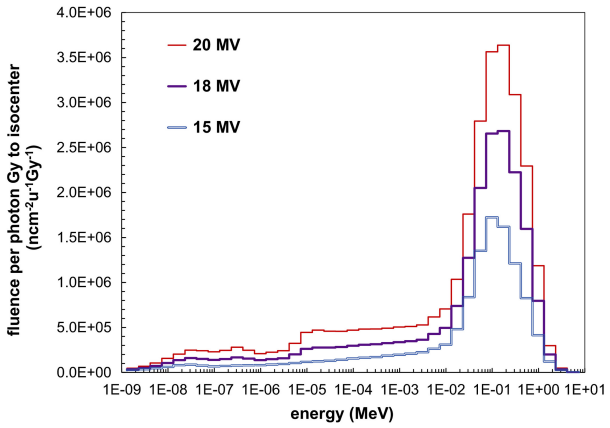

Figure 2.14: *Neutron fluence spectrum per unit lethargy per photon Gy to isocenter, measured in the patient plane at 40 cm from isocenter for three different x-ray beam energies from a Varian LINAC [44].*

Furthermore, neutrons can activate other elements inside the room, which remain radioactive and will con-

tribute to the radiation exposure of patient and workers entering into the room after treatment (exposure to leakage neutrons during treatments leads to a contribution to the effective dose of 7% for workers [47]), due to gamma and beta radiation emitted from decay of activation products. The radionuclides from activated components of a LINAC are generally short lived (from seconds to a few minutes), for example ^{15}O (half-life of 2 minutes) and ^{13}N (half-life 10 minutes) [46]. Because of that, air has to be removed efficiently, about 6–8 air exchanges per hour.

The use of a maze is almost mandatory in radiotherapy rooms. It increases the multiple scattering of neutrons and decreases the level of shielding at the door entrance. Also, the neutron field in the maze is function of the gantry angle and location of the target rotational plane.

Regarding the materials to be used in the barriers, since heavy metals (as lead) do not attenuate neutrons, an hydrogenous material (as concrete, heavy concrete or polyethylene) should be used since they can absorb most of the photoneutrons and neutron capture gamma rays originated in the room [9]. In general, the neutron fluence at any point in the room is composed of scattered and fast neutrons from the walls (the spectrum will be constant throughout the room); a thermal component which is also constant throughout the room; and a fast and possibly a thermal contribution, coming directly from the accelerator head, which will follow the inverse square law [46]. The thermal and scattered contributions are lower in energy than the direct component and contribute less per neutron to the absorbed dose.

Existing barriers of radiotherapy bunkers, that are optimised for shielding the radiation under determined set of parameters and RT techniques delivered, may be not efficient enough when changes in accelerator configuration are performed, when new external RT techniques are adopted or when the utilization rate changes.
In general, the dimensions of barriers will depend, among others, on:

- treatment modality (3D-CRT, IMRT, TBI, etc), workload and treatment energy,
- type of radiation to be shielded,
- the materials used to construct the barriers,
- the space available, including the height,
- the budget,
- the design project (the use of adjacent rooms), entrance design (direct entry with and without door or maze), structural obstructions as columns or utility suppliers (water, gas, electricity, communication, etc.),
- location of the accelerator.

Chapter 3

Structural shielding design for a megavoltage x-ray radiotherapy unit

The purpose of radiation shielding is to limit radiation exposure to members of the public and employees to an acceptable level. The NCRP-151 report presents recommendations and technical information related to the design and installation of structural shielding for megavoltage x- and gamma-ray radiotherapy facilities. This chapter describes the methodology adopted from the NCRP-151 for the calculation of primary, secondary barriers and door for both x-rays and neutrons, including also the TADR (time averaged dose equivalent rate) and IDR (instantaneous dose-equivalent rate) calculi. Finally, there is a section dedicated to describe the bunker characteristics and environment, which will remain constant along the study.

3.1 NCRP-151 Methodology

3.1.1 Primary and secondary barriers

The NCRP-151 methodology is based on the calculation of the transmission factor (*B*) through the barriers (primary and secondary) that will be used to assign the number of TVLs (tenth-value layer) or "*n*" of material needed, according to equation 3.1:

$$n = log_{10}\left(\frac{1}{\mathrm{B}}\right) \tag{3.1}$$

The transmission factor for primary barriers (wall, roof, floor or other structures designed to attenuate the primary beam), B_{pri}, is calculated as shown in equation 3.2:

$$B_{pri} = \frac{\mathrm{P\ d_{pri}^2}}{\mathrm{W_{pri}\ U\ T}} \tag{3.2}$$

where:

P, shielding design goal, expressed as dose equivalent per week (mSv/week);

d_{pri}, distance from the isocenter to the point protected (m) plus distance from x-ray target to isocenter, 1 m;

W_{pri}, workload or photon absorbed dose per week at the isocenter, 1 m from the x-ray target (Gy/week);

U, use factor;

T, occupancy factor.

The transmission factor for secondary barriers (wall, ceiling, floor or other structure designed to attenuate the leakage and scattered radiations) is computed separately considering two of the most important secondary radiation sources beyond the accelerator room: the scattered radiation from the patient and the leakage radiation. The barrier transmission factor for radiation scattered by patient, B_{ps}, and for leakage radiation, B_L, can be computed by equations 3.3 and 3.4:

$$B_{ps} = \frac{\mathrm{P}}{\mathrm{a}(\theta)\ \mathrm{W_{pri}}\ \mathrm{T}} d_{sca}^2 d_{sec}^2 \frac{400}{F} \tag{3.3}$$

where:

a(θ), fraction of the primary beam absorbed dose that scatters from the patient. Values are tabulated in the NCRP-151 document (Table B-4) as a function of the photon beam energy and the scattering angle;

d_{sca}, distance from the x-ray target to the patient (m), usually equals to 1 m;

d_{sec}, distance from the patient (origin of the scattered radiation) to the point protected (m);

F, field area at mid-depth of the patient at 1 m from x-ray target (cm^2);

400, refers the scatter fractions are normalized to those measured for a 20 x 20 cm^2 field size (cm^2);

P, W_{pri} and *T*, as previously defined.

$$B_L = \frac{\mathrm{P\ d_L^2}}{10^{-3}\ \mathrm{W_L\ T}} \tag{3.4}$$

where:

d_L, distance from the isocenter to the point protected (m);

10^{-3}, refers that leakage radiation is limited to 0.1% of the useful beam, by IEC [28];

W_L, leakage workload (Gy/week);

P and *T*, as previously defined.

Then, the thickness of the barriers (*t*) regarding primary, scattered and leakage radiation, t_{pri}, t_{ps}, t_L respectively, can be calculated using equation 3.5.

$$t = TVL_1 + (n-1)TVL_e \tag{3.5}$$

where:

TVL_1, first TVL (cm);

TVL_e, equilibrium TVL (cm).

The values of the TVLs depend on the primary beam energy, shielding material, type of radiation to shield (primary, patient scattered or leakage) and scattering angle (values in Appendix A, from NCRP-151 report [9]).

The thickness of a secondary barrier (t_s) is then calculated from the values of t_{ps} and t_L and applying the two-source rule. If both thicknesses are similar, the thickness of the barrier is determined by adding 1 HVL (half value layer) to the large of the two barrier thicknesses. If t_{ps} and t_L differ by a TVL or more, the larger barrier

thickness is used.

Finally, the thickness calculated with equation 3.5 should be evaluated in terms of time averaged dose equivalent rate (TADR) jointly with the instantaneous dose-equivalent rate (IDR).

The TADR is the barrier attenuated dose equivalent rate averaged over a specified time or period of operation, and it is proportional to IDR. According to NCRP-151 there are two periods of accelerator operation of particular interest to radiation protection: the week and the hour.

The weekly time averaged dose equivalent rate, R_w, is the TADR at a specified location averaged over a 40 h work-week and it is expressed in Sv/week. It is used to determine compliance with the shielding design goals. For primary barriers it is given by equation 3.6:

$$R_{w,pri} = \frac{IDR\, W_{pri} U_{pri}}{\dot{D}_0} \tag{3.6}$$

where:

IDR, the instantaneous dose equivalent rate (Sv/h) measured when accelerator is working at the absorbed-dose output rate $\dot{\mathrm{D}}_0$ (Gy/h) at 1 m from the source and measured at 30 cm beyond the barrier.

Similarly, for secondary barriers, the R_w has contributions from both, leakage and scattered radiation, as shown in equations 3.7 and 3.8 :

$$R_{w,s} = \left(IDR_L \, \frac{W_L}{\dot{D}_0}\right) \, + \, \left(IDR_{ps} \, \frac{W_{ps}\, U_{ps}}{\dot{D}_0}\right) \tag{3.7}$$

$$IDR_{ps} = IDR_{total} \, - \, IDR_L \tag{3.8}$$

where:

IDR_L, instantaneous dose equivalent rate measured at the secondary barrier (a point located 30 cm beyond this barrier) and in the absence of a phantom at the isocenter (Sv/h);

IDR_{total}, instantaneous dose equivalent rate measured at the same point in the presence of a phantom at the isocenter (Sv/h);

IDR_{ps}, instantaneous dose equivalent rate at the same point due to the patient scattered radiation (Sv/h).

Some regulatory bodies specify a limit for the time averaged dose equivalent rate based on the integrated dose equivalent in-any-one-hour (R_h) in uncontrolled areas, which is an extra safety condition that has been followed in this work, under the condition that this value cannot exceed 0.02 mSv in-any-one-hour [48]. R_h, in mSv, depends on the maximum number of treatments, N_{max}, that can be performed in any-one-hour as shown in equation 3.9:

$$R_h = \left(\frac{M}{40}\right) R_w, \qquad M = \left(\frac{N_{max}}{\bar{N}_h}\right) \tag{3.9}$$

where:

$\bar{N}_h$, average number of treatments per hour;

40, number of working hours per week;

M is always ≥ 1;

N_{max}, maximum number of treatments, includes the set-up time.

Width of primary barriers, *w* in cm, will depend on the distance from the x-ray target to the outside of the barrier (*d*) and can be calculated by equation 3.10, where it is considered the size of the diagonal of the largest beam (usually 35x35 cm^2 since the corners are clipped, at 100 cm SSD) plus 30 cm to each side [9].

$$w = 2 \cdot 30 \cdot \left(\sqrt{35^2 + 35^2} \cdot \frac{d}{d_{sca}} \right) \tag{3.10}$$

3.1.2 Maze and door

Maze wall is considered as a secondary barrier, and its thickness will determine to some extent the composition and thickness of the door.

Mainly because the neutron generation when using beam energies higher than 10 MV, the door composition and thickness is calculated considering two different scenarios: low-energy accelerator (less than 10 MV) and high-energy accelerator (higher than 10 MV). The goal is to reduce the total dose equivalent at the maze door from the mix of the different type of radiations involved: leakage and patient scattered radiation, neutron capture gamma rays and fast photoneutrons produced.

Low-energy accelerator

The total dose equivalent, H_{tot}, at the maze door from photon leakage and patient scattered radiation is estimated as shown in equation 3.11, considering the use factor of primary barriers as 0.25 and assuming both: the height-to-width ratio of the maze is between 1 and 2; and $2 < d_{zz}/\sqrt{(maze\ width\ \cdot\ height)} < 6$.

$$H_{tot} = 2.64\ H_C \tag{3.11}$$

If the primary beam is directed towards primary barrier C (see figure 3.1), the total dose equivalent from this barrier, H_C, (equation 3.12), in Sv/week, at the maze door is calculated by summing the dose equivalent components, as:

$$H_C = f\ H_s + H_{LS} + H_{ps} + H_{LT} \tag{3.12}$$

where:

H_s, dose equivalent per week due to scatter of the primary beam from the room surfaces (Sv/week);

H_{LS}, dose equivalent per week due to leakage photons from the head of accelerator scattered by the room surfaces (Sv/week);

H_{ps}, dose equivalent per week due to primary beam scattered from the patient (Sv/week);

H_{LT}, dose equivalent per week due to leakage radiation which is transmitted through the inner maze wall to the treatment door (Sv/week);

f, fraction of the primary beam transmitted through the patient, according the NCRP-151 has a value of 0.25 or 0.34, depending on the beam energy.

The dose equivalent due to scatter of primary beam from the room surfaces, H_s, is calculated with equation 3.13:

$$H_s = \frac{W_{pri}\ U_C\ \alpha_0\ A_0\ \alpha_z\ A_z}{(d_h\ d_r\ d_z)^2} \tag{3.13}$$

where:

U_C, use factor for wall C;

α_0, reflection coefficient scattering from surface A_0 (Tables B.8 from NCRP-151);

A_0, beam area at the first scattering surface (m^2);

α_z, reflection coefficient scattering from surface A_z (Tables B.8 from NCRP-151);

A_z, cross-sectional area (A_0 projected into the maze inner entry) (m^2);

d_h, perpendicular distance from the target to the first reflection surface, d_h=d_{pp}+*1*, (m);

d_r, distance from beam center at the first reflection to midline of maze, passing the edge of maze wall (m);

d_z, centerline distance along the maze (ending d_r) to the door (m).

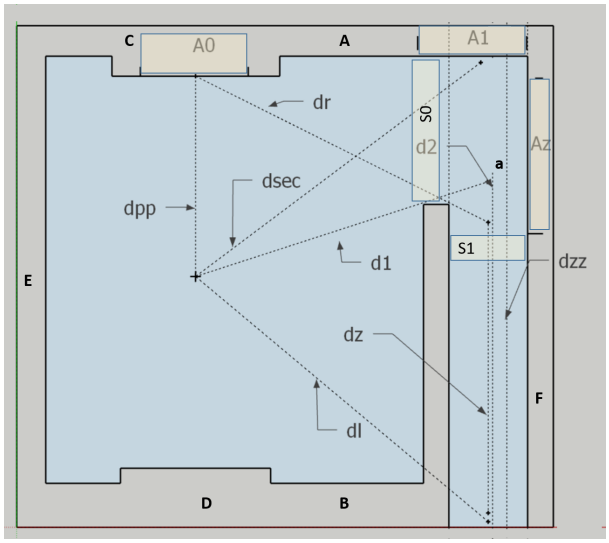

Figure 3.1: *Room layout for definition of parameters used to calculate door shielding (top view), adapted from [9].*

The dose equivalent due to leakage photons from the head of accelerator scattered by the room surfaces (H_{LS}) is calculated with equation 3.14:

$$H_{LS} = \frac{10^{-3}\ W_L\ U\ \alpha_1\ A_1}{(d_{sec}\ d_{zz})^2} \tag{3.14}$$

where:

10^{-3}, refers that head leakage radiation rate is limited to 0.1% of the useful beam, by IEC [28];

W_L, leakage workload (Gy/week);

α_1, reflection coefficient scattering from wall A of leakage radiation (Tables B.8 from NCRP-151);

A_1, area of wall C seen from the maze door (m^2);

d_{sec}, distance from isocenter to maze midline at wall A (m);

d_{zz}, centerline distance along the maze, (m).

The dose equivalent due to primary beam scattered from the patient, H_{ps}, is calculated with equation 3.15:

$$H_{ps} = \frac{a(\theta)\ W_{pri}\ U_C\ \alpha_1\ A_1}{(d_{sca}\ d_{sec}\ d_{zz})^2} \frac{F}{400} \tag{3.15}$$

where:

a(θ), scatter fraction for patient scattered radiation (Table B.4 from NCRP-151);

F, field area at mid-depth of the patient at 1 m from x-ray target (cm^2);

d_{sca}, distance from target to isocenter (m).

The dose equivalent due to leakage radiation transmitted through maze wall, H_{LT}, is calculated with equation 3.16:

$$H_{LT} = \frac{10^{-3}\ W_L\ U\ B}{d_l^2} \tag{3.16}$$

where:

B, transmission factor for maze barrier along the oblique path traced by d_l;

d_l, distance from target to the center of the maze door through the inner maze (m).

High-energy accelerator

The door shielding when using high-energy beams should mainly block neutron capture gamma rays and photoneutrons. The length of the maze affects this radiation distribution: if it is higher than 2.5 m, the photon field is dominated by neutron capture gamma rays, which can have up to 10 MeV energy for very short mazes [9]. The average energy of neutron capture gamma rays from concrete is 3.6 MeV.

The weekly dose equivalent (in Sv/week) at the door is then the sum of the contribution of neutron capture gamma rays, H_{cg}, and the contribution of photoneutrons H_n. H_{cg} is calculated with equation 3.17:

$$H_{cg} = W_L h_\varphi \tag{3.17}$$

where:

h_φ, dose equivalent from neutron capture gamma rays outside the door per unit of absorbed dose of x-rays at the isocenter (Sv/week), calculated with equation 3.18:

$$h_\varphi = K\ \varphi_A\ 10^{-d_2/TVD} \tag{3.18}$$

where:

K, value based on measurements: $6.9{\cdot}10^{-16}$ Sv m^2 [9];

φ_A, total neutron fluence ($1/m^2$) per absorbed dose of x-rays at the isocenter, at point *a* in figure 3.1;

d_2, distance from point *a* to the door (m);

TVD, tenth-value distance or distance required for the photon fluence decrease a 10-fold factor: $\sim$5.4 m for x-rays beam of 18 - 25 MV and $\sim$3.9 m for x-rays beam of 15 MV.

The total neutron fluence, φ_A is calculated with equation 3.19:

$$\varphi_A = \frac{\beta\ Q_n}{4\ \pi\ d_1^2} + \frac{5.4\ \beta\ Q_n}{2\ \pi\ S_r} + \frac{1.3\ Q_n}{2\ \pi\ S_r} \tag{3.19}$$

where:

β, transmission factor for neutrons that penetrate the head shielding (1 for Pb and 0.85 for W)[9];

d_1, distance from isocenter to point *a* in figure 3.1 (m);

Q_n, neutron source strength in neutrons emitted from the head of accelerator per gray of x-ray absorbed at isocenter, indicated in Table B.9 of NCRP-151;

S_r, total surface area of bunker (m^2).

The weekly dose equivalent at the door due to neutrons, H_n, is calculated with equation 3.20:

$$H_n = W_L H_{n,D} \tag{3.20}$$

where:

$H_{n,D}$, dose equivalent from neutrons at the maze entrance in Sievert per unit absorbed dose of x-rays at the isocenter (Sv m^2/n).

There are two methods to calculate $H_{n,D}$, the Kersey's method and the Wu and McGinley method, which results in a more realistic approach.

The Kersey's method calculates $H_{n,D}$ as (equation 3.21):

$$H_{n,D} = H_0\ \frac{S_0}{S_1}\ \left(\frac{d_0}{d_1}\right)^2\ 10^{-d_2/5} \tag{3.21}$$

where:

H_0, total neutron dose equivalent at a distance d_0 (1.41 m) from the target per gray (Table B.9 in NCRP-151) (mSv/Gy);

S_0, inner maze entrance cross-sectional area (m^2);

S_1, maze cross-sectional area (m^2);

d_1, distance from isocenter to the point *a* (figure 3.1) (m);

d_2, distance from point *a* to the entrance door (m).

The Wu and McGinley method calculates $H_{n,D}$ (Sv m^2/n) as (equation 3.22):

$$H_{n,D} = 2.4 \cdot 10^{-15}\ \varphi_A\ \sqrt{\frac{S_0}{S_1}}\ \left[1.64 \cdot 10^{-d_2/1.9} + 10^{-d_2/TVD}\right] \tag{3.22}$$

where:

TVD, as defined in equation 3.18 and in this case it is calculated as: $TVD = 2.06\ \sqrt{S_1}$,

Finally, the total weekly dose equivalent at the door H_w will be the sum of all the components from the leakage

and scattered radiations (H_{tot}, eq. 3.11), the neutron capture gamma rays (H_{cg}, eq. 3.17) and the neutrons (H_n, eq. 3.20):

$$H_w = H_{tot} + H_{cg} + H_n \tag{3.23}$$

The number of TVLs (*n*) of lead or borated polyethylene (BPE) is computed using equation 3.1, and the transmission factors (*B*) for each contribution can be calculated by dividing the desired goal protection outside the door (usually one half of P) by the value obtained for each component of H_w. For accelerator with energy below 10 MeV, the radiation field transmitted through the door can be considered as photons with energies of 0.2 MeV [9], and lead will be a good material to attenuate them.

Many doors with maze length on the order of 8 m or higher have lead and BPE or paraffin, being the typical arrangement as: lead, BPE/paraffin, lead. Typical thickness are about 0.6 - 1.2 mm for lead and 2 - 4 cm of BPE. In this configuration, the lead from the inside of the room will reduce the energy of the neutrons by nonelastic scattering, making more effective the BPE to stop the neutrons and the lead from the outside will attenuate the neutron capture gamma rays from the BPE (with energy of 478 keV). The main goal should be to simplify the door in order to obtain a light and inexpensive one. Typical TVL values for neutrons can be found in table A.5 from Appendix A.

The three common parameters in equations 3.2, 3.3, 3.4: P, W and T will be discussed in detail in the following subsections.

3.1.3 Shielding design goal, P

The shielding design goal (P) refers to the dose equivalent (*H*), expressed in mSv/week, and it is one of the variables needed to calculate the thickness of barriers. It may have different values, according to the area to be shielded (controlled and uncontrolled) and the regulation to be followed as shown in table 3.1:

Table 3.1: *Shielding design goal values for controlled and non-controlled areas.*

Area	NCRP-151	DL 180/2002
Controlled	5 mSv/year (0.1 mSv/week)	20 mSv/year (0.4 mSv/week)
Non-controlled	1 mSv/year (0.02 mSv/week)	1 mSv/year (0.02 mSv/week)

A controlled area is a limited-access area where only those individuals who are specifically trained can stay (besides the patient). These areas are under the supervision of the person in charge of radiation protection. Treatment rooms and control consoles are good examples of this type of area.

As can be observed in table 3.1, the shielding design goals considered by the NCRP-151 for workers (in controlled areas) is lower than the value considered in the Portuguese law [10], which is based on the limit of the effective dose in a consecutive five-years period (100 mSv). This difference is due to the conservative recommendations contained in the NCRP report. For non-controlled areas (those which are not controlled) the P values are the same for both documents, a limit of 1mSv per year is considered.

In fact, the quantity that is limited by law is the effective dose (E), but this quantity is not a physical neither a measurable quantity. According with the ICRP-103 [41], it should be used for planning and optimisation in

radiological protection. On the other hand, equivalent dose (H) is the product of the weighting factor of type and quality of radiation (w_R) and the absorbed dose (D), w_R=1 for gamma and x-rays.

$$H = \Sigma w_R D \tag{3.24}$$

3.1.4 Workload, W

The workload is the absorbed dose from photons delivered by the LINAC at the isocenter integrated over a period of one week. To calculate the workload for conventional treatments, equation 3.25 can be used, based on a 5 working days in a week:

$$W_{conv} = 5\ N\ D \tag{3.25}$$

where:

N, number of treatments per day (8 hours);

D, absorbed dose per treatment (Gy/treatment).

For TBI, where the patient is not located at the isocenter but at a distance d_{TBI} the workload at isocenter can be calculated considering the TBI absorbed dose to the patient, D_{TBI}, as (equation 3.26):

$$W_{TBI}(1m) = D_{TBI}\ d_{TBI}^2 \tag{3.26}$$

When multiple techniques are performed in the same room, or different radiation beam energies are used, the workload should consider all the individual contributions. In this value, it should be also included the dose delivered during quality controls (QC) or calibrations performed in the room.

As it will be discussed in the next subsections, the workload can be spread into primary (when the beam is directed towards primary barriers), patient scattered and leakage workload.

3.1.5 Occupancy factor, T

The occupancy factor is used to calculate the thickness of a barrier and it refers to the amount of time a single person spends in the area beyond that barrier, when accelerator is working. The values are also regulated by national laws, but in this work those recommended by the NCRP-151 have been considered. They can be found in the Appendix B, Table B.1 of the document [9]. For control area and door, the occupancy factor is recommended to be unity (the maximum value).

The values are refereed to a 40 working hours per week. For example, an uncontrolled area having an assigned occupancy factor of 20/40 (0.5) implies that an individual would spend an average of 20 h per week in that area every workweek for a year.

3.2 NCRP-151 Implementation

Due to the numerous variables considered in this work (x-ray energy beam, type of RT techniques, number of treatments and materials), it was developed a dedicated Excel document able to calculate the thicknesses of the

barriers, assuming the NCRP-151 methodology. The Excel works as shown in the flowchart (see figure 3.2).

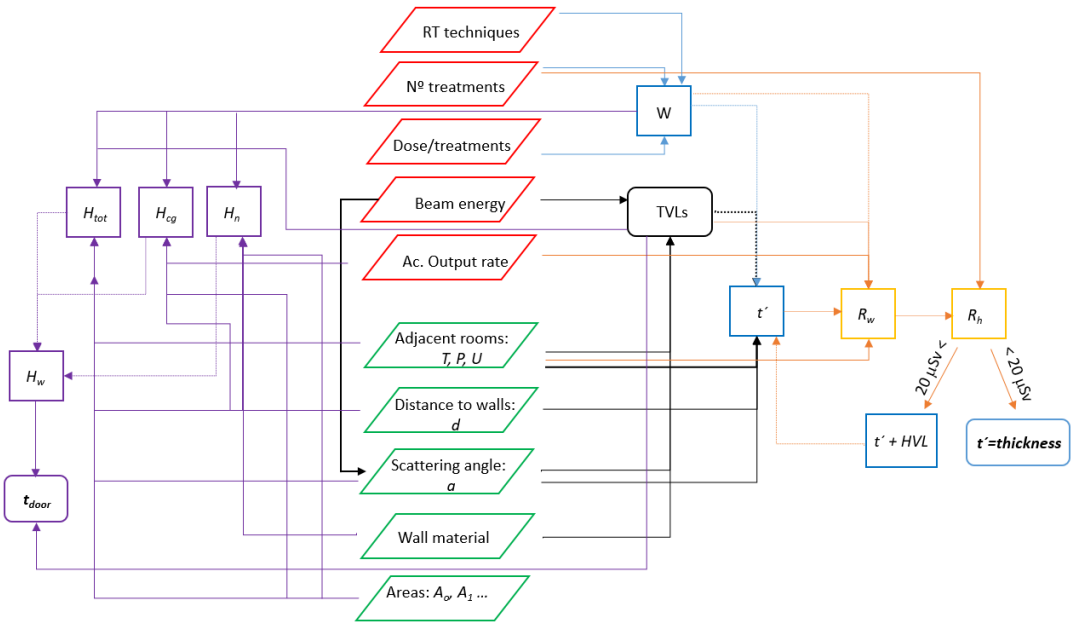

Figure 3.2: *Flowchart of Excel document to calculate the barrier thicknesses. Red, green parallelograms are input data.*

The design of the radiotherapy bunker will depend on the RT treatment delivery due to the intrinsic characteristics of each one, and briefly described in the next subsections.

3D conformal radiotherapy technique (3DCRT)

In this technique the patient is situated at the isocenter of the LINAC and workload for calculating the primary and secondary barriers has the same value, calculated as described in section 3.1.4, as in conventional treatment. In general, all equations described in section 3.1 can be applied without any modification.

There are 3 primary barriers (besides the floor) and the width can be computed by using equation 3.10.

Intensity-modulated radiotherapy (IMRT)

The dose received by the patient remains the same than in the 3D-CRT technique (or a conventional treatment), but due to the configuration of MLCs (which generate fluences maps using small segments of the beam outside central beam axis) the monitor units delivered per field are higher than the nominal value (1 MU/cGy). The ratio of the average monitor unit per unit of prescribed absorbed dose needed for IMRT (MU_{IMRT}) and the monitor unit per unit of absorbed dose for conventional treatment (MU_{conv}) is called the IMRT factor, C_{IMRT}, which is between 2 and 5, depending on the configuration of the MLCs to deliver dose.

The workload for the primary barriers will remain the same than in conventional treatment, and also for the patient components of the secondary barriers. On the other hand, leakage workload will increase by the IMRT factor, and thus will affect the thickness of the secondary barriers (see table 3.2).

There are also 3 primary barriers (besides the floor) and the width can be computed by using equation 3.10.

Total body irradiation (TBI)

In TBI procedures the patient is usually located away from the isocenter (d_{TBI}, about 4 m or more) and the beam is fixed during treatment towards one single barrier (primary), increasing thus its use factor and the workload for this primary barrier (W_{TBI}). As in IMRT, the workload for leakage radiation is also higher, in this case by a C_{TBI} factor between 10 and 15 [49].

In some room arrangements, the source of scattered radiation (the TBI patient and wall behind patient) will be much closer to the room entrance than to the isocenter, and the consequent dose equivalent rate at the entrance could be higher than that for conventional treatments.

Stereotactic radiation therapy (SRT)

For this procedure a conventional LINAC using 6 MV x-rays will be used. Use factors remains the same than in 3D-CRT technique, while the mean absorbed dose per treatment is higher than the used in 3D-CRT. SRT delivers also high monitor units, presenting thus high values of leakage radiation by a C_{SRT} factor of about 15 [36] and because of that all primary barrier calculations must also account for leakage contributions.

There are special accelerators configured to delivery this technique as described in section 2.3.5. The Cyberknife produces a small size primary beam (typically 1.5 cm in diameter) and can point to almost all points of the room (except ceiling), and because of that all barriers are considered as primary, with a recommended use factor of 0.05 [36]. Another characteristic of Cyberknife is the distance from the x-ray target to the treatment volume, which is about 0.8 m, thus the primary workload (W_{SRT}) will decrease.

Table 3.2 summarizes the workloads, distances and use factors of barriers when different RT treatments are delivered. Workload has been split into primary (W_{pri}), leakage (W_L) and patient scattered (W_{ps}) [50]. The primary workload is the sum of radiation contributions from treatments techniques towards a primary barrier (equation 3.27) and the leakage workload is the sum of radiation contributions towards any barrier (equation 3.28). Workload due to radiation scattered by patient coincides with the primary workload.

Table 3.2: *Workload, distances and use factors according to treatment technique.*

Treatment technique	$\mathbf{W}_{pri}$	$\mathbf{W}_L$	$\mathbf{W}_{ps}$	$\mathbf{d}_{sca}$	$\mathbf{U}_{pri}$	$\mathbf{U}_L$
3D-CRT	W_{conv}	W_{conv}	W_{conv}	1 m	0.25	1
IMRT	W_{IMRT}=W_{conv}	C_{IMRT} W_{IMRT}	W_{IMRT}	1 m	0.25	1
TBI	W_{TBI}= 5 N D_{TBI} $d_{TBI}{}^2$	C_{TBI} W_{TBI}	W_{TBI}	$d_{TBI} \geq$ 4m	1	1
SRT	W_{SRT}= 5 N D_{SRT} $d_{sca}{}^2$	C_{SRT} W_{SRT}	W_{SRT}	1 m	0.25	1
QC	W_{QC}	W_{QC}	W_{QC}	1 m	0.25	1

$$W_{pri} = W_{3DCRT} + W_{IMRT} + W_{TBI} + W_{SRT} + W_{QC} \tag{3.27}$$

$$W_L = W_{3DCRT} + C_{IMRT} \cdot W_{IMRT} + C_{TBI} \cdot W_{TBI} + C_{SRT} \cdot W_{SRT} + W_{QC} \tag{3.28}$$

The thickness of all barriers were checked in terms of dose equivalent rate in any hour (R_h). Although the limit of 20 μSv/week is only applied to uncontrolled areas [48], it also has been followed for controlled areas, to ensure the ALARA principle and to avoid possible compliance challenges.

3.3 Accelerator bunker design

3.3.1 Dimensions

According to IAEA [51] the minimum recommended inside dimensions for a radiotherapy bunker are 7 m x 7 m. Nevertheless, these dimensions should be reconsidered according to specifications of accelerator and its dimensions, and also to treatment therapies performed, as TBI.

The final dimensions should provide space for the accelerator unit (including the couch extension, gantry stand, gantry movements, accessories, etc.), imaging system, auxiliary systems (electrical equipment, air conditioning, exhaust and ventilation systems), quick and comfortable access (for patients and workers), storage room (cabinets, worktable, wash hand basin...), etc.

Since one of the objectives of this work is to compare the thickness of barriers for proper shielding, it was decided to fix the external dimensions of the room. In this way, the distances from target to the point to protect are going to remain constant (not those related with the door calculations) and the barriers will be planned towards the interior of the pre-defined space. Thus, the final clear area will be different for each case study. Since ideally, there is no space limitation, a 15 m x 14 m space was considered as starting point. The height is approximately 3 meters, and a dropped ceiling at 2.75 m was supposed in order to reduce the cross-section of neutrons and to accommodate the necessary auxiliary systems. The isocenter of accelerator is located at 5 m from the external E wall, 7 m from external D (or C) wall (see figure 3.3) and 1.3 m from floor.

In figures 3.3 and 3.4 are shown the room layouts where primary (C, D and G), secondary barriers (A, B, E, F, H) and maze barrier are identified. Also, the movement and extension of the couch are indicated in figure 3.3.

Since the work considers the use of 15 MV energy beam, the maze is almost mandatory to reduce the dose equivalent at the door. For this reason, a maze (9 m long and width of 2.2 m) was considered, following the recommendations from IAEA [51], and ensuring an adequate stretchers circulation, and also complying with height-to-width ratio between 1 and 2 and $2< d_{zz}/\sqrt{(maze\ width\ \cdot\ height)} <6$.

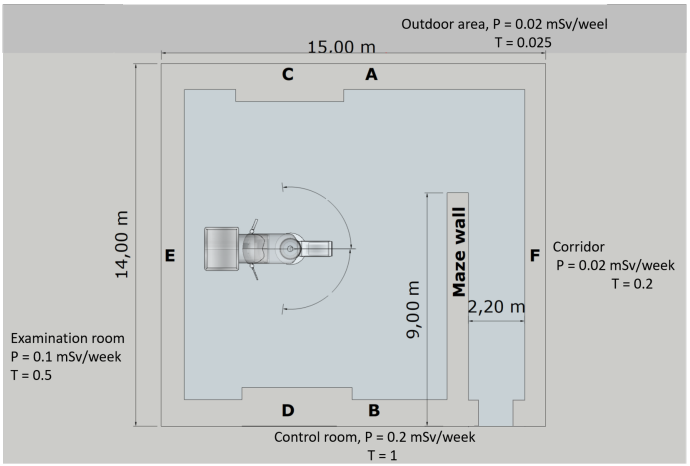

Figure 3.3: *Room layout and labels used for primary (C, D), secondary barriers (A, B, E, F) and maze wall (top view).*

Width of primary barriers C and D were calculated according the equation 3.10 and following the recommendations of the NCRP-151 report, the higher width is maintained over the primary-barrier region (barriers C, D and G), allowing simply arrangement during construction.

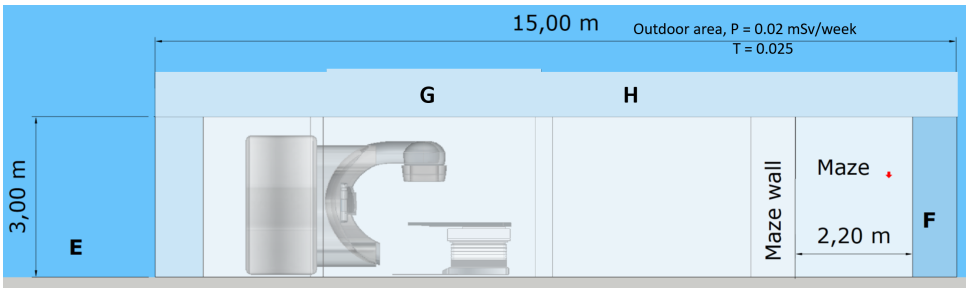

Figure 3.4: *Room layout and labels used for primary (G), secondary barriers (E, F, H) and maze wall (front view).*

Distances from target to the point to be protected used to calculate the thicknesses of barriers are summarized in table 3.3. They include the 0.3 m distance from the wall to the point to be protected, as recommended in the NCRP document [9]. Distance for barrier G (roof) changes according to the scenario in order to maintain the height (3 m) constant in and it is calculated by an iterative approach [52].

3.3.2 Adjacent rooms

The accelerator has been oriented in such a way the gantry rotation axis is perpendicular to the maze wall. It was assumed that primary beam rotates around the isocenter with a symmetric distribution of gantry treatment angles (0, 90, 180 and 270) except for TBI where the beam will be directed towards wall C.

The adjacent spaces beyond the barriers were considered as:

- Barriers C and A. An outdoor area for vehicular drop off (unattended), corresponding to an occupancy factor of 0.025. It is an uncontrolled area.
- Barriers D, B and door correspond to the control room (controlled area), with an occupancy factor of 1.
- Barrier E. The space beyond this barrier is a controlled area used for patient examination, with an occupancy factor of 1/2 (0.5).
- Barrier F is an uncontrolled corridor, with an occupancy factor of 1/5 (0.2).
- Barriers G and H correspond to the roof, an open space with no adjacent buildings. The HVAC machineries will be located there. An occupancy factor of 1/40 (0.025) was assumed.

Values are summarized in table 3.3, where scattering angle for calculating the scatter fraction ($a(\theta)$ in equation 3.3) has been added.

3.3.3 Door

Depending on the dose equivalent value at the door and also on the origin of this dose equivalent (photons or neutrons) the use of a door can be an option. In all cases, the use of a maze will reduce the dose-equivalent value reducing also the complexity of the door. Besides the composition, weight, assembly, opening time, safety mechanisms, maintenance or space are other important factors to take into account. A swing door will be considered with dimensions of 1.65 m x 2.15 m height, overlapping the wall at all sides 15 cm. Most of the shielded doors use layers of lead and borated (5%) polyethylene (BPE), which composition is calculated for each

Table 3.3: *Barriers parameters.*

Barrier	Type	P, mSv/week	T	U	scat. angle	Distance, m
C	N.C.	0.02	0.025	0.25/ 1*	-	7.3
D	C.	0.1	1	0.25	-	7.3
G	N.C.	0.02	0.025	0.25	-	4.0**
A	N.C.	0.02	0.025	1	21	7.9
B	C.	0.1	1	1	25	7.9
E	C.	0.1	0.5	1	90	5.3
F	N.C.	0.02	0.2	1	90	10.3
H	N.C.	0.02	0.025	1	$\sim$46	$\sim$4.5
Maze barrier	C.	0.1	1	1	-	-

* Beam toward the Barrier C during TBI treatments.

** Distance is calculated for each scenario to obtain a 3 m height room.

N.C. for not controlled area; C. for controlled area.

scenario, although the commercially available thicknesses will determine the final door composition, as listed in tables A.6 and A.7, where prices have been included.

3.3.4 Materials for barriers

All secondary barriers are made of ordinary concrete (density of 2.35 g/cm^3) while for primary barriers are made of ordinary or high density (HD) concrete (3.2 g/cm^3). TVLs and prices used for these materials are summarized in Appendix A (tables A.1, A.2 and A.3). Prices (90 €/m^3 for ordinary concrete and 600 €/m^3 for HD concrete) were obtained from different estimations and budgets [53–55].

3.3.5 Accelerator parameters

No particular manufacturer or accelerator has been used in this study. For this reason the accelerator data presented in table 3.4 are based on data from other units installed at the Radiotherapy Department at Santa Maria Hospital and also on those presented in Table B.9 from NCRP-151 [9], the maximum values have been chosen for each variable.

Table 3.4: *Linear accelerator parameters.*

Nominal photon energies, MV	6, 10, 15 and 18
Maximum absorbed-dose output rate at isocenter, $\dot{D}_0$, Gy/h	360
Absorbed dose at isocenter per treatment, Gy/tr.	2.5
Maximum field size at isocenter, cm^2	40 x 40
Treatment delivery techniques	3D-CRT, IMRT, VMAT, SRS, TBI
Leakage radiation/primary beam ratio	0.001
Neutron dose equivalent at 1.41 m from target per absorbed dose of x-rays at isocenter, H_0, mSv/Gy	1.3
Neutrons emitted from the accelerator head per absorbed dose of x-rays at isocenter, Q_n	$1.22 \cdot 10^{12}$

3.3.6 Treatment parameters

Treatments parameters are based on historical data of the Radiotherapy Department at Santa Maria Hospital and they are summarized in table 3.5.

Table 3.5: *Treatment parameters.*

Number of weeks (5 days) per year, week/y	50
Total number of treatments per week	250
Average number of patients per day per LINAC	50
Average number of patients per hour, $\bar{N}_h$	3.85
Maximum number of patients per hour	5
M (max. nº patients per hour/average patients per hour)	1.3
Mean absorbed dose per treatment in 3D-CRT, Gy	2.5
Mean absorbed dose per treatment in IMRT, Gy	2.5
IMRT factor, C_{IMRT}	3.3
Mean absorbed dose per treatment in SRS, Gy	12.5
SRS factor, C_{SRS}	15
Mean absorbed dose per treatment in TBI, Gy	12
TBI factor, C_{TBI}	15

3.4 The Portuguese regulation

Nowadays, in Portugal the Decree Law 222/2008 [12] which transposed the Council Directive 96/29/EURATOM of 13 May 1996 [56]), establishes the dose limits for exposed workers and public.

Article 9 establishes the dose limits for exposed workers:

"1. The limit on effective dose for exposed workers shall be 100 millisieverts (mSv) in a consecutive five-year period, subject to a maximum effective dose of 50 mSv in any single year."

"2. Without prejudice to paragraph 1:

a) the limit on equivalent dose for the lens of the eye shall be 150 mSv in a year;

b) the limit on equivalent dose for the skin shall be 500 mSv in a year. This limit shall apply to the dose averaged over any area of 1 cm^2, regardless of the area exposed;

c) the limit on equivalent dose for the hands, forearms, feet and ankles shall be 500 mSv in a year."

Article 13 establishes the dose limits for members of the public:

"1. Without prejudice to Article 14, the dose limits for members of the public shall be as laid down in paragraphs 2 and 3."

"2. The limit for effective dose shall be 1 mSv in a year. However, in special circumstances, a higher effective dose may be authorized in a single year, provided that the average over five consecutive years does not exceed 1 mSv per year."

"3. Without prejudice to paragraph 2:

a) the limit on equivalent dose for the lens of the eye shall be 15 mSv in a year;

b) the limit on equivalent dose for the skin shall be 50 mSv in a year averaged over any 1 cm² area of skin, regardless of the area exposed."

The recent Council Directive 2013/59/EURATOM of 5 December 2013 [13] in *Article 9* establishes:

"2. The limit on the effective dose for occupational exposure shall be 20 mSv in any single year. However, in special circumstances or for certain exposure situations specified in national legislation, a higher effective dose of up to 50 mSv may be authorised by the competent authority in a single year, provided that the average annual dose over any five consecutive years, including the years for which the limit has been exceeded, does not exceed 20 mSv."

Also the new Directive recomends to follow the new ICRP guidance on the limit for equivalent dose for the lens of the eye in occupational exposure. The ICRP-118 [37] recommends for occupational exposure in planned exposure situations, an equivalent dose limit for the lens of the eye of 20 mSv/year, averaged over defined periods of 5 years, with no single year exceeding 50 mSv. Limits for the skin and extremities remains unchanged.

The dose limits for public exposure are set at 1mSy/year (effective dose), 15 mSv for the lens of the eye (equivalent dose) and 50 mSV for skin over any 1 cm^2 (equivalent dose).

The specific requirements for radiotherapy design in Portugal are described in the DL 180/2002 of 8 August 2002, Article 52 [10], which follows the DIN-6847 standard from 1977 [11].

Chapter 4

Results

In this chapter are given the barriers´dimensions of the bunker described in the previous chapter that will change according to the type of construction material and the technique to be used. In this sense, different scenarios have been considered: dedicated bunkers for each radiotherapy technique (3D-CRT, IMRT, SRS and TBI) and bunkers with different mixed techniques and beam energies.

4.1 Dedicated bunkers

Barrier thickness comply with the limit (0.02 mSv) for the time averaged dose equivalent rate in-any-one-hour (R_h) for uncontrolled areas that some regulatory bodies specify, as the NRC [48], and it has been extended to controlled areas. Additionally, the sum of dose equivalent values from patient scattered and leakage radiation, H_{sum}, should be below the P value for each area. Workload relative to quality controls and calibrations are included in the 3D-CRT treatments.

4.1.1 3D-CRT

This technique is among the most used in radiotherapy and three cases have been analyzed: 100% of treatments performed either at 6 MV or 15 MV, and 50% of treatments performed with both x-ray energies.

This is the simplest scenario that can be considered since in these three cases the workload values for primary, patient scatter and leakage radiation remain constant (625 Gy/week). The barrier thicknesses are dependent on the TVLs for 6 and 15 MV beam energies, distances, design goal and occupancy factors of each area to protect.

Regarding primary barriers made of ordinary concrete, as shown in figure 4.1 and table 4.1, in all cases barrier D (which correspond to the control room) is the thicker one, followed by the barrier G and C, also barriers are thicker as the energy of the x-rays increase.

This trend is not valid for HD concrete barriers, where small differences between barriers are observed. Barriers D and G have the same thickness (1.13 m) for high and low photon energies and lower for the case of two energies mix (1.05 and 1.06 m respectively). In general, barriers made of HD concrete are thinner than those made of ordinary concrete, presenting also higher H_{sum} values, very close to 20 μSv/week in some cases.

Concerning secondary barriers, made of ordinary concrete, the thicker barrier correspond to barrier B, followed

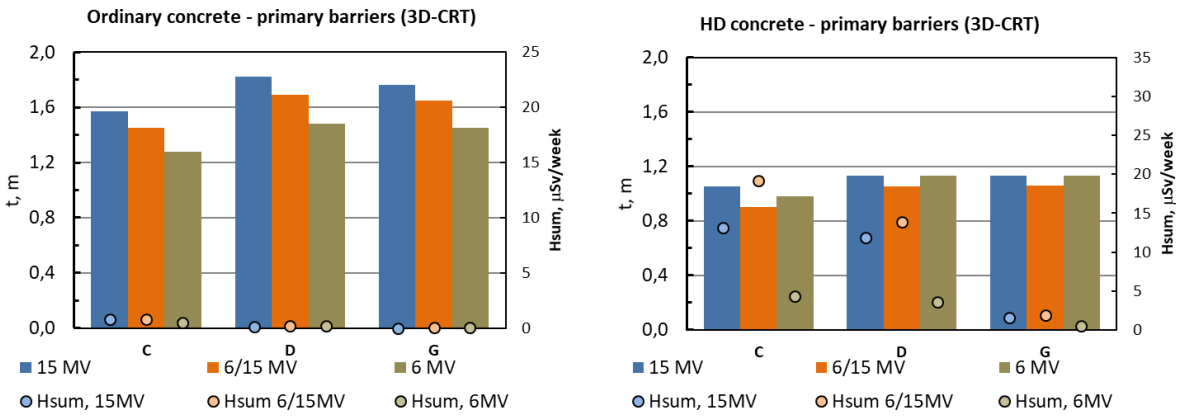

(a) (b)

Figure 4.1: *Thickness and dose equivalent, H_{sum}, values for primary barriers (3D-CRT). a) Ordinary concrete; b) High density concrete.*

Table 4.1: *Results obtained for a dedicated bunker to 3D-CRT (primary and secondary barriers). Thickness, (t) in m, R_h and H_{sum} in µSv/week.*

Nominal beam energy	Material construction		Primary barriers C	D	G	Secondary barriers A	B	E	H	F	M
15 MV	concrete	t	1.57	1.82	1.76	0.89	1.27	0.81	0.66	0.72	0.46
		R_h	13.0	3.2	13.0	13.8	1.7	3.1	10.0	1.0	-
		H_{sum}	0.8	0.1	0.01	10.6	51.7	47.2	11.3	9.5	-
	HD concrete	t	1.05	1.13	1.13						
		R_h	6.5	3.2	13.0						
		H_{sum}	13.1	11.9	1.6						
6/15 MV	concrete	t	1.45	1.69	1.65	0.89	1.15	0.71	0.67	0.62	0.47
		R_h	15.0	3.6	14.5	9.6	2.2	5.0	7.7	1.6	-
		H_{sum}	0.8	0.2	0.02	7.5	67.1	76.6	8.8	16.0	-
	HD concrete	t	0.90	1.05	1.06						
		R_h	19.7	4.7	18.9						
		H_{sum}	19.2	13.9	1.9						
6 MV	concrete	t	1.28	1.48	1.45	0.76	1.06	0.75	0.61	0.67	0.43
		R_h	13.0	3.2	13.0	14.2	1.7	2.9	10.1	0.9	-
		H_{sum}	0.5	0.2	0.03	10.9	53.2	45.1	11.2	9.1	-
	HD concrete	t	0.98	1.13	1.13						
		R_h	13.0	3.2	13.0						
		H_{sum}	4.3	3.6	0.5						

by barriers A, E, F and H, and they also present the highest values for 15 MV energy beam (figure 4.2). The highest values of H_{sum} are obtained for the mix of energies especially for barriers B and E, both controlled areas.

Regarding the door composition, table 4.2 presents the values obtained for the weekly total dose equivalent at the door, H_w, for the three cases jointly with the different contributions. Due to the presence of neutrons, BPE is needed for the 15MV and the 6/15 MV cases (5.08 cm) while lead is needed in all cases. Figure 4.3 shows the configuration and thickness of the materials, two sheets of lead of 0.79 mm each for 15 and 6/15 MV and a single layer of 1.98 mm thick of lead for the 6 MV case.

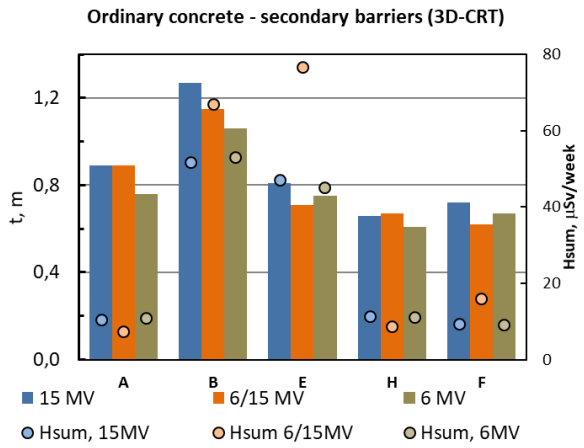

Figure 4.2: *Thickness and dose equivalent values, H_{sum}, for secondary barriers (3D-CRT).*

Table 4.2: *Total dose equivalent at the door, H_w in µSv/week, for a 3D-CRT dedicated bunker as a function of primary x-ray beam energy.*

	15 MV	6/15 MV	6 MV
H_{tot}	84.9	76.2	95.5
H_{cg}	4.6	2.3	-
H_n	501.4	250.7	-
H_w	590.9	329.2	95.5

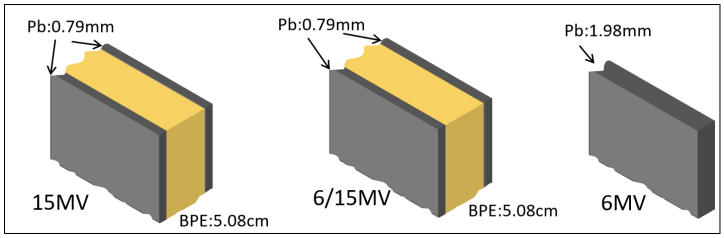

Figure 4.3: *Door thickness composition for a 3D-CRT dedicated bunker as a function of primary x-ray beam energy.*

4.1.2 IMRT

Again, three cases have been analysed: 100% of treatments performed either at 6 MV or 15 MV, and 50% performed with both x-ray energies. As in the previous case, the barrier thicknesses are dependent on the TVL values for 6 and 15 MV energy beams, distances, design goal and occupancy factors of each area to protect.

In terms of calculi, the IMRT technique introduces more leakage workload, increased by the C_{IMRT} factor, which in this case is 3.3. If only IMRT technique is used in the room, the workload values are: W_{pri}=625 and W_L=2062.5 Gy/week, independently of the beam energy.

Results are summarized in table 4.3 and shown in figure 4.4 where data from room dedicated to 3D-CRT (at 6 MV) are included for comparison. While thicknesses remains the same that in previous case for primary barriers, H_{sum} values increase for all barriers, mainly due to the leakage component. This is more evident for the HD concrete case, but it should be noted that due to lack of available data for this type of concrete (TVL for leakage radiation and patient scattered radiation, [9, 43, 57]), data used are those for ordinary concrete, that are higher than the real. Among the secondary barriers (figure 4.5), the thicker one corresponds again to barrier B.

Barriers A and B remains with the same thickness and the others have increased a TVL, except barrier H which has increased 6 cm for the 6/15 MV case, while R_h and H_{sum} present values slightly higher than in previous case.

Table 4.3: *Results obtained for a dedicated bunker to IMRT (primary and secondary barriers). Thickness, (t) in m, R_h and H_{sum} in µSv/week.*

Nominal beam energy	Material construction		Primary barriers C	D	G	Secondary barriers A	B	E	H	F	M
15 MV	concrete	t	1.57	1.82	1.76	0.89	1.27	0.98	0.83	0.89	0.58
		R_h	13.0	3.2	13.0	15.6	1.8	3.1	8.1	0.9	-
		H_{sum}	0.8	0.2	0.03	12.0	55.6	47.0	9.8	9.4	-
	HD concrete	t	1.05	1.13	1.13						
		R_h	6.5	3.2	13.0						
		H_{sum}	13.6	24.3	3.2						
6/15 MV	concrete	t	1.45	1.69	1.65	0.89	1.15	0.89	0.73	0.79	0.59
		R_h	15.0	3.6	14.5	11.0	2.4	4.6	13.1	1.5	-
		H_{sum}	0.9	0.3	0.04	8.5	73.7	71.2	15.8	14.7	-
	HD concrete	t	0.90	1.06	1.01						
		R_h	19.7	4.7	18.9						
		H_{sum}	20.4	29.2	4.0						
6 MV	concrete	t	1.28	1.48	1.45	0.76	1.06	0.90	0.76	0.82	0.53
		R_h	13.0	3.2	13.0	16.9	2.0	2.9	7.8	0.9	-
		H_{sum}	0.6	0.5	0.1	13.0	60.5	44.5	9.4	8.9	-
	HD concrete	t	0.98	1.13	1.13						
		R_h	13.0	3.2	13.0						
		H_{sum}	4.7	8.6	1.1						

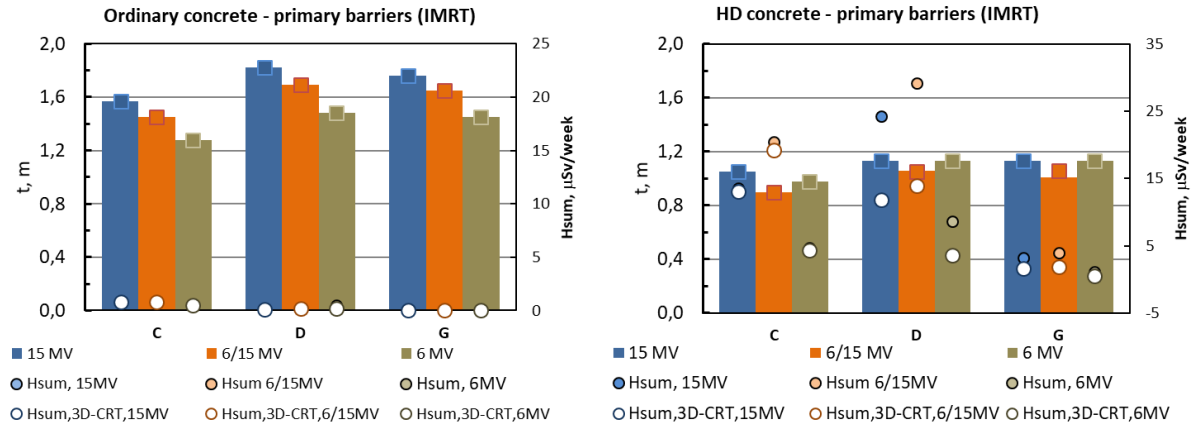

(a) (b)

Figure 4.4: *Thickness and dose equivalent values, H_{sum}, for primary barriers (IMRT). Data from 3D-CRT at 6 MV included (square: thickness; white circle: H_{sum}). a) Ordinary concrete; b) High density concrete.*

In table 4.4 are given the values obtained for the weekly total dose equivalent at the door (H_w) and the different contributions, for the three cases. As in previous scenario, BPE is needed for the 15MV and the 6/15 MV cases as well as lead but for IMRT the materials are thicker because the dose equivalent values are higher due to the leakage workload. Thicknesses are: a 7.62 cm of BPE between 2 layers of lead (0.79 mm) for 15 and 6/15 MV cases and a single lead layer of 1.98 mm thick for the 6 MV case.

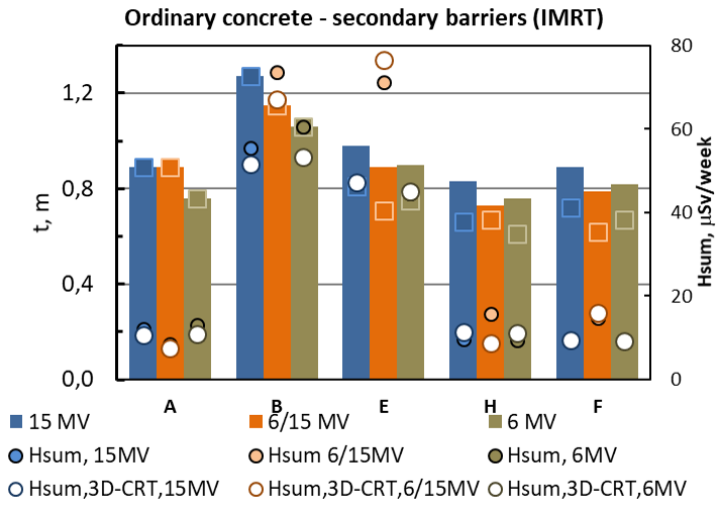

Figure 4.5: *Thickness and dose equivalent, H_{sum}, values for secondary barriers (IMRT).Data from 3D-CRT at 6 MV are included. (square: thickness; white circle: H_{sum}).*

Table 4.4: *Total dose equivalent at the door, H_w in µSv/week, for a IMRT dedicated bunker as a function of primary x-ray beam energy.*

	15 MV	6/15 MV	6 MV
H_{tot}	86.9	75.5	98.3
H_{cg}	15.7	7.7	-
H_n	1 654.5	827.3	-
H_w	1 757.1	910.4	98.3

4.1.3 SRS

This case is dedicated to a bunker used only for SRS technique using a conventional LINAC with x-ray beam of 6 MV. In this case, the number of treatments per week is lower than in 3D-CRT and IMRT cases, as shown in table 4.5, although M (needed to calculate R_h) is equal than in the previous cases. Due to the high SRS factor (C_{SRS}=15) the leakage workload will be much higher than the primary workload (W_{pri} = 60·12.5 = 750 Gy/week and W_L = 15· 750 = 1 1250 Gy/week). The other parameters as use factor, goal design and distances are those shown in table 3.3.

Table 4.5: *Treatment parameters for a bunker dedicated to SRT.*

Total number of treatments per week	60
Average number of treatments per day	12
Average number of treatments per hour, $\bar{N}_h$	1.5
Number of treatments per hour, max. recommended	2
M (max. nº treatments per hour/average treatments per hour)	1.3
Mean absorbed dose per treatment in SRS, Gy	12.5
SRS factor, C_{SRS}	15

Results are summarized in table 4.6 and shown in figure 4.6, where data from room dedicated to 3D-CRT at 6 MV are included for comparison. Thicknesses of primary barriers are almost the same (only 2 cm of difference) for both, ordinary and HD concrete while secondary barriers have increased by various HVL or a TVL. The

maximum difference is found in barrier H (47 cm). Due to the close value of H_{sum} to the limit for barrier E (90 µSv/week) the addition of a HVL should be considered.

Table 4.6: *Results obtained for a dedicated bunker to SRS (primary and secondary barriers). Thickness, (t) in m, R_h and H_{sum} in µSv/week.*

Nominal beam energy	Material construction		Primary barriers C	D	G	Secondary barriers A	B	E	H	F	M
6 MV	concrete	t	1.30	1.50	1.47	0.94	1.20	1.11	1.08	1.03	0.76
		R_h	13.3	3.3	13.3	15.2	2.1	5.9	10.5	3.0	-
		H_{sum}	0.8	2.1	0.3	11.4	63.5	88.7	7.9	17.8	-
6 MV	HD concrete	t	1.00	1.15	1.15						
		R_h	13.3	3.3	13.3						
		H_{sum}	7.2	34.6	4.6						

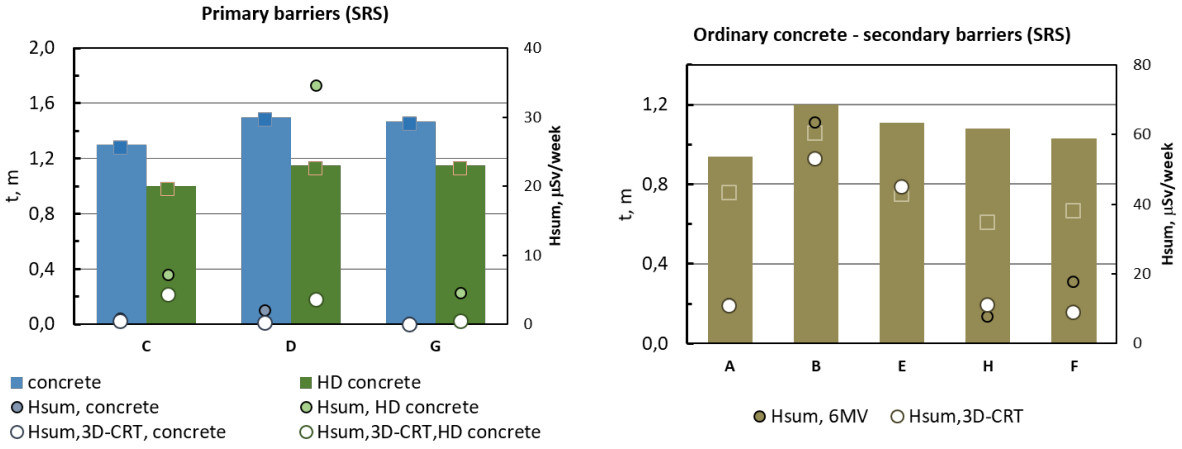

(a) (b)

Figure 4.6: *Thickness and dose equivalent, H_{sum}, values for primary and secondary barriers (SRS). Data from 3D-CRT at 6 MV included (square: thickness; white circle: H_{sum}). a) primary barriers; b) secondary barriers.*

The total dose equivalent at the door, that due to the absence of neutrons, it is equal to the dose equivalent from photon leakage and patient scattered radiation (H_{tot}) is 246.8 µSv/week. The different contributions values are given in table 4.6, being the main contribution that attributed to leakage radiation transmitted through the maze wall (H_{LT}), which is 76 cm thick. The door will need only lead, a thickness of 4.76 mm will be enough to reduce the dose equivalent to half of the shielding design goal.

Table 4.7: *Total dose equivalent at the door, H_w in µSv/week, for a SRS dedicated bunker.*

H_s	H_{ls}	H_{ps}	H_{LT}	$H_{tot} = H_w$
13.1	17.2	21.9	50.0	246.8

4.1.4 TBI

The bunker dedicated to TBI technique, applied by means of a LINAC with beam energy of 6 MV, has only a primary barrier, since the beam is always pointing towards the same barrier (in this case barrier C), as

a consequence this barrier has a use factor of 1. The other walls are then secondary barriers, and changes in the parameters to calculate the thickness should be done as shown in table 4.8. The patient is positioned at 4 m from the x-ray target and the absorbed dose per treatment is higher (see table 4.9), which will influence the primary workload (equation 3.26). The leakage workload is also increased by the C_{TBI} factor. Values considered for the workloads are: W_{pri} = 40·12·4^2 = 7 680 Gy/week and W_L = 15· 7 680 = 115 200 Gy/week.

Table 4.8: *Barriers and treatment parameters for TBI technique.*

Barrier	Type	P, mSv/week	T	U	scat. angle	Distance, m
C	N.C.	0.02	0.025	1	-	7.3
A	N.C.	0.02	0.025	1	30	7.9
B	C.	0.1	1	1	0	7.3
E	C.	0.1	0.5	1	90	5.3
F	N.C.	0.02	0.2	1	90	10.3
H	N.C.	0.02	0.025	1	0	4.0
Maze	C.	0.1	1	1	-	-

Table 4.9: *Treatment parameters for a bunker dedicated to TBI.*

Total number of treatments per week	40
Average number of treatments per day	8
Average Number of treatments per hour, $\bar{N}_h$	1
Number of treatments per hour, max. recommended	2
M (max. nº treatments per hour/average treatments per hour)	2
Distance x-ray target to patient (d_{TBI}), m	4
Mean absorbed dose per treatment in TBI, Gy	12
TBI factor, C_{TBI}	15

Results are summarized in table 4.10 and shown in figure 4.7, where data from 3D-CRT bunker at 6 MV are included. Thickness of primary barrier C has increased 66 cm for ordinary concrete and about 50 cm for HD concrete when compared to the 3D-CRT data. Secondary barriers are also thicker (between 0.5 and 0.8 m), being barriers E and H those with the highest increment, while the values of H_{sum} remains very close to those obtained for 3D-CRT technique.

As in the case of SRS, the total dose equivalent at the door is equal to the dose equivalent from photon leakage and patient scattered radiation. Values are given in table 4.11, being the lower contribution that attributed to

Table 4.10: *Results obtained for a dedicated bunker to TBI (primary and secondary barriers). Thickness, (t) in m, R_h and H_{sum} in μSv/week.*

Nominal beam	Material		Primary barriers			Secondary barriers					
energy	construction		C	D	G	A	B	E	H	F	M
6 MV	concrete	t	1.94	-	-	1.21	1.62	1.51	1.44	1.32	0.98
		R_h	10.0	-	-	17.0	2.1	3.9	15.9	4.4	-
		H_{sum}	0.3	-	-	8.5	41.1	39.4	8.0	17.8	-
6 MV	HD concrete	t	1.49	-	-						
		R_h	10.0	-	-						
		H_{sum}	6.6	-	-						

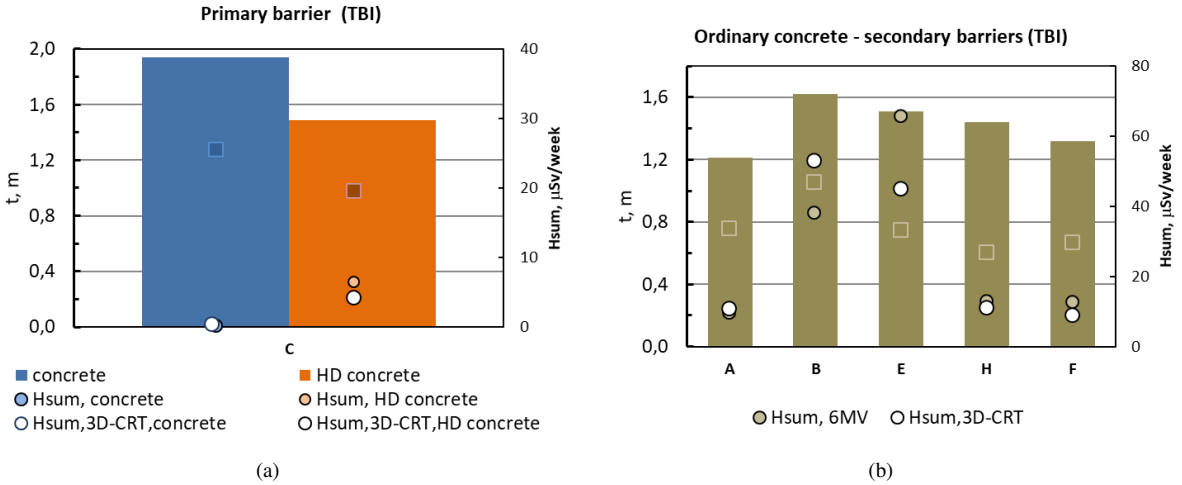

(a) (b)

Figure 4.7: *Thickness and dose equivalent, H_{sum}, values for primary and secondary barriers (TBI). Data from 3D-CRT at 6 MV included (square: thickness; white circle: H_{sum}). a) primary barriers; b) secondary barriers.*

leakage radiation transmitted through the maze wall (H_{LT}). The door will need 2x6.35 mm of lead sheets to reduce the dose at the door to 50 µSv/week, which means a 700 kg of weight.

Table 4.11: *Total dose equivalent at the door, H_w in µSv/week, for a TBI dedicated bunker.*

H_s	H_{ls}	H_{ps}	H_{LT}	$H_{tot} = H_w$
474.3	708.2	902.4	200.0	5 205.5

4.2 Bunkers for multiple techniques

As in previous section, barrier thickness comply with R_h limit for uncontrolled and controlled areas and also H_{sum} (the sum of all dose equivalent from patient scattered and leakage) should be below the P value. Workload relative to quality controls and calibrations are included in the 3D-CRT treatments. Examples of barriers calculations are given in Appendix B.

4.2.1 3D-CRT and IMRT

The effectiveness of IMRT technique is out of any doubt, nevertheless the suitable and optimize beam energy to be used remains unclear. The main reasons are: the significant increase in leakage radiation which increases the risk of radiation-induced cancer and other biological effects; the neutron contribution when photon energies are greater than 10 MV, which increases the dose equivalent to the patient and workers.

Several contributions to this open question can be found in [58–60] and references therein. The general consensus is that the use of high energy photons presents more risks and uncertainties than gains, so the use of 6 MV photons for IMRT should be incentivized. This is based on that there is no reported clinical benefit with respect to target coverage and normal tissue sparing when comparing 15 MV IMRT versus 6 MV IMRT.

Because of that, in this room IMRT technique is limited to the use of 6 MV photon beam, while 3D-CRT can be performed at both energies. The two following cases have been studied, being case b more realistic (considering

the historical data of Santa Maria Hospital):

- Case a. 50% of cases treated with 15 MV photons (3D-CRT technique) while IMRT is performed with 6 MV x-rays (50%),
- Case b. 25% of cases treated with 15 MV photons (3D-CRT technique) while at 6 MV x-rays are performed both techniques: IMRT (50%) and 3D-CRT (25 %).

The total W_{pri} and W_L for both cases is the same (1 1969 Gy/week), but the distribution is different (see table 4.12). In figures 4.8 and 4.9 it is shown how this distribution affects the thickness of the primary and secondary walls respectively, and they are compared with the 3D-CRT data (at 6 MV). All data, including R_h and H_{sum} are presented in table 4.13 and a detailed barrier calculation for case a can be found in Appendix B.

Regarding the primary barriers, when ordinary concrete is used, in both cases the thicknesses increase, being higher for the case a (22 cm) than for case b (17 cm), which is the one with the highest value of primary workload at high energy (312.5 versus 157.5 Gy/week). Against expected, when primary barriers are made of HD concrete the thicknesses decrease by about 8 cm for both cases, but in counterpart de sum of all dose equivalent (leakage and patient scattered), H_{sum}, increases up to values close to 20 μSv/week (except for the roof).

Table 4.12: *Workload (W) in Gy/week for different distribution of treatment techniques (3D-CRT and IMRT).*

		$6MV$	$15MV$	6 MV		15 MV	
		% treatments/week (nº of treatments)		W_{pri}	W_L	W_{pri}	W_L
Case a	$3D-CRT$	0% (0)	50% (125)	-	-	312.5	312.5
	$IMRT$	50% (125)	0% (0)	312.5	1 031.3	-	-
	Total	125	125	**312.5**	**1 031.3**	**312.5**	**312.5**
Case b	$3D-CRT$	25% (62)	25% (63)	155	155	157.5	157.5
	$IMRT$	50% (125)	0% (0)	312.5	1031.3	-	-
	Total	187	63	**467.5**	**1 186.3**	**157.5**	**157.5**

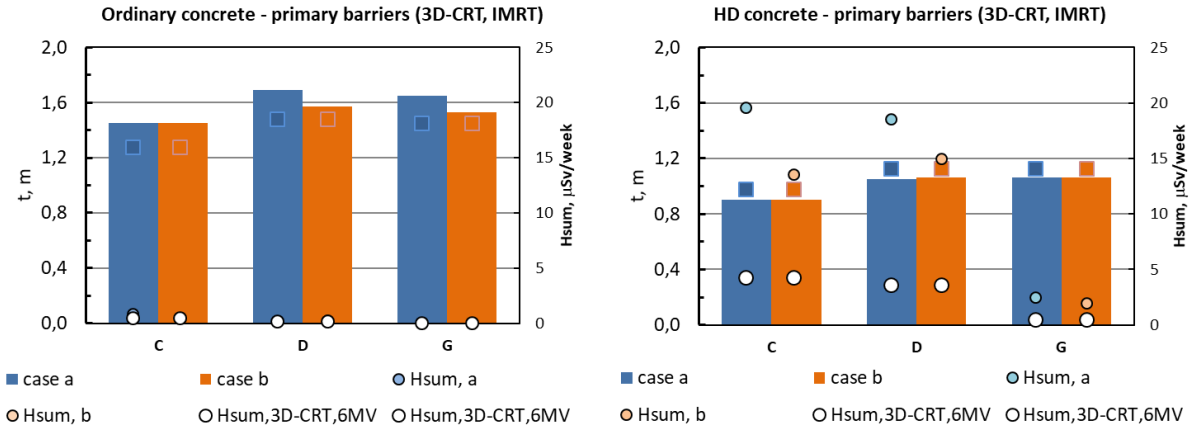

(a) (b)

Figure 4.8: *Thickness and dose equivalent, H_{sum}, values for primary barriers (3D-CRT, IMRT). Data from 3D-CRT at 6 MV included (square: thickness; white circle: H_{sum}). a) Ordinary concrete; b) High density concrete.*

Concerning the secondary barriers (figure 4.9), all of them increase in both cases, about 7 cm in case b and 9 cm in case a. In fact, the values obtained for these two cases are very close, being the main difference the H_{sum}

Table 4.13: *Results obtained for a bunker dedicated to 3D-CRT and IMRT (primary and secondary barriers). Thickness, (t) in m, R_h and H_{sum} in μSv/week.*

Case	Material construction		Primary barriers C	D	G	Secondary barriers A	B	E	H	F	M
Case a	concrete	t	1.45	1.69	1.65	0.89	1.15	0.81	0.68	0.73	0.55
		R_h	15.0	3.6	14.5	10.1	2.2	4.3	11.8	1.3	-
		H_{sum}	0.9	0.2	0.02	7.8	69.0	65.9	13.9	12.9	-
	HD concrete	t	0.90	1.05	1.06						
		R_h	19.7	4.7	18.9						
		H_{sum}	19.6	18.6	2.5						
Case b	concrete	t	1.45	1.57	1.53	0.86	1.17	0.83	0.70	0.75	0.56
		R_h	9.5	4.5	18.3	9.7	1.4	3.4	9.6	1.0	-
		H_{sum}	0.5	0.3	0.04	7.5	43.6	52.9	11.4	10.5	-
	HD concrete	t	0.90	1.06	1.06						
		R_h	16.4	3.8	15.3						
		H_{sum}	13.6	15.0	2.0						

values, which are higher for case a. Special attention should be given to barriers B and E (for case a) due to the high values obtained for the dose equivalent (close to 70 μSv/week).

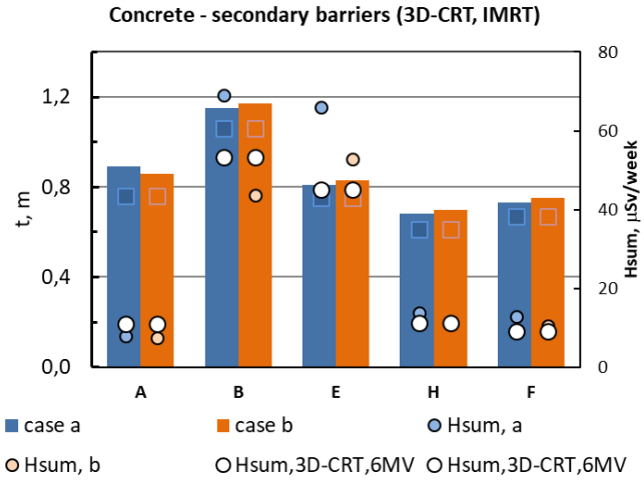

Figure 4.9: *Thickness and dose equivalent, H_{sum}, values for secondary barriers (3D-CRT, IMRT). Data from 3D-CRT at 6 MV included. (square: thickness; white circle: H_{sum}).*

Table 4.14: *Total dose equivalent at the door, H_w in μSv/week, for a 3D-CRT and IMRT bunker.*

	Case a	Case b
H_{tot}	67.9	62.8
H_{cg}	2.3	1.2
H_n	250.7	127.3
H_w	320.9	191.3

In table 4.14 are given the values obtained for the total dose equivalent at the door for both cases jointly with the different contributions. BPE is needed for both cases, but the thickness needed for case a is higher (5.08 cm vs 2.54 cm) as shown in figure 4.10, due to the higher value of workload at high energy (312.5 vs 157.5 Gy/week).

Also in both cases lead is needed, being 2 sheets of the minimum available thickness (0.398 mm) enough, which can be removed if the maze barrier increases by a HVL in both cases. Nevertheless, neutrons can generate gamma rays, so at least the face of the door closes to the control room should have at least the minimum thickness of lead.

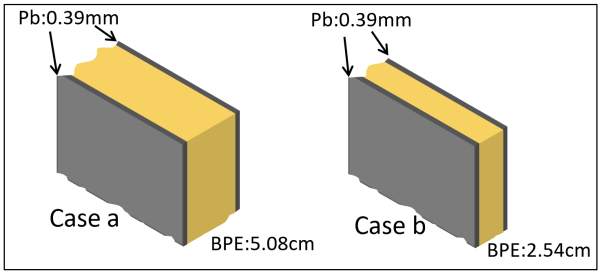

Figure 4.10: *Door thickness composition for a 3D-CRT and IMRT bunker.*

4.2.2 3D-CRT, IMRT and SRS

This case considers the scenario of three treatments techniques (3D-CRT, IMRT and SRS) using two different energy photon beams (6 and 15 MV), distributed as: 3D-CRT (20%) and IMRT (28%) at both energies and SRS (4%) at 6MV. Barriers and treatments parameters are those from tables 3.3 and 3.5. The workload values used are summarized in the following table 4.15:

Table 4.15: *Workload (W) in Gy/week for different distribution of treatment techniques (3D-CRT, IMRT and SRS).*

	$6MV$	$15MV$	6 MV		15 MV	
	% treatments/week (nº of treatments)		W_{pri}	W_L	W_{pri}	W_L
$3D-CRT$	20% (50)	20% (50)	125.0	125.0	125.0	125.0
$IMRT$	28% (70)	28% (70)	175.0	577.5	175.0	577.5
SRS	4% (10)	-	125.0	1 875.0	-	-
Total	130	120	**425.0**	**2 577.5**	**300**	**702.5**

In figure 4.11 are shown the thickness of barriers (primary and secondary) compared with the 3D-CRT data at 6 MV. All data, including R_h and H_{sum} are in table 4.16.

Different results are obtained, depending on the material used to build the primary barriers. When ordinary concrete is used, all thicknesses increase (between 17 and 21 cm) while if HD concrete is used, thickness remains equals than in the case of 3D-CRT or even decrease, as in the case of barrier D. Again, this decrement is at the cost of an increasing of all dose equivalent value, H_{sum}, specifically for barrier D.

The high value of the leakage workload in this scenario is may be the more remarkable issue, and this is reflected in the secondary barriers thicknesses. All of them increase in different way: barrier A increases 13 cm, barrier B, 20 cm and the others 18 cm. H_{sum} values are close to that reported for 3D-CRT case, except barrier E with a dose equivalent close to 70 μSv/week.

In table 4.17 are given the values obtained for the total dose equivalent at the door and the different contributions. Due to the presence of neutrons, a 5.08 cm of BPE embedded between two lead sheets (0.79 mm each) is needed, similar to that obtained for the dedicate room to 3D-CRT at 15 MV.

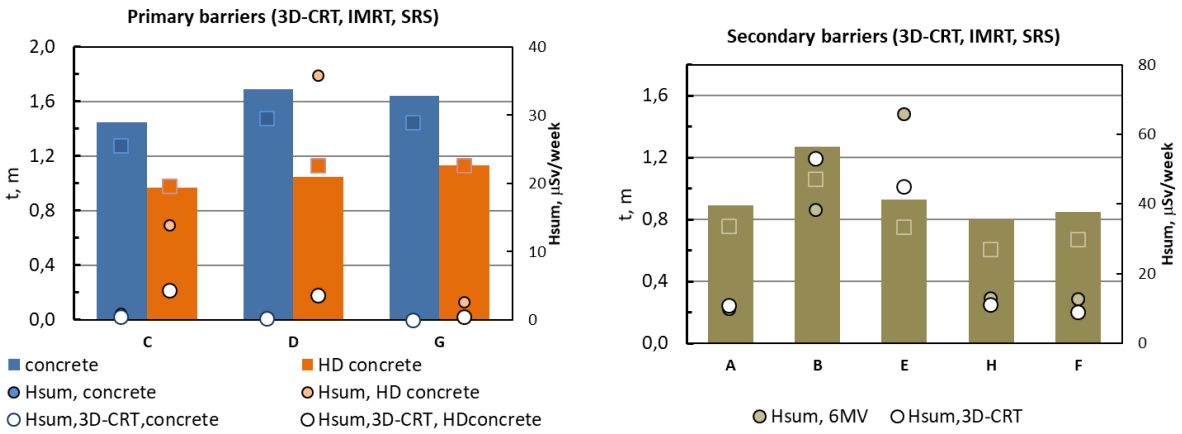

(a) (b)

Figure 4.11: *Thickness and dose equivalent, H_{sum}, values for primary and secondary barriers (3D-CRT, IMRT, SRS). Data from 3D-CRT at 6 MV included (square: thickness; white circle: H_{sum}). a) primary barriers; b) secondary barriers.*

Table 4.16: *Results obtained for a bunker dedicated to 3DCRT, IMRT and SRS (primary and secondary barriers). Thickness, (t) in m, R_h and H_{sum} in µSv/week.*

		Primary barriers			Secondary barriers					
		C	D	G	A	B	E	H	F	M
concrete	t	1.45	1.69	1.64	0.89	1.27	0.93	0.80	0.85	0.64
	R_h	15.1	3.8	15.2	12.8	1.2	4.3	10.7	1.3	-
	H_{sum}	0.9	0.3	0.04	9.9	38.3	65.8	13.1	12.8	-
HD concrete	t	0.97	1.05	1.13						
	R_h	11.0	5.4	10.5						
	H_{sum}	13.9	35.9	2.6						

Table 4.17: *Total dose equivalent at the door, H_w in µSv/week, for (3D-CRT, IMRT and SRS).*

H_{tot}	H_{cg}	H_n	H_w
78.1	5.4	591.4	674.9

4.2.3 3D-CRT, IMRT, SRS and TBI

In this last scenario, all techniques are applied in the same bunker distributed as: 20% of treatments per week using 3D-CRT at both energies (6MV and 15MV), 28% using IMRT at both energies, 1.6% using TBI and 2.4% using SRS, last two techniques using 6 MV photon beam. Workload values are summarized in table 4.18.

During barrier calculations, as in the case of a bunker dedicated to TBI, the beam is pointing towards barrier C and also for calculating the time averaged dose equivalent rate in-any-one-hour (R_h), the worst scenario has been considered and then M is equals to 2 (table 4.9).

The main difference between this case and the previous one is the distribution of the workload: while at 15 MV remains the same for both cases, at 6 MV this case has a lower value of W_{pri}, except for barrier C, and the leakage workload is about 5 times higher. This distribution is reflected in the thicknesses of primary barriers (see figure 4.12 a and table 4.19), where the biggest increment in registered for barrier C in both cases (ordinary and HD concrete). For HD concrete, barrier D has the same thickness than the 3D-CRT at 6 MV case, but attention

Table 4.18: *Workload (W) in Gy/week for different distribution of treatment techniques (3D-CRT, IMRT, SRS and TBI).*

	$6MV$	$15MV$	6 MV		15 MV	
	% treatments/week (nº of treatments)		W_{pri}	W_L	W_{pri}	W_L
$3D-CRT$	20% (50)	20% (50)	125	125	125	125
$IMRT$	28% (70)	28% (70)	175	577.5	175	577.5
SRS	2.4% (6)	-	75	1 125	-	-
TBI	1.6% (4)	-	768*	11 520	-	-
Total	130	120	**375***	**13 347.5**	**300**	**702.5**

* Beam is only towards Barrier C during TBI treatments.

$W_{pri,C} \cdot U_C = 375 \cdot 0.25 + 768 \cdot 1 = 861.8$ Gy/week

should be paid to the high value of H_{sum} (close to 60 μSv/week), nevertheless, it should be recall that TVL data from ordinary concrete have been used. Detailed barrier calculation can be found in Appendix B.

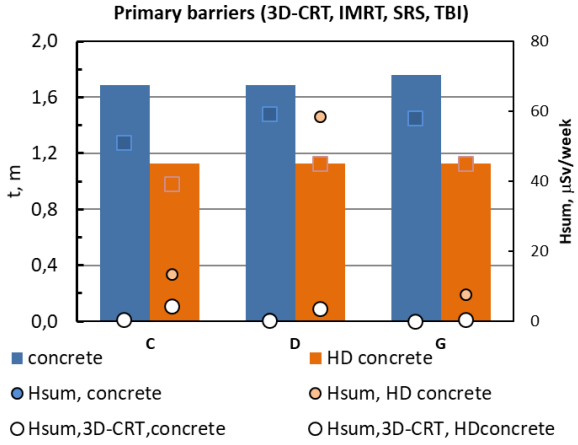

(a)

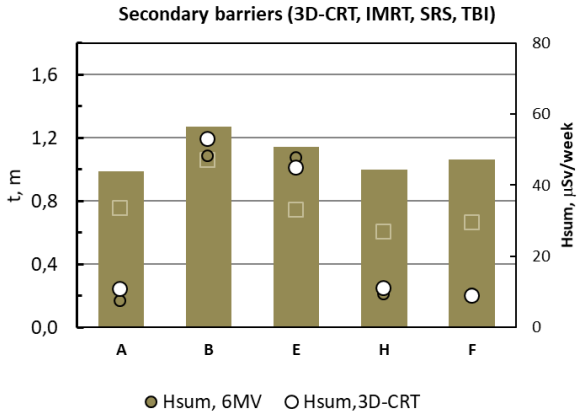

(b)

Figure 4.12: *Thickness and dose equivalent, H_{sum}, values for primary and secondary barriers (3D-CRT, IMRT, SRS and TBI). Data from 3D-CRT at 6 MV included (square: thickness; white circle: H_{sum}). a) primary barriers; b) secondary secondary.*

Concerning the secondary barriers (figure 4.12 b), all of them have increased. The highest increment (39 cm) is for barriers E, F and H, followed by barrier A (23 cm) and then barrier B (20 cm).

Table 4.19: *Results obtained for a bunker dedicated to 3DCRT, IMRT, SRS and TBI (primary and secondary barriers). Thickness, (t) in m, R_h and H_{sum} in μSv/week.*

		Primary barriers			Secondary barriers					
		C	D	G	A	B	E	H	F	M
concrete	t	1.69	1.69	1.76	0.99	1.27	1.14	1.00	1.06	0.79
	R_h	10,8	5,7	11,3	15.1	2.4	4.8	19.0	2.4	-
	H_{sum}	0.4	0.8	0.04	7.6	48.3	47.8	9.5	9.5	-
HD concrete	t	1.13	1.13	1.13						
	R_h	15.0	3.9	15.5						
	H_{sum}	13.6	58.5	7.8						

Table 4.20: *Total dose equivalent at the door, H_w in μSv/week, for (3D-CRT, IMRT, SRS and TBI).*

$\mathbf{H}_{tot}$	$\mathbf{H}_{cg}$	$\mathbf{H}_n$	$\mathbf{H}_w$
408.5	4.7	514.4	927.6

In table 4.20 are given the values obtained for the total dose equivalent at the door. The door should be composed by two sheets of lead of 3.17 mm each and in the middle 2 inchs of BPE (5.08 cm). In this case, the increment of the maze barrier will have no influence in the H_{tot} where the main contribution came from the patient scattered radiation.

Chapter 5

Economic impact

This chapter is dedicated to discuss the impact of using different RT techniques in the budget, just considering the cost of materials used for construction: concrete (ordinary and high density concrete), lead and borated polyethylene. Other parameters, as the maze barrier thickness, the dose equivalent (H_{sum}) values, or changes in the surrounding areas will also affect the final budget.

Radiotherapy techniques

Only costs attributed to material construction: concrete (or HD concrete) for walls and ceiling, and lead and BPE for doors were considered in this cost comparison exercise. Total cost of materials for different bunkers are shown in figures 5.1, 5.2 and table 5.1 where, as it has been done along this work, prices are compared with the 3D-CRT dedicated bunker at 6 MV. Layouts of bunkers are shown in figure 5.4. Prices obtained are below the costs (which are final prices) published by Van Dyk (between $ 567 497 and $ 253 800 for a bunker of 141 m^2) [2] or by the Tavistock Institute (over £500 000) [61].

In general, primary barriers volume using ordinary concrete represent about 62% of the volume needed by the secondary barrier, and about 42% of the volume if primary barriers are made of HD concrete.

Considering only the volume to be constructed and the type of door to be installed, the highest price among the dedicated bunkers, is found for the bunker dedicated to TBI due to the volume needed by the secondary barriers (about the double than in most of the other cases), as shown in table 5.1 and figure 5.2. Because of that, and due to the low quantity of HD concrete needed for the primary barrier (only barrier C), this case exhibit the lowest increment (25%) when comparing the price of ordinary and mix of ordinary and HD concrete. This bunker is also the one with the highest increment relative to the 3D-CRT case when only ordinary concrete is used, about 43 %. Besides the volume of the secondary barriers, door is also responsible for this big difference. Although in both situations, the energy of the photons is the same, 6 MV, the leakage workload in the TBI case is the main responsible for the thickness of lead needed and it is reflected in the dimensions and final price of the door, almost 7 times more expensive than the 3D-CRT door.

Similar analysis can be done for the bunker dedicated to 3D-CRT, IMRT, SRS and TBI, where besides the high volume of secondary barriers, it is also among the highest volumes of primary barriers. Furthermore, due to

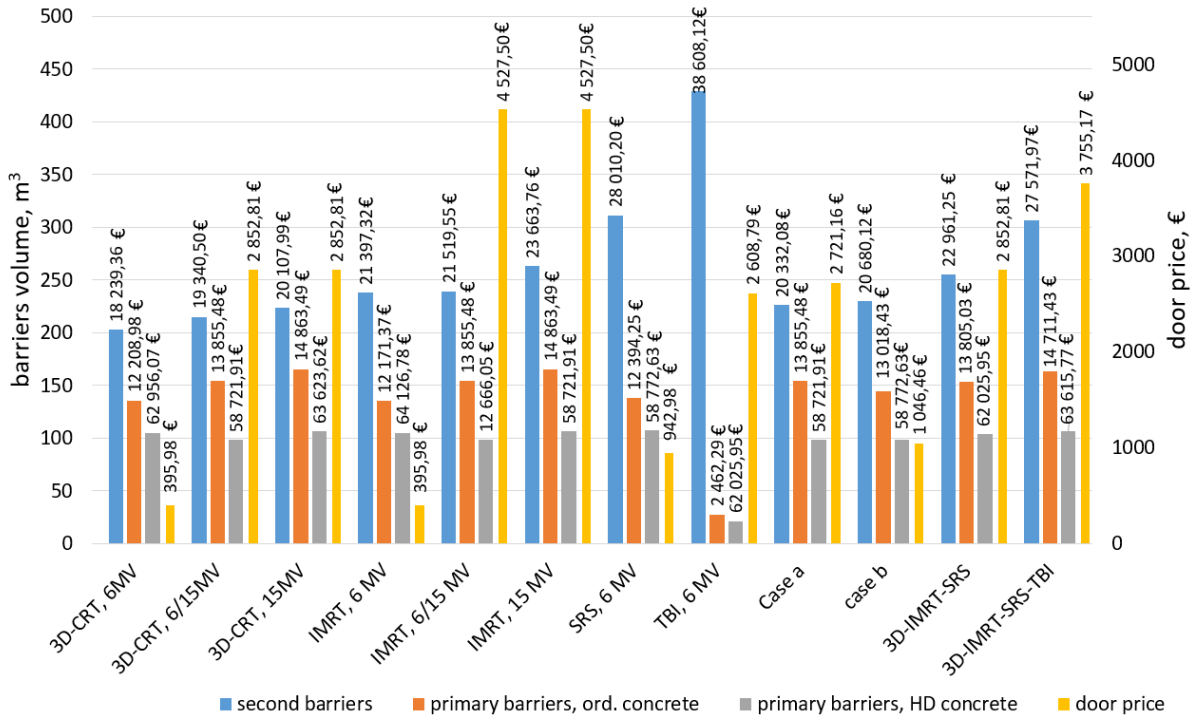

Figure 5.1: *Barriers volume, in m^3, as a function of the RT technique. Prices, in €, are included.*

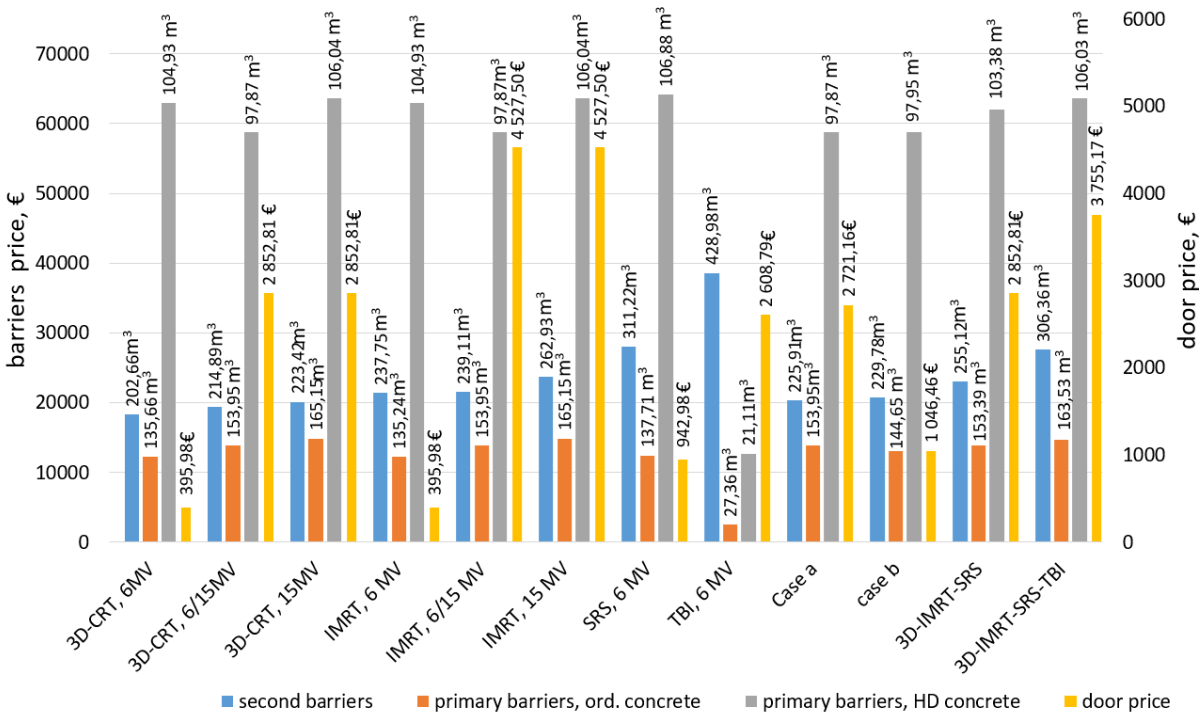

Figure 5.2: *Barriers prices, in €, as a function of the RT technique. Volumes, in m^3, are included.*

the presence of neutrons and photons, the door is among the most expensive doors.

In general, as the use of RT technique implies an increment on the workload (mainly the leakage workload), there is an increment on the volume required, mainly due to secondary barriers. Among the same RT technique, the volume slightly increases as the energy of the x-rays increases.

Doors made only of lead are the cheapest (except the one dedicated to SRS bunker, due to its thickness). In

fact, due to the costly and the limited offer in the market of BPE, all those bunkers which use 15 MV photon beams, either alone or jointly with 6 MV photon beam, present the most expensive doors.

Maze barrier dependence

Door composition of a bunker is dependent on the origin and quantity of the dose equivalent value at the door, H_w, which also depends on the maze barrier thickness by means of the H_{tot} contribution. From the studied bunkers some has been selected to study the dependency of budget as a function of maze barrier thickness.

In the case of the bunker dedicated to 3D-CRT using a 15 MV beam, section 4.1.1, door shown in figure 4.3 can be simplified if barrier maze increases. If the maze barrier-slant increases a TVL (36 cm), given then a maze barrier of 0.83 m thick and a 900 € investment in ordinary concrete, the distribution of equivalent dose at the door changes, being the contribution of neutrons the most important one (0.5 mSv/week), while the H_{tot} and H_{cg} are 24 and 5 mSv/week, respectively. Thus, only 2 inchs of BPE (5.1 cm) will be needed, although, since neutrons can generate gamma rays, at least the face of the door closes to the control room should have at least the minimum thickness of lead 0.39 mm. The door price will be reduced to 2 616.60 €. In this case, a negative balance is obtained if the maze door increase (−660 €), because the neutron contribution is not affected by the maze barrier thickness.

Similar analysis can be done for the bunker dedicated to IMRT using only 6 MV photon beam. A doorless bunker (or a bunker with a simple door) can be obtained if the maze barrier is increased by 1 HVL, up to 0.86 m thick (see table 4.3) with a cost of about 800 €. Then, the dose equivalent at door, H_w, can be reduced up to 36.8 µSv/week. Again, the balance is negative (−660 €), but other considerations such as door maintenance should be considered in the final decision.

Increase the maze barrier is not always the way to simplify the door. An example can be found for the TBI bunker, where even if the maze thickness is increased up 1.2 m reducing then the H_{LT} contribution (from 200 to 13.45 µSv/week), it is not enough to reduce the thickness of the door, due mainly to the other high contributions: H_s, H_{ls} and H_{ps} to H_{tot}(seen table 4.11).

Patient and leakage dose equivalent dependence

Contrary to what was expected, the time averaged dose equivalent rate in-any-one-hour limit (20 µSv/week), R_h, is not as restrictive as the limit imposed to the dose equivalent due to patient scattered and leakage radiation, H_{sum}, (see example in B.0.2) which should be below the P value for each area. Furthermore, the close values to the limit obtained for H_{sum} in some barriers for controlled areas should be carefully considered.

Three examples were chosen in order to evaluate the extra budget needed to reduce these H_{sum} high values up to 20 µSv/week. Only secondary barriers are considered (mainly barriers B and E), since only barriers made of HD concrete present high H_{sum} values, which can be related with the use of TVL values of ordinary concrete due to the absence of these data for HD concrete [9, 43, 57].

The first example is the bunker dedicated to IMRT using 6 and 15 MV photon beams. In order to reduce the sum of dose equivalent from the initial values (73.7 and 71.2 µSv/week for barriers B and E respectively as shown in table 4.3) to 16.6 and 14.7 µSv/week, the barriers should be increased in 0.25 and 0.21 m respectively. This

means an increment of the volume needed of ordinary concrete of 14 m^3, about 1 212 € (3.1% of the total cost for this bunker (see table 5.1).

Another example is found in the bunker dedicated to SRS technique, where barriers B and E present H_{sum} values equals to 63.5 and 88.7 µSv/week respectively (see table 4.6). It is needed to add 0.20 m to both barriers to achieve H_{sum} values of 13.8 and 17.5 µSv/week respectively, obtaining then final thicknesses of 1.40 m for barrier B and 1.31 m for barrier E. The price of ordinary concrete needed (11.5 m^3) is 1 034€, about 2.5% of the price for this bunker, including the door as shown in table 5.1.

Finally, if barriers B and E from the bunker dedicated to all RT techniques (described in section 4.2.3 and Appendix B), increase 0.25 and 0.21 m respectively, the sum of the equivalent dose values for these barriers are reduced to 9.8 and 8.8 µSv/week. These thicknesses increment mean an increment of 13.0 m^3 of ordinary concrete, about 1 170 €, 2.5% of the price for this bunker (table 5.1).

Adjacent rooms

Type of adjacent rooms to the bunker (controlled or uncontrolled aras) and their occupancy factor, T, will influence the thickness of barriers. In this sense, some of the surrounding areas of the bunkers studied in the previous section have been changed to study the effect in the barriers and price, assuming that only ordinary concrete is used and the maximum H_{sum} should be below 20 µSv/week. Changes are:

- Barriers G and H. The roof is now a controlled area and the occupancy factor remains the same (0.025);
- Barrier E. The examination room beyond this barrier is now a receptionist area, so is an uncontrolled area and the occupancy factor is 1.

Barriers G and H for the bunker dedicated to IMRT with both energies decrease only 4 and 1.4 cm respectively, which means a volume decrease of 2.5 m^3, nevertheless barrier E increases 33 cm, about 7.5 m^3. In total, an investment of about 675 € (1.6% of the final price) is needed to maintain the radiological protection of this bunker.

Similar results are obtained for the bunker dedicated to SRS (section 4.1.3). While barrier G decreases 2.0 cm, barrier H remains with the same thickness (1.08 m) and barrier E increases 29 cm. In total, there is an increase of ordinary concrete volume of 8.7 m^3, which means about 786 € (1.9% of the total price).

For the bunker dedicated to all RT techniques (section 4.2.3) different changes are registered. Barrier G decreases 4 cm, barrier H increases only 2 cm and barrier E increases 29 cm. In total, the volume needed is about 10 m^3 with a price of about 921 € (2.0% of the total price).

Accelerator and isocenter position

In order to analyse the impact of accelerator position (and thus, the isocenter position) into the budget, the three bunkers from previous section has been analysed.

The accelerator position is now in such a way the gantry rotation axis is parallel to the maze wall, then primary barriers are: the previous barrier E and the maze barrier (see figure 5.3), besides the ceiling. The new position of isocenter is 5 m from external wall C, 5 m from external wall E and 1.3 m from the floor.

In this new configuration all secondary barriers will be affected, while among the primary barriers, besides maintaining the width, only barrier C will change due to the distance to the point to protect (5.3 m) and the space

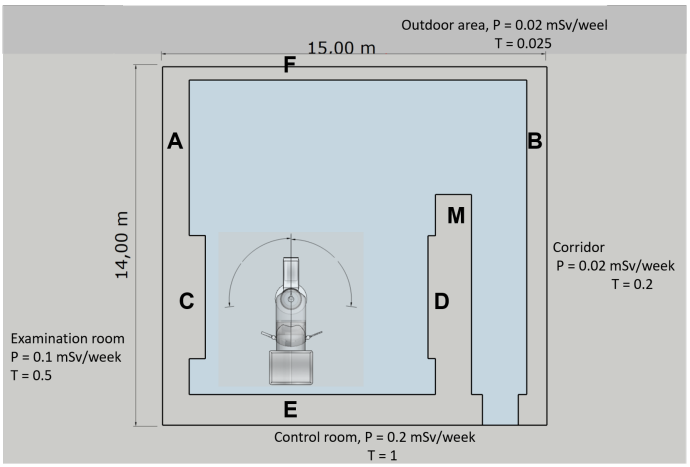

Figure 5.3: *Bunker layout and labels used for primary (C, D) and secondary barriers: A, B, E, F. (top view).*

to be protected (a controlled area with an occupancy factor of 0.5). Also, length of barrier G (roof) is lower, since the maze will no need protection from the primary beam, reducing then the volume associated to this barrier.

The first bunker analysed in this new configuration is the one dedicated to IMRT with the two photon beam energies. Primary barriers volume is reduced up to 140.51 or 96.49 m^3 of ordinary and HD concrete respectively, while secondary barriers volume increases up to 243.55 m^3. In terms of price, there is no big difference in comparison with the initial configuration bunker, only 810 and 428 € for ordinary and HD/ordinary concrete respectively. The main difference in this new bunker is related with the door due to the distances, which affect both the photon and neutron distribution at the door. The width of BPE needed to protect from neutrons is lower, 5.08 cm while only 0.39 mm of lead in the outside of the door will be enough to reduce the dose due to the photons originated from the BPE. This new door composition will also reduce the final price of the bunker.

If the bunker dedicated to SRS is considered, similar results are obtained. Barrier C increases 8 cm while the other primary barriers remains with the same thickness. In the same way, volume of secondary barriers increase 12.5 m^3. Also, due to the maze barrier thickness (1.20 m), in this case as secondary barrier, the corresponding contribution to H_{tot} is negligible and then lead thickness needed for the door is 1.98 mm. The final price for this bunker is 40 502.68 € for ordinary concrete and 86 396.98 € for the mix of ordinary and HD concrete.

For the bunker dedicated to all RT techniques, the beam during TBI treatments is pointing towards barrier D (in the maze barrier) ir order to maintain the t_{TBI} distance of 4 m. In this case, barriers C and D increase for both ordinary and HD concrete materials, increasing also the volume needed for primary barriers up to 148 and 96 m^3 respectively. Secondary barriers also increase, and the volume of ordinary concrete needed is 315 m^3. The door composition also changes, in general all dose contributions are half of those values presented in table 4.20. The BPE needed is 2.96 cm, but due to the available thicknesses in market, the BPE thickness should be 5.08 cm. Lead thickness is also reduced, and two sheets of lead of 1.98 mm thick each, will be enough. In terms of prices this bunker presents a decrease of about 1 076 € if ordinary concrete is used and about 5 600 € if ordinary and HD concrete are used.

Table 5.1: *Material costs, in €, for different type of bunkers. Density of ordinary concrete: (2.35 g/cm^3); density of HD concrete (3.2 g/cm^3). Dimensions of BPE:121.92 cm x 243.84 cm; Dimensions of lead: 500 cm x 100 cm.*

		Dedicated bunkers														Mix bunkers							
		3D-CRT						IMRT						SRS		TBI		3D-CRT+IMRT				3D-CRT+IMRT+SRS		3D-CRT+IMRT+SRS+TBI	
		6 MV		6/15 MV		15 MV		6 MV		6/15 MV		15 MV		6 MV		6 MV		Case a		Case b		6/15 MV		6/15 MV	
Description	Unit price, €	Quantity, m^3	Amount, €	Quantity, m^3	Amount, €	Quantity, m^3	Amount, €	Quantity, m^3	Amount, €	Quantity, m^3	Amount, €	Quantity, m^3	Amount, €	Quantity, m^3	Amount, €	Quantity, m^3	Amount, €	Quantity, m^3	Amount, €	Quantity, m^3	Amount, €	Quantity, m^3	Amount, €	Quantity, m^3	Amount €
Ordinary concrete, secondary barriers	90.00	202.66	18 239.36	214.89	19 340.50	223.42	20 107.99	237.75	21 397.32	239.11	21 519.55	262.93	23 663.76	311.22	28 010.20	428.98	38 608.12	225.91	20 332.08	229.78	20 680.12	255.12	22 961.25	306.36	27 571.97
Ordinary concrete, primary barriers	90.00	135.66	12 208.25	153.95	13 855.48	165.15	14 863.49	135.24	12 171.37	153.95	13 855.48	165.15	14 863.49	137.71	12 394.25	27.36	2 462.29	153.95	13 855.48	144.65	13 018.43	153.39	13 805.03	163.53	14 711.43
HD concrete, primary barriers	600.00	104.93	62 956.07	97.87	58 721.91	106.04	63 623.62	104.93	62 956.07	97.87	58 721.91	106.04	63 623.62	106.88	64 126.78	21.11	12 666.05	97.87	58 721.91	97.95	58 772.63	103.38	62 025.95	106.03	63 615.77
subtotal, ordinary concrete			30 448.34		33 195.98		34 971.48		33 568.69		35 375.02		38 527.25		40 404.45		41 070.41		34 187.56		33 698.55		36 766.27		42 289.44
subtotal, ordinary and HD concrete			81 195.43		78 062.41		83 731.61		84 353.39		80 241.45		87 287.38		92 136.98		51 274.17		79 053.99		79 452.75		84 987.20		91 187.74
increment, %			167%		135%		139%		151%		127%		127%		128%		25%		131%		136%		131%		116%
Borated Polyethylene, 2.54 cm	837.34																			1	837.34				
Borated Polyethylene, 5.08 cm	2 512.04			1	2 512.04	1	2 512.04											1	2 512.04			1	2 512.04	1	2 512.04
Borated Polyethylene, 7.62 cm	4 186.73									1	4 186.73	1	4 186.73												
Lead, 0.39 mm	104.56																	2	209.12	2	209.12				
Lead, 0.79 mm	170.39			2	340.77	2	340.77			2	340.77	2	340.77									2	340.77		
Lead, 1.98 mm	395.98	1	395.98					1	395.98																
Lead, 3.17 mm	621.56																							2	1 243.13
Lead, 4.76 mm	942.98													1	942.98										
Lead, 6.35 mm	1 304.40															2	2 608.79								
subtotal door			395.98		2 852.81		2 852.81		395.98		4 527.50		4 527.50		942.98		2 608.79		2 721.16		1 046.46		2 852.81		3 755.17
Total, walls ordinary concrete and door, €			30 844.32		36 048.79		37 824.29		33 964.67		39 902.53		43 054.76		41 347.43		43 679.20		36 908.72		34 745.01		39 619.09		46 044.57
Total, walls HD concrete and door, €			81 591.41		80 915.23		86 584.42		84 749.37		84 768.96		91 814.89		93 079.96		53 882.96		81 775.15		80 499.21		87 840.01		94 942.91
Increment relative to 3D-CRT at 6 MV, ordinary concrete			-		17%		23%		10%		29%		40%		34%		42%		20%		13%		28%		49%
Increment relative to 3D-CRT at 6 MV, HD concrete			-		-1%		6%		4%		4%		13%		14%		-34%		0.2%		-1%		8%		16%

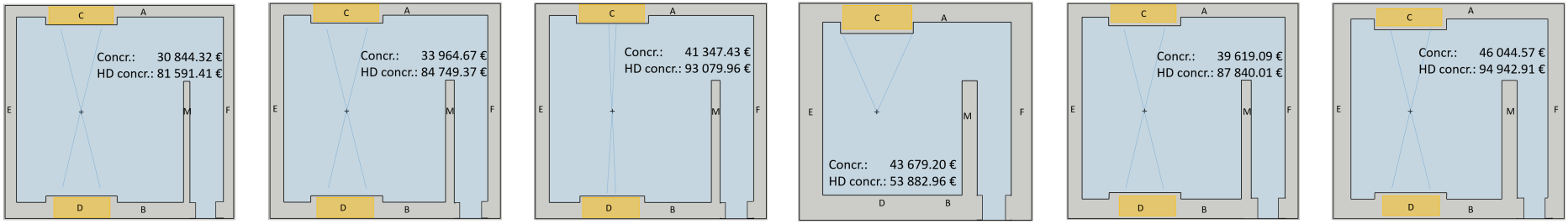

(a) 3D-CRT, 6 MV (b) IMRT, 6 MV (c) SRS, 6 MV (d) TBI, 6 MV (e) 3D-CRT+IMRT+SRS (f) 3D-CRT+IMRT+SRS+TBI

Figure 5.4: *Bunker layouts for different radiotherapy techniques (top view). Primary barriers, made of ordinary concrete, are orange-shadowed.*

Chapter 6

Conclusions

This research project involved the study of shielding barriers for bunkers dedicated to single radiotherapy treatments (dedicated bunkers) or to a more realistic situation, a mix of radiotherapy treatments with different distributions. Thicknesses of barriers were calculated following the NCRP-151 methodology, by means of the development of a Excel document. Changes in thickness barriers are correlated with the volume of material needed to construct the bunker and also to the budget needed.

Among the dedicated bunkers, the one for TBI is the most expensive, mainly due to the volume of ordinary concrete needed for the secondary barriers, presenting also the most expensive door due to the thickness of lead needed to shield the secondary radiation, mainly leakage radiation. This bunker is followed, in terms of price, by the SRS bunker. According with the historical data available in Santa Maria Hospital, due to the reduced number of treatments performed using these two RT techniques, the investment in theses bunkers would not be justified, besides the investment on LINAC and related items acquisition.

The cheapest bunker is the one dedicated to 3D-CRT, followed by the bunker dedicated to IMRT. In both cases, as the energy of beam used increases, the prices also increase since the thicknesses needed are larger.

In general, the use of HD concrete for primary barriers implies an average budget increment of 74% when compared with the budget using ordinary concrete (without considering the door). This extra investment can be justified if constrains, as space, exist. The use of photons with energy of 15 MV involves expensive doors, mainly due to the need of using borated polyethylene, a costly material to protect from neutrons generated at this energy.

When a bunker has been designed and constructed under well determined conditions, as RT technique to be performed inside, the introduction of new techniques will be reflected in the wall thicknesses. Can be highlighted:

- Introduction of IMRT or SRS techniques will be reflected mainly in the volume of secondary barriers.

- Introduction TBI will be reflected in both, primary and secondary barriers. The primary barrier towards the beam is pointing will have the higher increment, while the secondary barriers, due to the leakage and patient scattered radiation will also increase.

Not only changes affecting the RT techniques used in the bunker will affect the barriers, changes in surrounding areas will also modify the bunker. For example, change a controlled area to uncontrolled, or even transform a waiting room to a reception area will change the occupancy factor, which has a relationship with the thickness of the barriers. The investment needed to ensure the radiation protection of public and workers, considering the

studies carried out in this work, supposes a low percentage (less than 2%) of the initial investment.

In agreement with the Principle of optimisation of protection (or ALARA principle), reduce the dose equivalent due to leakage and patient scattered radiation, H_{sum}, in controlled areas to 20 µS/week requires only less than 1 300 €(considering the cases studies).

The NCRP-151 report is a widely consulted document using cumbersome calculation formalism, which in the frame of this work it has been interpreted in a Excel document. This document takes the input data and provides the thickness of barriers jointly with the time averaged dose-equivalent rate in-any-one-hour (R_h) and the sum of dose equivalent due to patient scattered and leakage radiation (H_{sum}). It is the user who is responsible to check if these values are above the limit and evaluate if the barrier should be increased. The Excel document also calculates the dose-equivalent at the door and provides the different thickness of materials needed, being the user responsible for choosing the final composition. It is intended to supply this document to be used as a tool for a first evaluation of barrier thicknesses needed, including also the door. Nevertheless, since each bunker has its own characteristics (which should be reflected in final calculations), individualized and detailed calculi should be wisely done.

Furthermore, the results obtained in this work using the NCRP-151 methodology should be compared with calculations obtained from Monte Carlo simulations and, when possible, with experimental measurements. Also, data regarding the TVL for leakage and patient scattered radiation when HD concrete is used, should be updated when available.

Finally, as it has been shown, there is a relationship between the RT techniques implemented in a bunker and the barrier thicknesses. In Portugal, most of the LINACs installed a decade ago to perform only 3D-CRT are nowadays performing IMRT and SRS techniques without any change in the bunker. A survey should be performed to check if the barriers are appropriate or if a reinforcement is needed.

Bibliography

[1] *Planning National Radiotherapy Services: A Practical Tool*. IAEA Human Health Series. International Atomic Energy Agency, Vienna, 2011.

[2] J. Van Dyk, E. Zubizarreta, and Y. Lievens. Cost evaluation to optimise radiation therapy implementation in different income settings: A time-driven activity-based analysis. *Radiotherapy and Oncology*, 125(2):178–185, 2017. DOI: 10.1016/j.radonc.2017.08.021.

[3] C. Grau, N. Defourny, J. Malicki, P. Dunscombe, J. M. Borras, M. Coffey, B. Slotman, et al. Radiotherapy equipment and departments in the European countries: Final results from the ESTRO-HERO survey. *Radiotherapy and Oncology*, 112(2):155–164, 2014. DOI: 10.1016/j.radonc.2014.08.029.

[4] N. R. Datta, M. Samiei, and S. Bodis. Radiotherapy infrastructure and human resources in Europe – Present status and its implications for 2020. *European Journal of Cancer*, 50(15):2735–2743, 2014. DOI: 10.1016/j.ejca.2014.06.012.

[5] DIrectory of RAdiotherapy Centres DIRAC IAEA. https://dirac.iaea.org/, last access, October 2018.

[6] R. Atun, D. A. Jaffray, M. B. Barton, F. Bray, M. Baumann, B. Vikram, T. P. Hanna, F. M. Knaul, Y. Lievens, T. Y. M. Lui, et al. Expanding global access to radiotherapy. *The Lancet Oncology*, 16(10):1153–1186, 2015. DOI:10.1016/S1470-2045(15)00222-3.

[7] A. Rodríguez, M. Algara, D. Monge, J. López-Torrecilla, F. Caballero, R. Morera, R. Escó, et al. Infrastructure and equipment for radiation oncology in the Spanish National Health System: analysis of external beam radiotherapy 2015–2020. *Clinical and Translational Oncology*, 20(3):402–410, 2018. DOI:10.1007/s12094-017-1727-x.

[8] B. J. Slotman and P. H. Vos. Planning of radiotherapy capacity and productivity. *Radiotherapy and Oncology*, 106(2): 266–270, 2013. DOI:10.1016/j.radonc.2013.02.006.

[9] *NCRP Report No. 151 - Structural Shielding Design and Evaluation for Megavoltage x- and gamma-Ray Radiotherapy Facilities*. National Council on Radiation Protection and Measurements, 2005.

[10] *Decreto-Lei 180/2002 of 8 August 2002*. Diário da República - I Série A, Ministério da Saúde.

[11] *Medizinische Elektronenbeschleuniger-Anlagen*. DIN-6847, Deutsches Institut fur Normung of November 1977.

[12] *Decreto-Lei 222/2008 of 17 November 2008*. Diário da República - I Série A, Ministério da Saúde.

[13] *Council Directive 2013/59/EURATOM of 5 December 2013*. The Council of the European Union, Official Journal of the European Union.

[14] R. F. Mould. Röntgen and the discovery of x-rays. *The British Journal of Radiology*, 68(815):1145–1176, 1995. DOI: 10.1259/0007-1285-68-815-1145.

[15] M. Lederman. The early history of radiotherapy: 1895–1939. *International Journal of Radiation Oncology-Biology-Physics*, 7(5):639–648, 1981. DOI: 10.1016/0360-3016(81)90379-5.

[16] H. Becquerel. Phosphorescence of uranium salts in liquid air. *Journal of the Röntgen Society*, 3(13):141–141, 1907. DOI: 10.1259/jrs.1907.0094.

[17] R. F. Mould. The discovery of radium in 1898 by Maria Sklodowska-Curie (1867-1934) and Pierre Curie (1859-1906) with commentary on their life and times. *The British Journal of Radiology*, 71(852):1229–1254, 1998. DOI: 10.1259/bjr.71.852.10318996.

[18] W. Morton. *The x-ray or photography of the invisible and its value in surgery*. https://archive.org/details/b21500393. Simpkin, Marshall, Hamilton, Kent, London, 1896.

[19] http://www.independent.co.uk/voices/campaigns/give-to-gosh/great-ormond-street-hospitals-history-revealed-in-photography-archive-that-stretches-back-150-years-a6803516.html, last access October, 2018.

[20] https://www.med-dept.com/medical-kits-contents/u-s-army-x-ray-field-unit/, last access October, 2018.

[21] https://www.historad.com/en/symbol/en/100-years-radiotherapy-netherlands-cancer-institute-science/improved-safety-of-x-ray-machines/, last access October, 2018.

[22] H. Domenech. *Radiation Safety - Management and Programs*. Springer International Publishing Switzerland, 2017.

[23] T. Terasima and L. J. Tolmach. Changes in x-ray sensitivity of hela cells during the division cycle. *Nature*, 190:1210, 1961. DOI: 10.1038/1901210a0.

[24] C. C. Stobbe, S. J. Park, and J. D. Chapman. The radiation hypersensitivity of cells at mitosis. *International Journal of Radiation Biology*, 78(12):1149–1157, 2002. DOI: 10.1080/09553000210166570.

[25] J. Bergonié and L. Tribondeau. Interprétation de quelques résultats de la radiothérapie et essai de fixation d'une technique rationnelle. *Comptes-rendus de l'Académie des Sciences*, 143:983–984, 1906. DOI: 10670/1.b8y7ww.

[26] *Radiation Oncology Physics*. International Atomic Energy Agency, Vienna, 2005. ISBN:92-0-107304-6.

[27] T. Maruyama, S. Sakata, Y. Kumamoto, and T. Hashizume. Spectra of primary x-ray and secondary photons from shielding materials for 4-30 MV x-rays. *Health Physics*, 28:777–791, 1975.

[28] International Electrotechnical Commission. Amendment 1. Medical electrical equipment – Part 2-1: Particular requirements for the safety of electron accelerators in the range 1 Mev to 50 Mev, IEC 60601-2-1-AM1, 2002.

[29] *IAEA TRS 398: Absorbed Dose Determination in External Beam Radiotherapy: An International Code of Practice for Dosimetry based on Standards of Absorbed Dose to Water*. International Atomic Energy Agency, Vienna, 2000. ISSN: 1011-4289.

[30] C. H. Hsieh, M. L. Hou, M. H. Chiang, H. C. Tai, H. J. Tien, L. Y. Wang, T. H. Tsai, and Y. J. Chen. Head and neck irradiation modulates pharmacokinetics of 5 fluorouracil and cisplatin. *Journal of Translational Medicine*, 11(1):231, 2013. DOI: 10.1186/1479-5876-11-231.

[31] B. Fraass, S. Jolly, and A. Eisbruch. *Clinical Radiation Oncology (Third Edition). Chapter 15: Conformal therapy and intensity-modulated radiation therapy*. W.B. Saunders, Philadelphia, 2012.

[32] E. Bakiu, E. Telhaj, E. Kozma, F. Ruçi, and P. Malkaj. Comparison of 3DCRT and IMRT tratment plans. *Acta Informatica Medica*, 21(3):211–212, 2013. DOI: 10.5455/aim.2013.21.211-212.

[33] Elekta. https://www.elekta.com/radiotherapy/treatment-solutions/beam-shaping/agility.html, last access October, 2018.

[34] G. Narayanasamy, W. Cruz, D. L. Saenz, S. Stathakis, N. Papanikolaou, and N. Kirby. Effect of electron contamination on in vivo dosimetry for lung block shielding during TBI. *Journal of Applied Clinical Medical Physics*, 17(3):486–491, 2016. DOI: 10.1120/jacmp.v17i3.6128.

[35] *AAPM Report 17. The physical aspects of total and half body photon irradiation*. AAPM American Association of Physicists in Medicine, 1986.

[36] J. Rogers. *Ch 5. CyberKnife treatment room design and radiation protection*. Bucholz, Richard, Gagnon, Gerszten, Kresl, Levendag, Schulz and Raymond, 2005.

[37] *ICRP Publication 118. ICRP Statement on tissue reactions and early and late effects of radiation in normal tissues and organs; Threshold doses for tissue reactions in a radiation protection context*. ICRP International Commission on Radiological Protection, 2012.

[38] E. Nakashima. Radiation dose response estimation with emphasis on low dose range using restricted cubic splines: Application to all solid cancer mortality data, 1950–2003, in atomic bomb survivors. *Health Physics*, 109(1):15–24, 2015. DOI: 10.1097/HP.0000000000000293.

[39] *ICRP Publication 60. 1990 Recommendations of the International Commission on Radiological Protection*. ICRP International Commission on Radiological Protection, 1991.

[40] *Fundamental Safety Principles*. IAEA Safety Standards Series. International Atomic Energy Agency, Vienna, 2006. http://www-pub.iaea.org/books/IAEABooks/7592/Fundamental-Safety-Principles.

[41] *ICRP Publication 103. The 2007 Recommendations of the International Commission on Radiological Protection*. ICRP International Commission on Radiological Protection, 2007.

[42] K. S. Krane. *Introductory Nuclear Physics*. John Wiley & Sons, Inc., 1988. ISBN: 0-471-80553-X.

[43] R. Barish. Evaluation of a new high-density shielding material. *Health physics*, 64:412–6, 1993.

[44] S. F. Kry, B. Bednarz, R. M. Howell, L. Dauer, D. Followill, E. Klein, H. Paganetti, B. Wang, C.-S. Wuu, and X. George Xu. AAPM TG 158: Measurement and calculation of doses outside the treated volume from external-beam radiation therapy. *Medical Physics*, 44(10):e391–e429, 2017. DOI: 10.1002/mp.12462.

[45] R. M. Howell, S. F. Kry, E. Burgett, N. E. Hertel, and D. S. Followill. Secondary neutron spectra from modern Varian, Siemens, and Elekta linacs with multileaf collimators. *Medical Physics*, 36(9Part1):4027–4038, 2009. DOI: 10.1118/1.3159300.

[46] *NCRP Report No. 79 - Neutron contamination from medical electron accelerators*. National Council on Radiation Protection and Measurements, 1984.

[47] L. Donadille, F. Trompier, I. Robbes, S. Derreumaux, J. Mantione, B. Asselineau, K. Amgarou, et al. Radiation protection of workers associated with secondary neutrons produced by medical linear accelerators. *Radiation Measurements*, 43(2): 939–943, 2008. DOI: /10.1016/j.radmeas.2008.01.018.

[48] *U.S. Nuclear Regulatory Commission (NRC), 10CRF20, 2005.* last access October, 2018. https://www.nrc.gov/reading-rm/doc-collections/cfr/part020/part020-1302.html.

[49] R. Barish. On designing room shielding for total-body irradiation. *Health Physics*, 1996.

[50] J. E. Rodgers. Radiation therapy vault shielding calculational methods when IMRT and TBI procedures contribute. *Journal of Applied Clinical Medical Physics*, 2(3):157–164, 2001. DOI: 10.1120/jacmp.v2i3.2609.

[51] *Radiotherapy facilities: Master planning and concept design considerations*. IAEA Human Health Reports. International Atomic Energy Agency, Vienna, 2014.

[52] R. J. Barish. Shielding design for multiple-energy linear accelerators. *Health Physics*, 106(5):614–617, 2014. DOI: 10.1097/HP.0000000000000036.

[53] www.dufrane.com, Personal communication, August, 2018.

[54] https://contratacion.gobex.es, last access October, 2018.

[55] http://www.varja.com.pt/, last access October, 2018.

[56] *Council Directive 96/29/EURATOM of 13 May 1996*. The Council of the European Union, Official Journal of the European Union.

[57] A. Facure and A. X. Silva. The use of high-density concretes in radiotherapy treatment room design. *Applied Radiation and Isotopes*, 65(9):1023–1028, 2007. DOI: 10.1016/j.apradiso.2007.04.006.

[58] S. F. de Boer, Y. Kumek, W. Jaggernauth, and M. B. Podgorsak. The effect of beam energy on the quality of IMRT plans for prostate conformal radiotherapy. *Technology in Cancer Research and Treatment*, 6(2):139–146, 2007. DOI: 10.1177/153303460700600211.

[59] D. S. Followill, F. Nüsslin, and C. G. Orton. IMRT should not be administered at photon energies greater than 10 MV. *Medical Physics*, 34(6Part1):1877–1879, 2007. DOI: 10.1118/1.2734751.

[60] J. S. Welsh, T. R. Mackie, and J. P. Limmer. High-energy photons in IMRT: Uncertainties and risks for questionable gain. *Technology in Cancer Research and Treatment*, 6(2):147–149, 2007. DOI: 10.1177/153303460700600212.

[61] J. Cullen, D. Drabble, C. Castellanos, and L. Brissett. Recommendations for achieving a world-class radiotherapy service in the UK. Report for Cancer Research, UK. 2014. http://www.tavinstitute.org/wp-content/uploads/2014/05/Tavistock-Projects-Recommendations-for-achieving-a-world-class-radiotherapy-service-in-the-UK-.pdf.

[62] M. J. Pereira Rodrigues. *Avaliação de Métodos de Cálculo de Barreiras de Proteção Radiológica em Instalações de Radioterapia Externa e Braquiterapia*. Master Thesis, Universidade de Lisboa, 2012.

[63] https://www.pureleadproducts.com/lead-sheet/, last access October, 2018.

[64] *AMAT*. www.pbamat.com, Personal communication, October, 2018.

[65] *MidlandLead*. www.midlandlead.co.uk, Personal communication, October, 2018.

[66] https://www.eplastics.com/sheets/borated-polyethylene, last access October, 2018.

Appendix A

Supporting Tables

Table A.1: *Primary barriers TVLs [9] and prices [53–55] for ordinary and HD concrete as a function of nominal energy photon beam. Prices for a volume of 1 m x 1 m x TVL_1 m*

	6 MV		15 MV		6 MV	15 MV
	TVL_1, cm	TVL_e, cm	TVL_1, cm	TVL_e, cm	TVL_1, €	TVL_1, €
concrete (2.35 g/cm^3)	37	33	44	41	33.3	39.6
high concrete (3.2 g/cm^3)	24	24	26	26	144.0	156.0

Table A.2: *Patient scattered radiation TVLs [9] and prices [53–55] for ordinary concrete (2.35 g/cm^3) as a function of nominal energy photon beam and scattering angle. Prices for a volume of 1 m x 1 m x TVL m*

	TVL, cm		price, €	
scattering angle	6 MV	15 MV	6 MV	15 MV
15º	34	42	30.6	37.8
30º	26	31	23.4	27.9
45º	23	26	20.7	23.4
90º	17	18	15.3	16.2

Table A.3: *Leakage radiation TVLs [9] and prices [53–55] for ordinary concrete (2.35 g/cm^3) as a function of nominal energy photon beam. Prices for a volume of 1 m x 1 m x TVL_1 m*

	6 MV		15 MV		6 MV	15 MV
	TVL_1, cm	TVL_e, cm	TVL_1, cm	TVL_e, cm	TVL_1, €	TVL_1, €
concrete	34	29	36	33	30.6	32.4

Table A.4: *Scatter fractions a(θ) at 1 m from human-size phantom, $d_{target-phantom}$ = 1 m, F = 400 cm^2 [9].*

	Scatter fractions a(θ)	
scattering angle	6 MV	18 MV
10º	$1.04 \cdot 10^{-2}$	$1.42 \cdot 10^{-2}$
20º	$6.73 \cdot 10^{-3}$	$5.39 \cdot 10^{-3}$
30º	$2.77 \cdot 10^{-3}$	$2.53 \cdot 10^{-3}$
45º	$1.39 \cdot 10^{-3}$	$8.64 \cdot 10^{-4}$
90º	$4.26 \cdot 10^{-4}$	$1.89 \cdot 10^{-4}$

Table A.5: *Door shielding materials TVLs (cm) [9, 46, 62].*

Material	TVL	Comment
Lead	0.3 - 0.6	shield low energy scattered and transmitted leakage photons (H_{tot})
Lead	6.1	shield neutron capture gamma rays with energy about 3.6 MeV (H_{cg})
BPE	4.5	shield neutrons with energy about 100 keV (H_n)
Paraffin	8	shield neutrons with energy about 100 keV (H_n)

Table A.6: *Lead thickness sheets available in the market [63] and prices [64, 65]. Prices for a volume of 5 m x 1 m x thickness mm*

Inch	Decimal	millimeter	price, €
1/64”	0.0156	0.3968	104.56
1/32”	0.0312	0.7937	170.39
5/128”	0.0391	0.9922	
3/64”	0.0469	1.1906	
1/16”	0.0625	1.5875	
5/64”	0.0781	1.9844	395.98
3/32”	0.0937	2.3812	
1/8”	0.1250	3.1750	621.56
5/32”	0.1562	3.9687	
3/16”	0.1875	4.7625	942.98
1/4”	0.2500	6.3500	1 304.40

Table A.7: *BPE thickness sheets and prices available in the market [66]. Prices for a volume of 121 cm x 243.84 cm x thickness cm*

Inch	centimetres	price, €
1”	2.54	837.34
2”	5.08	2 512.04
3”	7.62	4 186.73

Appendix B

Barriers calculations. Example

B.0.1 Bunker dedicated to 3D-CRT and IMRT: Case a.

This section shows how barrier thicknesses of a bunker were calculated considering two techniques distributed as: 3D-CRT (50%) at 15 MV and IMRT (50%) at 6 MV, which corresponds to case a (see section 4.2.1). Distances, occupancy factors, shielding goals and use factors are those presented in table 3.3. Workloads values are those presented in table 4.12:

Primary barriers

Parameters used to calculate the thickness of primary barrier **C** are summarized in table B.1.

Table B.1: *Parameters used to calculate the thickness of primary barrier C (3D-CRT and IMRT). Workload in Gy/week.*

P, mSv/week	0.02	U	0.25	T	1/40	d_{pri}, m	7.3
W_{pri} (15 MV)	312.5	W_{pri} (6 MV)	312.5	W_L (15 MV)	312.5	W_L (6 MV)	1 031.3

To calculate the thickness barrier for 15 MV accelerating voltage, equation 3.2 is used:

$$B_{pri} = \frac{20 \cdot 10^{-6} \cdot (7.3+1)^2}{312.5 \cdot 0.25 \cdot 0.025} = 7.1 \cdot 10^{-4}$$

The required number of TVLs is (from equation 3.1):

$$n = log_{10}\Big(\frac{1}{7.1 \cdot 10^{-4}}\Big) = 3.15$$

The thickness, using ordinary concrete is:

$$t_{pri} = 44 \ + \ (3.15 - 1) \cdot 41 = 132.2 \ cm$$

To check if this thickness is adequate for 6 MV workload, the transmitted dose equivalent (H) per week is calculated using equation 3.2, where P is replaced by H and the transmission factor of the 132 cm thick barrier is

calculated considering the corresponding TVLs values:

$$H(6MV) = 10^{-\left\{1+\left[\frac{(t-TVL_1)}{TVL_e}\right]\right\}} \cdot W \cdot U \cdot T \cdot (d_{pri}+1)^{-2}$$

$$H(6MV) = 10^{-\left\{1+\left[\frac{(132-37)}{33}\right]\right\}} \cdot 312.5 \cdot 0.25 \cdot 0.025 \cdot (7.3+1)^{-2} = \ 3.7\ \mu Sv/week$$

The dose equivalent is about 20 % of the shielding design goal (20 μSv/week), and this barrier seems adequate from this point of view. Nevertheless, other considerations should be taken into account, as the dose equivalent rate in any-one-hour (R_h). The values of IDR are calculated as [9]:

$$IDR(15MV) = \frac{360 \cdot 7.1 \cdot 10^{-4}}{(7.3+1)^2} = 3.7 \cdot 10^{-3}\ Sv/h$$

$$IDR(6MV) = 360 \cdot 10^{-\left\{1+\left[\frac{(132-37)}{33}\right]\right\}} \cdot (7.3+1)^{-2} = \ 6.8 \cdot 10^{-4}\ Sv/h$$

The weekly time averaged dose equivalent rate for both energies,R_w, are calculated using the equation 3.6:

$$R_w(15MV) = \frac{3.7 \cdot 10^{-3} \cdot 312.5 \cdot 0.25}{360} = 8.0 \cdot 10^{-4}\ Sv/week$$

$$R_w(6MV) = \frac{6.8 \cdot 10^{-4} \cdot 312.5 \cdot 0.25}{360} = 1,5 \cdot 10^{-4}\ Sv/week$$

Then, the dose equivalent in any-one-hour combining both energies is (equation 3.9):

$$R_h = \frac{M}{40} \cdot R_w = \frac{1.3}{40} \cdot (8.0 \cdot 10^{-4}\ + 1,5 \cdot 10^{-4}) = 30.8\ \mu Sv\ in\ any\ one\ hour$$

Since the value obtained is higher than 20 μSv limit, additional shielding is needed (at least 1 HVL). With the new thickness (t = 132.2 + 0.301 · 41 = 145 cm) the new value for R_h is:

$$IDR(15MV) = 1.8 \cdot 10^{-3}\ Sv/h \qquad IDR(6MV) = 2.9 \cdot 10^{-4}\ Sv/h$$

$$R_w(15MV) = 4.0 \cdot 10^{-4}\ Sv/week \qquad R_w(6MV) = 6.2 \cdot 10^{-5}\ Sv/week$$

$$R_h = 15.0\ \mu Sv\ in\ any\ one\ hour$$

So the thickness of 145 cm just meet the R_h limit.

This primary barrier should be checked in terms of secondary radiation (from patient and leakage). The transmission factors for both energies are:

$$B_{ps}(15MV) = 10^{-\left(\frac{145}{42}\right)} = 3.6 \cdot 10^{-4}\ \ ;\ \ B_{ps}(6MV) = 10^{-\left(\frac{145}{34}\right)} = 5.6 \cdot 10^{-5}$$

$$B_L(15MV) = 10^{-\left\{1+\left[\frac{(145-36)}{33}\right]\right\}} = \ 5.1 \cdot 10^{-5}\ \ ;\ \ B_L(6MV) = 10^{-\left\{1+\left[\frac{(145-34)}{29}\right]\right\}} = \ 1.5 \cdot 10^{-5}$$

The dose equivalent for energies are (using equations 3.3 and 3.4) are:

$$H_{ps}(15MV) = \frac{3.6 \cdot 10^{-4} \cdot 1.42 \cdot 10^{-2} \cdot (40 \cdot 40) \cdot 312.5 \cdot 0.25 \cdot 0.025}{400 \cdot 7.3^2 \cdot 1^2} = 0.8\ \mu Sv/week$$

$$H_{ps}(6MV) = \frac{5.6 \cdot 10^{-5} \cdot 1.04 \cdot 10^{-2} \cdot (40 \cdot 40) \cdot 312.5 \cdot 0.25 \cdot 0.025}{400 \cdot 7.3^2 \cdot 1^2} = 0.1\ \mu Sv/week$$

$$H_L(15MV) = \frac{5.1 \cdot 10^{-5} \cdot 10^{-3} \cdot 312.5 \cdot 0.025}{7.3^2} = 7.5 \cdot 10^{-3}\ \mu Sv/week$$

$$H_L(6MV) = \frac{1.5 \cdot 10^{-5} \cdot 10^{-3} \cdot 1031.3 \cdot 0.025}{7.3^2} = 7.5 \cdot 10^{-3}\ \mu Sv/week$$

The total dose equivalent, H_{sum}, is below the shielding design goal, so the wall thickness for this primary barrier is adequate to shield the scattered radiation.

Analogue calculi for primary barriers D and G can be done, results are summarized in table B.2. Values obtained for ordinary (2.35 g/cm^3) and high density (3.2 g/cm^3) concrete are presented.

Secondary Barrier

Since barrier A is a secondary barrier, the transmission factor for patient and leakage radiation (B_{ps} and B_L) are calculated with equations 3.3 and 3.4. Values of scatter fraction from patient are those from table A.4.

$$B_{ps}(15MV) = \frac{20 \cdot 10^{-6} \cdot 1^2 \cdot 7.9^2 \cdot 400}{5.39 \cdot 10^{-3} \cdot 312.5 \cdot 0.025 \cdot (40 \cdot 40)} = 3.0 \cdot 10^{-2}$$

$$B_{ps}(6MV) = \frac{20 \cdot 10^{-6} \cdot 1^2 \cdot 7.9^2 \cdot 400}{6.73 \cdot 10^{-3} \cdot 312.5 \cdot 0.025 \cdot (40 \cdot 40)} = 2.4 \cdot 10^{-2}$$

$$B_L(15MV) = \frac{20 \cdot 10^{-6} \cdot 7.9^2}{10^{-3} \cdot 312.5 \cdot 0.025} = 1.6 \cdot 10^{-1} \quad ; \quad B_L(6MV) = \frac{20 \cdot 10^{-6} \cdot 7.9^2}{10^{-3} \cdot 1031.3 \cdot 0.025} = 4.8 \cdot 10^{-2}$$

These values lead to a thicknesses of:

$$n_{ps}(15MV) = 1.53; \quad t_{ps}(15MV) = 42 \cdot 1.53 = 64.2\ cm$$
$$n_{ps}(6MV) = 1.62; \quad t_{ps}(6MV) = 34 \cdot 1.62 = 55.2\ cm$$
$$n_L(15MV) = 0.8; \quad t_L(15MV) = (1 \cdot 33) = 33\ cm$$
$$n_L(6MV) = 1.32; \quad t_L(6MV) = 34 + (0.32 \cdot 29) = 43.1\ cm$$

Since the difference of both thicknesses for patient scattered radiation (9 cm) is lower than the TVL value, 1 HVL (for 15 MV) to the largest thickness is added. Then, the final thickness for patient radiation is $t_{ps} = 64.2 + 0.301 \cdot 42 = 76.8\ cm$. In the same way, for leakage radiation, the final thickness is $t_L = 43.1 + 0.301 \cdot 36 = 54.0\ cm$. Finally, the difference between t_{ps} and t_L is 22.8 cm, lower than the TVL (42 cm), thus the final barrier thickness for this secondary barrier is $t_s = 76.8 + 0.301 \cdot 42 = 89.5\ cm$.

As has been done with primary barrier C, the individual dose equivalent components should be calculated,

Table B.2: *Parameters and values for primary barriers: C, D and G, using ordinary (2.35 g/cm^3) and high density (3.2 g/cm^3) concrete, 3D-CRT and IMRT. * A HVL has been added.*

		Concrete			High concrete		
		C	D	G	C	D	G
Input data							
P	mSv/week	0.02	0.1	0.02	0.02	0.1	0.02
T		0.025	1	0.025	0.025	1	0.025
W_{pri}	Gy/week		312.5			312.5	
W_l	Gy/week		312.5 / 1031.3			312.5 / 1031.3	
U			0.25			0.25	
d_{pri}	m	7.3	7.3	3.7	7.3	7.3	3.1
d_{sca}	m		1.0			1.0	
Scat.angle	degrees	10	30	30	10	30	30
Output data							
t	**cm**	**145***	**169**	**165***	**90***	**105**	**106***
Width	m	4.7	4.7	7.7	4.7	4.7	4.7
R_h	µSv	15.0	3.6	14.5	19.7	4.7	18.9
H_{ps}(15MV)	µSv/week	0.8	0.1	0,01	15.2	5.9	0,8
H_{ps}(6MV)	µSv/week	0.1	0.01	$>$ 0,01	3.5	1.4	0,2
H_L(15MV)	µSv/week	0.01	0.1	$>$0,01	0.3	4.6	0,6
H_L(6MV)	µSv/week	0.01	0.04	0,01	0.7	6.7	0,9
H_{sum}	µSv/week	0.9	0.2	0,02	19.6	18.6	2.5

values are:

$$H_{ps}(15MV) = 5.0\ \mu Sv/week \quad H_{ps}(6MV) = 2.0\ \mu Sv/week$$
$$H_L(15MV) = 0.3\ \mu Sv/week \quad H_L(6MV) = 0.5\ \mu Sv/week$$

The total dose equivalent, H_{sum}, is 7.8 µSv/week, which is below the shielding design goal.

Finally, the time averaged dose equivalent rate in any-one-hour was also calculated for this barrier. It is the sum of the IDR from patient and leakage radiations. Values are:

$$IDR_{ps}(15MV) = 9.2 \cdot 10^{-4}\ Sv/h \quad IDR_{ps}(6MV) = 3.6 \cdot 10^{-4}\ Sv/h$$
$$IDR_L(15MV) = 1.4 \cdot 10^{-5}\ Sv/h \quad IDR_L(6MV) = 7.1 \cdot 10^{-6}\ Sv/h$$

$$R_{w,ps}(15MV) = 2.0 \cdot 10^{-4}\ Sv/week \quad IDR_{w,ps}(6MV) = 7.9 \cdot 10^{-5}\ Sv/week$$
$$R_{w,L}(15MV) = 1.2 \cdot 10^{-5}\ Sv/week \quad IDR_L(6MV) = 2.0 \cdot 10^{-5}\ Sv/week$$
$$R_h(15MV) = 6.9\ \mu Sv/h \quad R_h(6MV) = 3.2\ \mu Sv/h$$

The maximum dose equivalent in any-one-hour, R_h, is 10.1 µSv, which is below the limit of 20 µSv.

For the other secondary barriers (B, E, F and H) similar calculations were done and results are summarized in table B.3. Although for barrier E it was not needed to add an extra HVL since R_h=9.8 µSv/week, the value obtained for H_{sum} (150.7 µSv/week) was considered high, because of that 1 HVL was added. Nevertheless, values of H_{sum} for barriers B and E may still be considered as high, an extra HVL should be added following the ALARA principle.

Table B.3: *Parameters and values for secondary barriers: A, B, E, F and H, using ordinary concrete (2.35 g/cm^3), 3D-CRT and IMRT. * A HVL has been added.*

		A	B	E	F	H
Input data						
P	mSv/week	0.02	0.1	0.1	0.02	0.02
T		0.025	1	0.5	0.2	0.025
W_{pri} (15/6 MV)	Gy/week			312.5		
W_L (15/6 MV)	Gy/week			312.5 / 1 031.3		
U				1		
d_{sec}	m	7.9	7.9	5.3	10.3	4.5
d_{sca}	m			1		
Scat.angle	degrees	20	20	90	90	45
Output data						
t	**cm**	**89***	**115**	**81***	**73**	**68**
t_{ps}	cm	77	102	39	30	33
t_L	cm	54	69	81	63	57
R_h	µSv/week	10.1	2.2	4.2	1.3	11.8
H_{ps}(15MV)	µSv/week	5.0	50.0	0.1	0.04	0.8
H_{ps}(6MV)	µSv/week	2.0	14.2	0.2	0.1	0.6
H_L(15MV)	µSv/week	0.3	2.1	23.3	4.3	4.1
H_L(6MV)	µSv/week	0.5	2.7	42.3	8.5	8.4
H_{sum}	µSv/week	7.8	69.0	65.9	12.9	13.9

Maze Barrier

The maze barrier thickness is calculated as a secondary barrier, being the main contributions: leakage radiation (at both photon energies) and the fast photoneutrons produced at 15 MV.

Considering first the leakage radiation, the transmission factors for 15 and 6 MV are $3.7{\cdot}10^{-2}$ and $1.1{\cdot}10^{-2}$ respectively (P = 0.1 mSv/week, T = 1, d = 10.8 m, W_L (15 MV)= 312.5 and W_L (6 MV)=1031.3 Gy/week). The number of TVLs (*n*) obtained are 1.43 and 1.95. The barrier slant thickness is 72.3 cm, since 1 HVL has been added to the t_{maze}.

$$n_{maze}(15MV) = 1.43; \quad t_{maze}(15MV) = 36 + (0.43 \cdot 33) = 50.1; cm$$
$$n_{maze}(6MV) = 1.95; \quad t_{maze}(6MV) = 34 + (0.95 \cdot 29) = 61.5\ cm$$

Considering the fast photoneutrons, first it is calculated the fast neutron fluence at the door in the absence of the maze, considering Q_n = $1.22 \cdot 10^{12}$ n/Gy and equation 3.19:

$$\varphi_n = \frac{1.22 \cdot 10^{12}}{4 \cdot \pi \cdot 10.8^2} = 8.32 \cdot 10^8\ n/cm^2 Gy$$

The neutron dose equivalent at the door, H_n, is then:

$$H_n = H_{ns} \cdot W_L \cdot \varphi_n = 5 \cdot 10^{-13} \cdot 312.5 \cdot 8.32 \cdot 10^8 = \ 13.0 \mu Sv/week$$

where H_{ns} is obtained from figure A.2 from NCRP-151 considering that 72.3 cm is equivalent to 170 g/cm^2.

Since 13.0 µSv/week is lower than the H_L for 72.3 cm (63.6 µSv/week), the maze barrier-slant thickness can be considered as 72 cm. Then the final thickness is 52 cm, considering a scattering angle of 45º.

Door

To calculate the door composition and thickness different contributions should be considered, as described in subsection 3.1.2 and equation 3.23. They were calculated considering the following values:

Table B.4: *Input data to calculate H_s, μSv/week (3D-CRT and IMRT techniques). (*) scattered angle of 45º, (**) 0.5 MeV energy. Units: W (Gy/week), distances (m), areas (m^2).*

	W	**U**	α_0 **(*)**	$\mathbf{A}_0$	α_z **(**)**	$\mathbf{A}_z$	$\mathbf{d}_h$	$\mathbf{d}_r$	$\mathbf{d}_z$	$\mathbf{H}_s$
6 MV	312.5	0.25	$4.7{\cdot}10^{-3}$	7.0	$15{\cdot}10^{-3}$	18.8	5.6+1	9.1	8.5	2.8
15 MV	312.5	0.25	$3{\cdot}10^{-3}$	7.0	$15{\cdot}10^{-3}$	18.8	5.6+1	9.1	8.5	1.8
total										4.6

Table B.5: *Input data to calculate H_{LS}, μSv/week (3D-CRT and IMRT techniques). (*) scattered angle of 0º. Units: W (Gy/week), distances (m), areas (m^2).*

	W	**U**	α_1 **(*)**	$\mathbf{A}_1$	$\mathbf{d}_{sec}$	$\mathbf{d}_{zz}$	$\mathbf{H}_{LS}$
6 MV	1031.3	0.25	$6.4{\cdot}10^{-3}$	8.6	10.3	13.1	0.8
15 MV	312.5	0.25	$4.5{\cdot}10^{-3}$	8.6	10.3	13.1	0.2
total							1.0

Table B.6: *Input data to calculate H_{ps}, μSv/week (3D-CRT and IMRT techniques). F=40 x 40 cm^2 (*) scattered angle of 45º, (**) 0.5 MeV energy. Units: W (Gy/week), distances (m), areas (m^2).*

	W	**U**	**a**(θ) **(*)**	α_1 **(**)**	$\mathbf{A}_1$	$\mathbf{d}_{sca}$	$\mathbf{d}_{sec}$	$\mathbf{d}_{zz}$	$\mathbf{H}_{ps}$
6 MV	312.5	0.25	$1.4{\cdot}10^{-3}$	$22{\cdot}10^{-3}$	8.6	1	10.3	13.1	4.5
15 MV	312.5	0.25	$8.6{\cdot}10^{-4}$	$22{\cdot}10^{-3}$	8.6	1	10.3	13.1	2.8
total									7.3

Table B.7: *Input data to calculate H_{LT}, μSv/week (3D-CRT and IMRT techniques). Units: W (Gy/week), distances (m).*

	W	**U**	**B**	$\mathbf{d}_l$	$\mathbf{H}_{LT}$
6 MV	1031.3	0.25	$4.8{\cdot}10^{-3}$	10.8	10.6
15 MV	312.5	0.25	$7.9{\cdot}10^{-3}$	10.8	5.3
total					15.9

Then, H_{tot} = 2.64 · (0.34 · 4.6 + 1.0 + 7.3 + 15.9) = 68.0 μSv/week, where f = 0.34 from [9].

Table B.8: *Input data to calculate H_{cg}, μSv/week (3D-CRT and IMRT techniques). K=$6.9{\cdot}10^{-16}$ Svm^2, Q_n=1.22 $\cdot 10^{12}$ n/Gy; β= 1. Units: W (Gy/week), distances (m), areas (m^2), φ_A (m^{-2}), h_φ (Sv/Gy).*

	$\mathbf{W}_L$	$\mathbf{d}_2$	**TVD**	$\mathbf{d}_1$	$\mathbf{S}_r$	φ_A	$\mathbf{h}_\varphi$	$\mathbf{H}_{cg}$
15 MV	312.5	9.5	3.9	8.7	381	$2.9{\cdot}10^{9}$	$7.4{\cdot}10^{-9}$	2.3

Table B.9: *Input data to calculate $H_{n,D}$ and H_n, µSv/week (3D-CRT and IMRT techniques). d_0=1.41 m, φ_A=2.9 · 10^9 m^{-2}, TVD=2.06 · ${S_1}^{1/2}$. Units: H_0 (mSv/Gy), distances (m), areas (m^2).*

	$\mathbf{H}_0$	$\mathbf{S}_0$	$\mathbf{S}_1$	$\mathbf{d}_2$	**TVD**	$\mathbf{H}_{n,D}$		$\mathbf{H}_n$
						Kersey's	Wu and McGinley	
15 MV	1.3	11.3	6.1	9.5	5.1	0.8	0.1	250.7

Finally, the H_w is:

Table B.10: *Value of H_w, µSv/week (3D-CRT and IMRT techniques)*

$\mathbf{H}_{tot}$	$\mathbf{H}_{cg}$	$\mathbf{H}_n$	$\mathbf{H}_w$
68.0	2.3	250.7	321.0
21.2 %	0.7 %	78.1 %	

The total dose equivalent at the door is 0.3 mSv/week, of which ∼21 % is from low energy scattered and transmitted leakage photons (H_{tot}), ∼1 % is from neutron capture gamma rays (H_{cg}) and ∼78 % is due to neutrons (H_n). The door should reduce the dose equivalent for each radiation to achieve at least one half of the shielding design goal (0.5 mSv/week), considering also the TVL data (table A.5).

To protect from neutrons, 3.15 cm of BPE will be enough to obtain one half of the shielding design goal but the closest thickness available in the market is 5.08 cm. To protect from the photons, 2 sheets of 0.39 mm each will reduce the dose equivalent to the half. The aproximately weight will be 200 kg.

B.0.2 Bunker dedicated to 3DCRT, IMRT, TBI and SRS. Barrier calculation

RT techniques and number of treatments for this bunker, jointly with the workloads values are summarized in table B.11. TBI treatment was assumed as one single fraction of 12 Gy treated at a distance of 4 m, using a 6 MV beam, directed towards barrier C.

Table B.11: *Workload (W) in Gy/week as a function of treatment technique and nominal energy photon beam .*

	$6MV$	$15MV$	6 MV		15 MV	
	% treatments/week (nº of treatments)		W_{pri}	W_L	W_{pri}	W_L
$3D-CRT$	20% (50)	20% (50)	125	125	125	125
$IMRT$	28% (70)	28% (70)	175	577.5	175	577.5
SRS	1.6% (6)	-	75	1 125	-	-
TBI	2.4% (4)	-	768*	11 520	-	-
Total	130	120	**375****	**13 347.5**	**300**	**702.5**

* Beam is only towards Barrier C during TBI treatments. ** $W=W_{3D-CRT}+W_{IMRT}+W_{SRS}$

$W_{pri,C}\cdot U_C$= 375·0.25 + 768·1 = 861.8 Gy/week

Primary Barriers

Parameters used to calculate the thickness for barrier **C** are those shown in table B.12.

To calculate the transmission factor for 15 MV photon beam, equation 3.2 is used:

$$B_{pri} = \frac{20 \cdot 10^{-6} \cdot (7.3+1)^2}{300 \cdot 0.25 \cdot 0.025} = 7.4 \cdot 10^{-4}$$

Table B.12: *Parameters used to calculate the thickness of primary barrier C (3D-CRT, IMRT, SRS and TBI). Workload in Gy/week.*

P, mSv/week	0.02	U	0.25 / 1*	T	1/40	d_{pri}, m	7.3
W_{pri} (15 MV)	300	W_{pri} (6 MV)	375 / 768*	W_L (15 MV)	702.5	W_L (6 MV)	13 347.5

* Beam is only towards Barrier C during TBI treatments. $W_{pri,C} \cdot U_C$= 375·0.25 + 768·1 = 861.8 Gy/week

The required number of TVLs, *n*, is (equation 3.1):

$$n = log_{10}\Big(\frac{1}{7.4 \cdot 10^{-4}}\Big) = 3.13$$

The thickness, using ordinary concrete and data from table A.1 is:

$$t_{pri} = 44 \ + \ (2.13 - 1) \cdot 41 = 131.5 \ cm$$

To check if this thickness is adequate for 6 MV workload, the transmitted dose equivalent (H) per week is calculated using 3.2, where P is replaced by H and the transmission factor of the 132 cm thick barrier is calculated considering the corresponding TVLs values:

$$H(6MV) = 10^{-\left\{1+\left[\frac{(t - TVL_1)}{TVL_e}\right]\right\}} \cdot W \cdot U \cdot T \cdot (d_{pri} + 1)^{-2}$$

$$H(6MV) = 10^{-\left\{1+\left[\frac{(132 - 37)}{33}\right]\right\}} \cdot (375 \cdot 0.25 + 768 \cdot 1) \cdot 0.025 \cdot (7.3 + 1)^{-2} = \ 42.9 \ \mu Sv/week$$

Since the result obtained is higher than the shielding design goal (20 μSv/h), a HVL is added. With a 144.7 cm thick barrier, the H (6MV) = 17.0 μSv/week, so this barrier seems to be adequate from this point of view. Nevertheless, other considerations should be taken into account, as the time averaged dose equivalent rate in any-one-hour, R_h. The IDR values are then calculated as [9]:

$$IDR(15MV) = 360 \cdot 10^{-\left\{1+\left[\frac{(145 - 44)}{41}\right]\right\}} \cdot (7.3 + 1)^{-2} = 1.8 \cdot 10^{-3} \ Sv/h$$

$$IDR(6MV) = 360 \cdot 10^{-\left\{1+\left[\frac{(145 - 37)}{33}\right]\right\}} \cdot (7.3 + 1)^{-2} = \ 2.8 \cdot 10^{-4} \ Sv/h$$

The weekly time averaged dose equivalent rate for both energies,R_w, is calculate using the equation 3.6, where $\dot{D}_0$ is 360 Gy/h according to the table 3.4.

$$R_w(15MV) = \frac{1.8 \cdot 10^{-3} \cdot 300 \cdot 0.25}{360} = 3.8 \cdot 10^{-4} \ Sv/week$$

$$R_w(6MV) = \frac{2.8 \cdot 10^{-4} \cdot (375 \cdot 0.25 + 768 \cdot 1)}{360} = 6.8 \cdot 10^{-4} \ Sv/week$$

Then, the dose equivalent in any-one-hour combining both energies, R_h (equation 3.9), is:

$$R_h = \frac{M}{40} \cdot R_w = \frac{2.0}{40} \cdot (3.8 \cdot 10^{-4} \ + 6.8 \cdot 10^{-4}) = 53.0 \ \mu Sv \ in \ any - one - hour$$

Since R_h is higher than the 20 μSv limit, additional shielding is needed (2 HVLs). With the new thickness ($t = 144.7 + 0.301 \cdot 41 \cdot 2 = 169\ cm$) the values obtained are:

$$IDR(15MV) = 4.6 \cdot 10^{-4}\ Sv/h \qquad IDR(6MV) = 5.1 \cdot 10^{-5}\ Sv/h$$
$$R_w(15MV) = 9.5 \cdot 10^{-5}\ Sv/week \qquad R_w(6MV) = 5.1 \cdot 10^{-5}\ Sv/week$$
$$R_h = 10.8\ \mu Sv\ in\ any\ one\ hour$$

So the thickness of 169 cm meets the R_h limit.
This primary barrier should be also checked in terms of secondary radiation (due to patient scattered and leakage). The transmission factors for both energies are:

$$B_{ps}(15MV) = 10^{-\left(\frac{169}{42}\right)} = 9.3 \cdot 10^{-5}\ ;\quad B_{ps}(6MV) = 10^{-\left(\frac{169}{34}\right)} = 1.0 \cdot 10^{-5}$$

$$B_L(15MV) = 10^{-\left\{1+\left[\frac{(169-36)}{33}\right]\right\}} = 9.1 \cdot 10^{-6}\ ;\quad B_L(6MV) = 10^{-\left\{1+\left[\frac{(169-34)}{29}\right]\right\}} = 2.1 \cdot 10^{-6}$$

The dose equivalent per week for both energies (using equations 3.3 and 3.4) are:

$$H_{ps}(15MV) = \frac{9.3 \cdot 10^{-5} \cdot 1.42 \cdot 10^{-2} \cdot (40 \cdot 40) \cdot 300 \cdot 0.25 \cdot 0.025}{400 \cdot 7.3^2 \cdot 1^2} = 0.2\ \mu Sv/week$$

$$H_{ps}(6MV) = \frac{1.0 \cdot 10^{-5} \cdot 1.04 \cdot 10^{-2} \cdot (40 \cdot 40) \cdot (375 \cdot 0.25 + 768 \cdot 1) \cdot 0.025}{400 \cdot 7.3^2 \cdot 1^2} = 0.2\ \mu Sv/week$$

$$H_L(15MV) = \frac{9.1 \cdot 10^{-6} \cdot 10^{-3} \cdot 702.5 \cdot 0.025}{7.3^2} = 2.9 \cdot 10^{-3}\ \mu Sv/week$$

$$H_L(6MV) = \frac{2.1 \cdot 10^{-6} \cdot 10^{-3} \cdot 13347.5 \cdot 0.025}{7.3^2} = 1.3 \cdot 10^{-2}\ \mu Sv/week$$

The total dose equivalent, H_{sum}, is 0.4 μSv/week, which is below the shielding design goal, so the wall thickness for this primary barrier is adequate to shield the secondary radiation.

Analogue analysis for primary barriers D and G can be done for ordinary and high density concrete. Results are summarized in table B.13. Although for barrier D, with HD concrete it was not needed to add an extra HVL since R_h=5.0 μSv/week, the value obtained for H_{sum} (107 μSv/week) was considered not valid, because of that 1 HVL was added.

Secondary Barriers

Thickness of secondary barrier A is going to be evaluated in the following pages, as an example of a secondary barrier. The transmission factor for patient and leakage radiation (B_{ps} and B_L) are calculated with equations 3.3 and 3.4. Values of scatter fraction from patient are those from table A.4.

$$B_{ps}(15MV) = \frac{20 \cdot 10^{-6} \cdot 1^2 \cdot 7.9^2 \cdot 400}{5.39 \cdot 10^{-3} \cdot 300 \cdot 0.025 \cdot (40 \cdot 40)} = 3.1 \cdot 10^{-2}$$

$$B_{ps}(6MV) = \frac{20 \cdot 10^{-6} \cdot 1^2 \cdot 7.9^2 \cdot 400}{6.73 \cdot 10^{-3} \cdot 375 \cdot 0.025 \cdot (40 \cdot 40)} = 2.0 \cdot 10^{-2}$$

$$B_L(15MV) = \frac{20 \cdot 10^{-6} \cdot 7.9^2}{10^{-3} \cdot 702.5 \cdot 0.025} = 7.1 \cdot 10^{-2}$$

$$B_L(6MV) = \frac{20 \cdot 10^{-6} \cdot 7.9^2}{10^{-3} \cdot 13347.5 \cdot 0.025} = 3.7 \cdot 10^{-3}$$

Table B.13: *Parameters and values for primary barriers: C, D and G, using ordinary (2.35 g/cm^3) and high density (3.2 g/cm^3) concrete, 3D-CRT, IMRT, SRS and TBI techniques.* ^{1*} *A HVL has been added;* ^{2*} *2 HVLs has been added;*^{3*} *3 HVLs has been added;*^{4*} *4 HVLs has been added.*

		Concrete			High concrete		
		C	D	G	C	D	G
Input data							
P	mSv/week	0.02	0.1	0.02	0.02	0.1	0.02
T		0.025	1	0.025	0.025	1	0.025
W_{pri}(15/6 MV)	Gy/week	300/768	300/375		300/768	300/375	
W_l(15/6 MV)	Gy/week		702.5 / 13 347.5			702.5 / 13 347.5	
U		025/1	025		0.25/1	0.25	
d_{pri}	m	7.3	7.3	3.7	7.3	7.3	3.2
d_{sca}	m		1.0			1.0	
Scat.angle	degrees	10	30	30	10	30	30
Output data							
t	**cm**	**169**^{3*}	**169**	**176**^{2*}	**113**^{4*}	**113**^{1*}	**113**^{2*}
Width	m	4.7	4.7	4.7	4.7	4.7	4.7
R_h	µSv	10.8	5.7	11.3	15.0	3.9	15.5
H_{sum}	µSv/week	0.4	0.8	0,04	13.6	58.5	7.8
H_{ps}(15MV)	µSv/week	0.2	0.05	>0,01	4.1	3.3	0.4
H_{ps}(6MV)	µSv/week	0.2	0.01	>0,01	8.1	0.9	0.1
H_L(15MV)	µSv/week	>0.01	0.1	0,01	0.2	6.2	0.8
H_L(6MV)	µSv/week	0.01	0.6	0.03	1.2	48.1	6.4

These values lead to thicknesses of:

$$n_{ps}(15MV) = 1.51; \quad t_{ps}(15MV) = 42 \cdot 1.51 = 63.4\ cm$$
$$n_{ps}(6MV) = 1.70; \quad t_{ps}(6MV) = 34 \cdot 1.70 = 57.8\ cm$$
$$n_L(15MV) = 1.15; \quad t_L(15MV) = 36 + (0.15 \cdot 33) = 40.9\ cm$$
$$n_L(6MV) = 2.43; \quad t_L(6MV) = 34 + (1.43 \cdot 29) = 75.5\ cm$$

Since the difference of both thicknesses for patient scattered radiation (5.6 cm) is lower than the TVL value, 1 HVL (for 15 MV) to the largest thickness is added. Then, the final thickness for patient radiation is $t_{ps} = 63.4 + 0.301 \cdot 42 = 76.0\ cm$. In the same way, for leakage radiation, the final thickness is $t_L = 75.5 + 0.301 \cdot 36 = 86.3\ cm$. Finally, the difference between t_{ps} and t_L is (10.3 cm) is lower than the TVL, thus the final barrier thickness for this secondary barrier is $t_s = 86.3 + 0.301 \cdot 42 = 98.9\ cm$.

As has been done with primary barrier C, the individual dose equivalent components should be calculated,

values are:

$$H_{ps}(15MV) = 2.9\ \mu Sv/week \quad H_{ps}(6MV) = 1.3\ \mu Sv/week$$
$$H_L(15MV) = 0.4\ \mu Sv/week \quad H_L(6MV) = 3.1\ \mu Sv/week$$

The total dose equivalent, H_{sum}, is 7.7 μSv/week, which is below the shielding design goal.

Finally, the time averaged dose equivalent rate in any-one-hour was also calculated for this barrier. Values are:

$$IDR_{ps}(15MV) = 5.5 \cdot 10^{-4}\ Sv/h \quad IDR_{ps}(6MV) = 1.9 \cdot 10^{-4}\ Sv/h$$
$$IDR_L(15MV) = 7.2 \cdot 10^{-6}\ Sv/h \quad IDR_L(6MV) = 3.3 \cdot 10^{-6}\ Sv/h$$

$$R_{w,ps}(15MV) = 1.2 \cdot 10^{-4}\ Sv/week \quad IDR_{w,ps}(6MV) = 5.0 \cdot 10^{-5}\ Sv/week$$
$$R_{w,L}(15MV) = 1.4 \cdot 10^{-5}\ Sv/week \quad IDR_L(6MV) = 1.2 \cdot 10^{-4}\ Sv/week$$
$$R_h(15MV) = 6.4 \cdot 10^{-6}\ Sv/h \quad R_h(6MV) = 8.7 \cdot 10^{-6}\ Sv/h$$

The maximum dose equivalent in any-one-hour, R_h, is 15.1 μSv, which is below the limit of 20 μSv.

For the other secondary barriers (B, E, F and H) similar calculations were done. Results are summarized in table B.14. Although for barriers B and E it was not needed to add an extra HVL since R_h was lower than 20 μSv/week, the values obtained for H_{sum} (higher than 100 μSv/week) were considered not valid, because of that 1 HVL was added to each barrier.

Table B.14: *Parameters and values for secondary barriers: A, B, E, F and H using ordinary concrete, 3D-CRT, IMRT, SRS and TBI techniques.*

		A	B	E	F	H
Input data						
P	mSv/week	0.02	0.1	0.1	0.02	0.02
T		0.025	1	0.5	0.2	0.025
W_{ps}(15/6 MV)	Gy/week			300 / 375		
W_L(15/6 MV)	Gy/week			702.5 / 13347.5		
U		1	1	1	1	1
d_{sec}	m	7.9	7.9	5.3	10.3	4.5
d_{sca}	m	1.0	1.0	1.0	1.0	1.0
Scat.angle	degrees	20	20	90	90	45
Output data						
t	**cm**	**99**	**127***	**114****	**106*****	**100**
t_{ps}	cm	76	114	40	36	42
t_L	cm	86	112	114	106	100
R_h	μSv	15.1	2.4	4.8	2.4	19.0
H_{sum}	μSv/week	7.6	48.3	47.8	9.5	9.5
H_{ps}(15MV)	μSv/week	2.8	25.0	>0.01	>0.01	0.04
H_{ps}(6MV)	μSv/week	1.3	7.6	>0,01	>0.01	0.03
H_L(15MV)	μSv/week	0.4	2.0	5.5	1.0	1.0
H_L(6MV)	μSv/week	3.1	13.7	42.3	8.5	8.5

* H_{sum}=108.6 μSv/week R_h=3.5 Sv/h; 1 HVL added.

** H_{sum}=111.8 μSv/week R_h=7.3 Sv/h; 1 HVL added.

*** H_{sum}=22.2 μSv/week R_h=2.2 Sv/h; 1 HVL added.

B.0.3 Maze barrier

The maze barrier thickness is calculated as a secondary barrier being the main contributions the leakage radiation (at both energies) and the fast photoneutrons produced at 15 MV.

Considering first the leakage radiation, the barrier transmission factor for 15 MV and 6 MV are: $1.6{\cdot}10^{-2}$ and $8.3{\cdot}10^{-4}$ (considering P = 0.1 mSv/week, T = 1, d = 10.5 m and W_L = 702.5 and 13 347.5 Gy/week, at 15 and 6 MV respectively). The number of TVLs (*n*) are 1.80 and 3.08. The barrier slant thickness is then 105 cm, since 1 HVL has been added to the t_{maze} at 6 MV.

$$n_{maze}(15MV) = 1.80; \quad t_{maze}(15MV) = 36 + (0.80 \cdot 33) = 62.4; cm$$
$$n_{maze}(6MV) = 3.08; \quad t_{maze}(6MV) = 34 + (2.08 \cdot 29) = 94.3\ cm$$

Considering the fast photoneutrons, first it is calculated the fast neutron fluence at the door in the absence of the maze, considering Q_n = $1.22 \cdot 10^{12}$ n/Gy and equation 3.19:

$$\varphi_n = \frac{1.22 \cdot 10^{12}}{4 \cdot \pi \cdot 10.5^2} = 8.8 \cdot 10^8\ n/cm^2 Gy$$

The neutron dose equivalent at the door, H_n, is then:

$$H_n = H_{ns} \cdot W_L \cdot \varphi_n = 9 \cdot 10^{-14} \cdot 702.5 \cdot 8.8 \cdot 10^8 = \ 6.2 \mu Sv/week$$

where H_{ns} is obtained from figure A.2 from NCRP-151 considering that 105 cm of ordinary concrete is equivalent to 247 g/cm^2.

Since 6.2 μSv/week is lower than the H_L (47.4 μSv/week), the maze barrier slant-line thickness can be considered as 105 cm, and the thickness as 79 cm considering the angle of scattering of 49º.

B.0.4 Door

To calculate the door composition and thickness different contributions should be considered, as described in subsection 3.1.2 and equation 3.23. They were calculated considering the following values:

Table B.15: *Input data to calculate H_s, μSv/week (3D-CRT, IMRT, SRS and TBI techniques). (*) scattered angle of 45º, (**) 0.5 MeV energy. Units: W (Gy/week), distances (m), areas (m^2).*

	W	**U**	α_0 **(*)**	$\mathbf{A}_0$	α_z **(**)**	$\mathbf{A}_z$	$\mathbf{d}_h$	$\mathbf{d}_r$	$\mathbf{d}_z$	$\mathbf{H}_s$
6 MV	375/768$^+$	0.25/1$^+$	$3.0{\cdot}10^{-3}$	7.0	$15{\cdot}10^{-3}$	18.0	6.5	8.9	8.5	34.9
15 MV	300	0.25	$4.7{\cdot}10^{-3}$	7.0	$15{\cdot}10^{-3}$	18.0	6.5	8.9	8.5	1.7
total										36.6

$^+$ Beam is only towards Barrier C during TBI treatments. $W_{pri,C}{\cdot}$U= 375·0.25 + 768·1 = 861.8 Gy/week

Table B.16: *Input data to calculate H_{LS}, μSv/week (3D-CRT, IMRT, SRS and TBI techniques). (*) scattered angle of 0º. Units: W (Gy/week), distances (m), areas (m^2).*

	W	**U**	α_1**(*)**	$\mathbf{A}_1$	$\mathbf{d}_{sec}$	$\mathbf{d}_{zz}$	$\mathbf{H}_{LS}$
6 MV	13347.5	0.25	$4.5{\cdot}10^{-3}$	9.1	10.1	13.0	11.2
15 MV	702.5	0.25	$6.4{\cdot}10^{-3}$	9.1	10.1	13.0	0.4
total							11.6

Table B.17: *Input data to calculate H_{ps}, μSv/week (3D-CRT, IMRT, SRS and TBI techniques). F=40 x 40 cm^2 (*) scattered angle of 45º, (**) 0.5 MeV energy. Units: W (Gy/week), distances (m), areas (m^2).*

	W	**U**	**a(θ) (*)**	**α_1 (**)**	**A_1**	**d_{sca}**	**d_{sec}**	**d_{zz}**	**H_{ps}**
6 MV	375/768$^+$	0.25/1$^+$	$8.6{\cdot}10^{-4}$	$22\cdot10^{-3}$	9.1	1	10.1	13.0	63.2
15 MV	300	0.25	$1.4{\cdot}10^{-3}$	$22\cdot10^{-3}$	9.1	1	10.1	13.0	3.0
total									66.2

$^+$ Beam is only towards Barrier C during TBI treatments.

$W_{pri,C}$·U= 375·0.25 + 768·1 = 861.8 Gy/week

Table B.18: *Input data to calculate H_{LT}, μSv/week (3D-CRT, IMRT, SRS and TBI techniques). Units: W (Gy/week), distances (m).)*

	W	**U**	**B**	**d_l**	**H_{LT}**
6 MV	13347.5	0.25	$3.5{\cdot}10^{-4}$	10.5	10.6
15 MV	702.5	0.25	$8.0{\cdot}10^{-4}$	10.5	1.3
total					11.9

Then, H_{tot} = 4 · (0.34 · 36.6 + 11.6 + 66.2 + 11.9) = 408 μSv/week, where f = 0.34 from [9] and since the coefficient 2.64 from the equation 3.11 is not valid for TBI technique, a coefficient of 4 was considered for conservative purpose [9].

Table B.19: *Input data to calculate H_{cg}, μSv/week (3D-CRT, IMRT, SRS and TBI techniques). K=$6.6{\cdot}10^{-16}$ Svm^2, Q_n = $1.22\cdot10^{12}$ n/Gy; β= 1. Units: W (Gy/week), distances (m), areas (m^2, φ_A (m^{-2}), h_φ (Sv/Gy).)*

	W_L	**d_2**	**TVD**	**d_1**	**S_r**	**φ_A**	**h_φ**	**H_{cg}**
15 MV	702.5	9.8	3.9	8.4	349	$3.2{\cdot}10^9$	$6.7{\cdot}10^{-9}$	4.7

Table B.20: *Input data to calculate $H_{n,D}$ and H_n μSv/week (3D-CRT, IMRT, SRS and TBI techniques). d_0=1.41 m, φ_A=$3.2{\cdot}10^9 m^{-2}$, TVD=2.06 · $S_1{}^{1/2}$. Units: H_0 (mSv/Gy), distances (m), areas (m^2).*

	H_0	**S_0**	**S_1**	**d_2**	**TVD**	**$H_{n,D}$** Kersey's	**$H_{n,D}$** Wu and McGinley	**H_n**
15 MV	1.3	11.0	6.1	9.8	5.1	0.7	0.1	514.4

Finally, the H_w is:

Table B.21: *Value of H_w, μSv/week (3D-CRT, IMRT, SRS and TBI techniques).*

H_{tot}	**H_{cg}**	**H_n**	**H_w**
408.5	4.7	514.4	927.6
44.0 %	0.5 %	55.5 %	

The total dose equivalent at the door is 0.9 mSv/week, of which ∼44 % is from low energy scattered and transmitted leakage photons, ∼1 % is from neutron capture gamma rays and ∼55 % is due to neutrons.

Door should reduce the dose equivalent for each radiation at least one half of the shielding design goal in this area (0.5 mSv/week), considering also the TVL data (table A.5).

The number of lead TVLs is then 0.87, being the TVL for lead equals to 6 mm (see table A.5), and the number of BPE TVLs is 1.01. The required thickness of lead is then 5.2 mm and for BPE is 4.6 cm. The configuration of the door will be 5.08 cm of BPE (2 inch, commercially available) between two sheets of lead with thickness of 3.175 mm each [63], about 570 kg of weight.